博士論文

The role of Interleukin-1 receptor type 2 in the development of collagen-induced arthritis and helper T cell differentiation
(コラーゲン誘導関節炎およびヘルパーT 細胞分化における IL-1R2 の役割)

東京大学
新領域創成科学研究科
メディカルゲノム専攻
清水　謙次

平成２７年３月卒業

Contents

I. Summary

Interleukin-1 (IL-1) is one of inflammatory cytokines and two types of receptor, type 1 and type 2, are known. Although IL-1 receptor type 2 (IL-1R2) is thought to be a decoy receptor, its pathophysiological roles and cell specificity remain to be elucidated. In chapter III, I attempted to solve these problems. When collagen-induced arthritis was performed, *Il1r2*$^{-/-}$ mice developed severer arthritis than wild-type (WT) mice. Surprisingly, the inhibitory effect of IL-1R2 was observed only on macrophages but not on neutrophils which highly express IL-1R2. Furthermore, I investigated intracellular roles of IL-1R2 in chapter IV, because intracellular functions of IL-1R2 are suggested in addition to the decoy receptor function. I found that IL-1R2 promotes Th17 differentiation in a IL-1 signal independent manner, suggesting an intracellular role of IL-1R2. I showed that IL-1R2 controls the transcription of RORγ(t)-dependent genes in collaboration with IL-1α.

II. Introduction

Functions of interleukin-1 (IL-1)

IL-1, consisting of two molecular species IL-1α and IL-1β, is an inflammatory cytokine that plays important roles in host defense against infection and inflammatory diseases (1, 2). IL-1 induces cell adhesion molecules, cytokines and chemokines in various types of cells including epithelial cells, endothelial cells, synovial cells and macrophages to induce inflammation. Especially, IL-1 disrupts vascular stability through induction of vasodilators and internalization of VE-cadherin on epithelial cells, causing exudation of fluid from blood vessels (3). IL-1 is also involved in the development of fever by inducing PGE_2 in the hypothalamus (4-6), activation and proliferation of lymphocytes (7), development of autoimmunity by breaking tolerance of T cells (8), bone resorption and erosion by activating osteoclasts (9, 10), regulation of lipid metabolism by regulating insulin secretion (11), and regulation of body weight by regulating sympathetic nerves (12).

Secretory mechanism of IL-1

Both IL-1α and IL-1β do not have signal sequence for secretion. They are secreted by unique mechanisms. Many types of cells constitutively express IL-1α, which is mainly localized at nuclei and is hardly secreted. When cells undergo necrosis, they release IL-1α with many other cellular contents. The molecules released upon necrosis which induce inflammation, like IL-1α, are called

danger-associated molecular patterns (DAMPs) (13). DAMPs include HSP70, HSP90, HMGB1, HDGF, SAP130 and S100 protein family members. There are also non-protein DAMPs such as ATP, DNA, RNA and uric acid crystal. Upon necrosis, Ca^{2+} influx induces activation of calpain and results in cleavage of full-length IL-1α to mature form. Full-length IL-1α has low biological activity than mature form (14). When cells are killed by NK cell-derived granzyme B, granzyme B itself cleaves full-length IL-1α to mature form.

In contrast to IL-1α, many types of cells do not express IL-1β in steady state. When myeloid cell sense pathogen-associated molecular patterns (PAMPs) or DAMPs, IL-1β is up-regulated in these cells. However full-length IL-1β has no biological effects. Caspase-1 dependent cleavage is needed for generation of mature IL-1β, which have biological effects. Activation of caspase-1 is mediated by large protein complexes called inflammasome consisting of sensor molecule, adaptor molecule and caspase-1. Binding of sensor molecules, NLRP1, NLRP3 and AIM2, to PAMPs or DAMPs, muramyl dipeptide, cathepsins and dsDNA respectively, results in oligomerization of inflammasome components. These sensor molecules bind to ASC, an adaptor molecule, via homotypic interaction of each pyrin domains (PYDs), then ASC recruits caspase-1 via homotypic interaction of each caspase activation and recruitment domains (CARDs). NAIP family members are non-canonical sensor molecules, which do not contain PYDs. Binding of NAIP2 and NAIP5 to rod, a component of bacterial type III secretion systems, and flagellin, a

component of flagella, respectively results in formation of ligand-NAIP-NLRC4 complex, then NLRC4 recruits caspase-1 via homotypic interaction of each CARDs (15). Mature IL-1β is released by plasma-membrane rupture caused by pyroptosis, caspase-1 dependent cell death, concurrently with IL-1β maturation. IL-18, one of IL-1 family member, is produced, cleaved and released in same manner as IL-1β. There is an exception that neutrophils can process IL-1β by neutrophil elastase (16).

Receptors for IL-1

There are two receptors for IL-1; IL-1 receptor type 1 (IL-1R1) and IL-1 receptor type 2 (IL-1R2). Although IL-1α and IL-1β have low amino acid sequence homology, both bind IL-1R1, followed by the recruitment of IL-1 receptor accessory protein (IL-1RAcP). Then, MyD88 is recruited to the complex via homotypic interaction of the TIR (toll/interleukin-1 receptor) domains of each three molecules to activate NF-κB and AP-1 through the IRAK-TRAF6-TAK1 signaling pathway. IL-1R2 also binds IL-1. However, IL-1R2 cannot transduce the signal, because it lacks the TIR domain, which is essential for the association with MyD88, in its intracellular region (Fig. 1). It was reported that, when IL-1R2 was blocked by anti-IL-1R2 antibody, polymorphonuclear cell survival was prolonged and the expression of cytokines, chemokines and adhesion molecules in response to IL-1 was enhanced in monocytes (17). Overexpression of IL-1R2 could inhibit IL-1 signal in

human 8387 sarcoma line (18) and human keratinocyte cell line HaCaT (19). Knockdown of IL-1R2 by siRNA results in upregulation of chemokine production from HaCaT upon stimulation with IL-1 (20). Transgenic mice, which express IL-1R2 in basal keratinocytes under control of human keratin 14 promoter, showed impaired inflammation during PMA-induced dermatitis (21). Therefore, the expression of IL-1R2 is rather inhibitory to IL-1 signaling, and IL-1R2 is thought to be a decoy receptor to attenuate IL-1 activity. However, the roles of IL-1R2 under physiological conditions and its cell specificity remain to be elucidated.

Localization of IL-1R2

IL-1R2 is type I membrane protein, which has three immunoglobulin-like domains in its extracellular region (Fig. 2). However not all IL-1R2 localize in cell surface (22). It's probably because the signal sequence of IL-1R2 is very short. Although average lengths of signal sequence are 23.72 amino acid (aa) and 24.21 aa in mouse and human respectively (Fig. 3), signal sequences of both mouse and human IL-1R2 are 13 aa (Fig. 2). In addition, it is also known that trans-membrane IL-1R2 undergoes shedding. Ectodomain of IL-1R2 is processed by α-secretase or β-secretase and remaining trans-membrane fragment is processed by γ-secretase (23). Released soluble IL-1R2 has intact three immunoglobulin-like domains and IL-1 binding capacity.

Negative regulator of IL-1

There are many negative regulator of IL-1 aside from IL-1R2. IL-1 receptor antagonist (IL-1Ra, gene symbol: *Il1rn*) is one of IL-1 specific negative regulators. Although IL-1Ra binds IL-1R1, IL-1Ra does not induce the signal, because IL-1Ra cannot recruit IL-1RAcP. *Il1rn*$^{-/-}$ mice spontaneously develop arthritis and psoriasis-like dermatitis in BALB/c background due to excess IL-1 signaling (24, 25). Other negative regulators also inhibit Toll-like receptors (TLRs) signaling, which use MyD88 to transduce intracellular signaling. But this is not in case of TLR3, which use TRIF to transduce intracellular signaling. SIGIRR, receptor for IL-37, inhibits IL-1 signal by two mechanisms. Extracellular domain of SIGIRR, which contains one immunoglobulin-like domain, interferes the heterodimerization of IL-1R1 and IL-1RAcP. Intracellular domain of SIGIRR, which contains TIR domain, competes with IL-1R1 for MyD88 binding (26). ST2, receptor for IL-33, contains TIR domain in its intracellular domain and inhibits IL-1 signal by competing with IL-1R1 for MyD88 binding (27). And also, a lot of phosphatases and E3 ubiquitin ligases are involved in negative regulation of intracellular signaling of IL-1 (28).

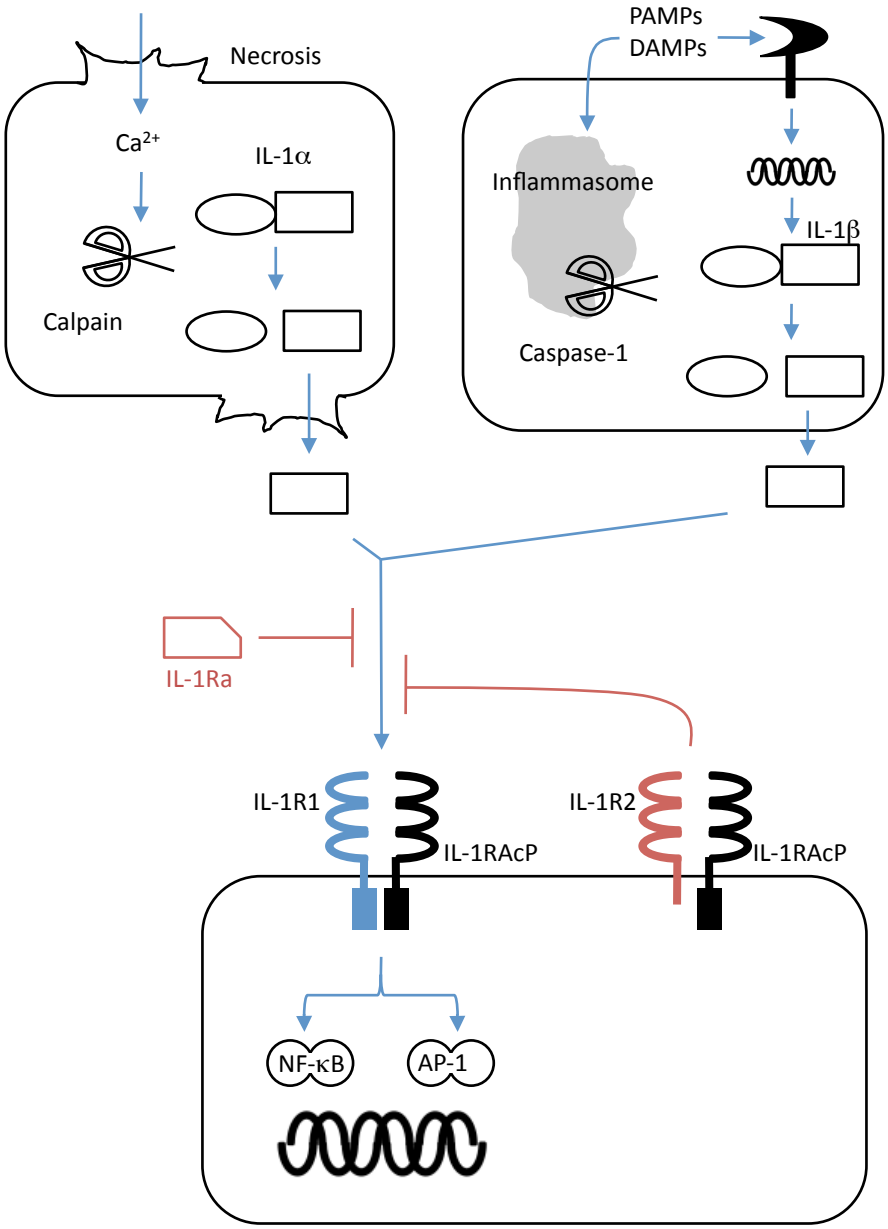

FIGURE. 1 Schematic for the IL-1 system

FIGURE. 2 Amino acid sequences of mouse IL-1R2 and human IL-1R2. Amino acid sequences of mouse IL-1R2 and human IL-1R2 were aligned by ClustalW v2.1 server. Common amino acids were marked by asterisks. Signal sequences were predicted by SignalP v4.1 server. Domains were predicted by GENE3D v12.0 server. Trans membrane regions were predicted by SOSUI v1.11 server.

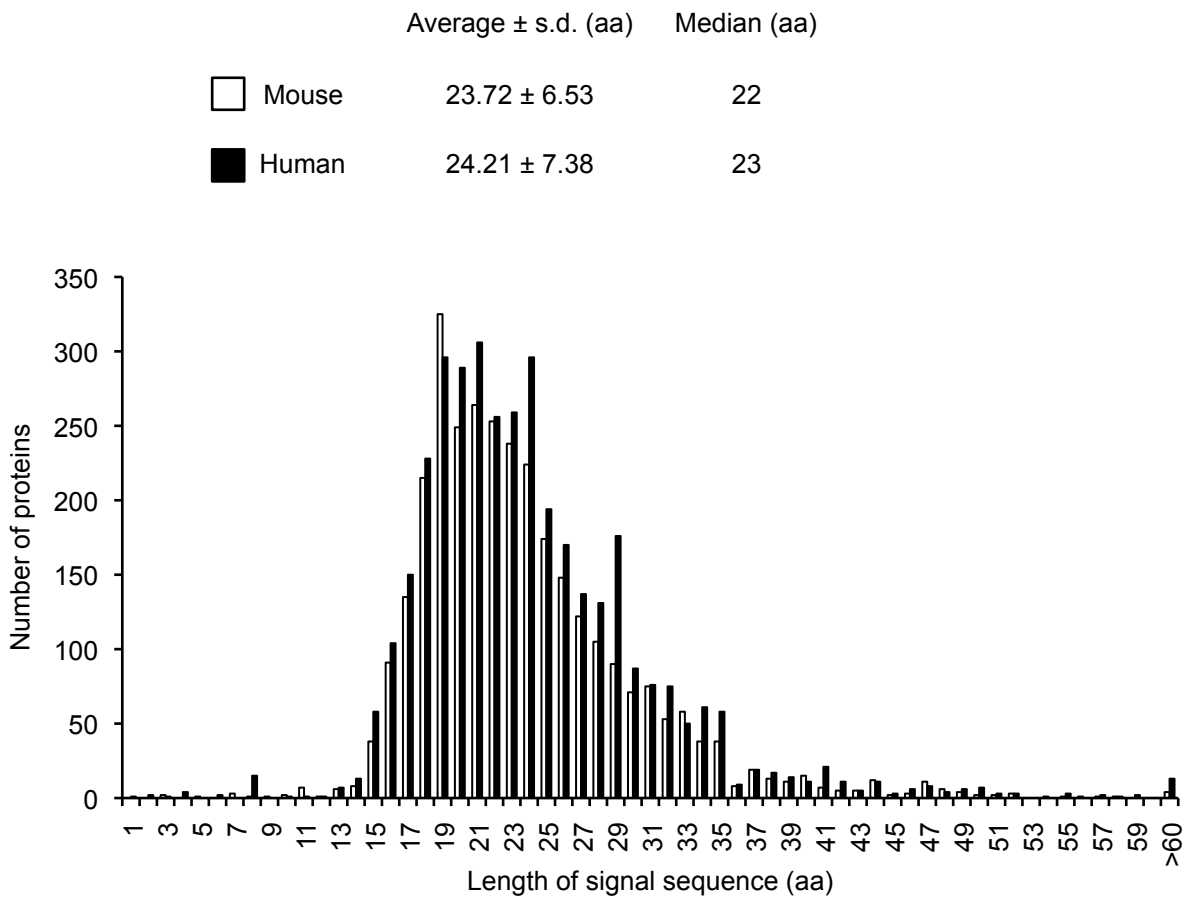

FIGURE. 3 Distribution of lengths of signal sequences.
List of signal sequence-bearing proteins and their lengths were obtained from Signal Peptide Database (http://www.signalpeptide.de/).

III

Interleukin-1 receptor type 2 suppresses collagen-induced arthritis by inhibiting interleukin-1 signal on macrophages

III-1. Abstract

Interleukin-1α and interleukin-1β, the term IL-1 refers IL-1α and IL-1β, play important roles in host defense against infection and inflammatory diseases. IL-1R1 is the receptor for IL-1, and IL-1R2 is suggested to be a decoy receptor, because it lacks signal transducing TIR domain in the cytoplasmic part. The roles of IL-1R2 in health and diseases, however, remain largely unknown. Here, I showed that *Il1r2*$^{-/-}$ mice were highly susceptible to collagen-induced arthritis, an animal model for rheumatoid arthritis in which the expression of IL-1R2 is augmented in inflammatory joints. *Il1r2* was highly expressed in neutrophils but only low in other cells including monocytes and macrophages. Antibody production and T cell responses against type II collagen were normal in *Il1r2*$^{-/-}$ mice. In spite of the high expression in neutrophils, no effects of *Il1r2* deficiency were observed in neutrophils. However, I found that the production of inflammatory mediators in *Il1r2*$^{-/-}$ macrophages were greatly enhanced upon IL-1 stimulation. These results suggest that IL-1R2 is an important regulator of arthritis by acting specifically on macrophages as a decoy receptor for IL-1.

III-2. Introduction

IL-1 in human diseases

It is well known that IL-1 plays an important role in several autoinflammatory diseases such as Familial Mediterranean fever (FMF) and cryopyrin-associated periodic syndrome (CAPS) (29). FMF is characterized by recurrent bouts of fevers, serositis and arthritis. People who have mutation in *MEFV* gene, coding pyrin, develop FMF during childhood. Pyrin interacts with ASC via homotypic interaction of each PYDs to prevent formation of inflammasome (30). Therefore, loss-of-function mutations in *MEFV* gene result in spontaneous activation of inflammasome followed by secretion of mature IL-1β. CAPS is characterized by systemic inflammation, joint deformities and developmental disabilities. People who have activating mutation in *NLRP3* gene, also known as cryopyrin, develop CAPS during childhood due to overproduction of IL-1β. Rheumatoid arthritis (RA) is a typical autoimmune disease affecting approximately 1% of people worldwide, irrespective of races. RA is characterized by chronic inflammation of synovial tissues in multiple joints that causes swelling of joints, pain, joint deformity, and loss of joint function. Line of Studies using animal models demonstrated that IL-1 is involved in RA (29, 31), and blockade of IL-1 signal can mildly remedy RA (32). But today, anti-TNF therapy and anti-IL-6 therapy are recommended as the first-line therapy for RA patients who have failed to recover by chemical treatments, since these are more effective than anti-IL-1 therapy. Because the concentration of

soluble IL-1R2 protein is increased in the synovial fluid (33) and plasma (34, 35) in RA patients and the promoter region of *IL1R2* gene is hypomethylated in RA patients' PBMC (35), the involvement of IL-1R2 is suggested in the pathogenesis.

Mouse models for RA

There are many mouse models to study pathogenesis of RA (36). The pathogenesis of these models have similarities and differences to each other. This should be same with the pathogenesis of RA, because each treatments are effective for not all RA patients. Genetically engineered spontaneous arthritis models, such as *Il1rn*$^{-/-}$ mice (24), HTLV-1 transgenic mice (37), TNF-α transgenic mice (38), SKG mice (39) and so on, are useful to understand how auto-reactive T cells and antibodies are generated. To investigate the roles of objective genes, it is demanded to generate mice deficient for these gene with another gene-modification for spontaneous arthritis. But this method is time-consuming especially when the genetic background of spontaneous arthritis model does not match that of deficient mice for objective gene. Induced arthritis models, such as Collagen-induced arthritis (CIA) (40), collagen-antibody-induced arthritis (CAIA) (41), antigen-induced arthritis (AIA) (42, 43) and so on, are good models to investigate the roles of objective genes in the pathogenesis of arthritis. On the other hands, these models are not suitable to understand how auto-reactive T cells and antibodies are generated, because these are generated by immunization of

antigens for induction of CIA and AIA, or auto-reactive antibodies are directly transferred for induction of CAIA. Proper arthritis models are to be selected for individual experiments.

Purpose of study in chapter 1

In Chapter 1, I investigated the role of IL-1R2 in the pathogenesis of arthritis by using *Il1r2*$^{-/-}$ mice. My results demonstrate that IL-1R2 is an important negative regulator of CIA by suppressing IL-1 functions in macrophages as a decoy receptor.

III-3. Materials and methods

Mice

C57BL/6J mice were purchased from Japan SLC (Hamamatsu, Japan) and kept in our mouse rooms for at least one week before use. Age- (7-10-week-old) and sex-matched mice were used for all experiments. *Rag2*$^{-/-}$ mice were obtained from the Central Institute for Experimental Animals. *Il1rn*$^{-/-}$ mice were generated as previously described (5) and backcrossed to C57BL/6J mice for eight generations. *Il1rn*$^{-/-}$*Il1r2*$^{-/-}$ mice were obtained by crossing *Il1rn*$^{-/-}$ mice and *Il1r2*$^{-/-}$ mice. *Il1r1*$^{-/-}$ mice were provided by Immunex (Amgen; Thousand Oaks, CA, USA) (44). All the mice were kept under specific pathogen-free conditions in environmentally controlled clean rooms in The Institute of Medical Science and The Graduate School of Agricultural and Life Science, The University of Tokyo, and Research institute for biomedical sciences, Tokyo University of Science. All experiments were approved by the institutional animal use committees and were conducted according to the institutional ethical guidelines for animal experiments and the safety guidelines for gene manipulation experiments.

Generation of Il1r2$^{-/-}$ *mice*

Il1r2$^{-/-}$ mice were generated by gene targeting using ES cells (Fig. 4). For the cloning of the homology arms of the targeting vector, *Il1r2* genomic clones were isolated from mouse 129

genomic phage libraries from Stratagene (129SvJ Mouse Genomic Library in the FIX II Vector; La Jolla, CA, USA) using the cDNA probe amplified by the following PCR primers: forward: CCCCCATTACATCGGAGAAGCCCA and reverse: TCCATGGACGTGTTGGATATCA. The 5.9 kb 5' arm fragment was generated by ligating two DNA fragments; the 5' side was cloned from a *Il1r2* genomic clone digested with EcoRV (EV) and EcoRI (EI), while the 3' side was amplified using the following PCR primers: forward: GAATTCTTACTTTCTTTCCAGTTTAAACA and reverse: GAAGTTGGTGCGGACAATGTTCATC. The 2.6 kb 3' arm fragment was cloned from the *Il1r2* genomic clone by digesting with EcoRV. Then, the chromosome region of E14.1 ES cells containing the second, third and fourth exons of the *Il1r2* gene, which ranged from the initiation codon ATG to a EcoRV site just after the fourth exon, was replaced by the 2.5 kb DNA fragment containing the *EGFP* gene and the neomycin resistance gene (neo) under the phosphoglycerate kinase (PGK) 1 promoter which was flanked by lox P sequences using homologous recombination techniques (Fig. 4) (45). A diphtheria toxin A (DT) gene under the MC1 promoter was ligated to the 3' end of the targeting vector for the negative selection.

Mutated ES clones were screened by Southern blot hybridization analysis using the 3' probe amplified by the following PCR primers: forward: TGGCCAGGAATACAACATCA and reverse: ATTTCCCAGGACGCCTTAGT. Chimeric mice were generated by aggregating ES cells with C57BL/6J blastocysts (45), and the *neo* gene was deleted by injecting the Cre recombinase

gene under the CAG promoter into fertilized eggs (46). *Il1r2* mutant mice were backcrossed to C57BL/6J mice for eleven generations.

I'm not involved in the generation of *Il1r2*$^{-/-}$ mice. Construction of targeting vector and ES cell screening were performed by Akiko Nakajima and Reiko Horai. Chimeric mice were generated by Hayato Kotaki. Cre-expressing vector was injected by Yang Liu.

Genotyping of Il1r2 mutant mice

The genotyping of *Il1r2* mutant mice was carried out using KOD-Fx Neo polymerase (TOYOBO; Osaka, Japan) and the following PCR primers: primer 1: CCAATGGAAGCTCAGGATCC, primer 2: CACCTGTGGGCTTCTCCGATG and primer 3: CGGCCATGATATAGACGTTG. Primers 1 and 2 were used to detect the wild-type (WT) allele (0.2 kb), and primers 1 and 3 were used to detect the mutant allele (0.5 kb). Template DNA was obtained by boiling 1 mm mouse tail with 50 mM NaOH at 95°C for 30 min, followed by neutralization with final 100 mM Tris-HCl (pH 8.0).

RT-PCR

Total RNA was isolated from bone marrow cells of WT and *Il1r2*$^{-/-}$ mice using Sepasol-RNA I Super (Nacalai Tesque; Kyoto, Japan). Target gene cDNA was amplified by PCR with KOD Fx

Neo and the following primers: for *Il1r2*, forward (exon3; P1): TGGGTGAAGGGTAACATACTCTGGA, forward (exon5; P2): GGCGCCATACTCTTGGATAA and reverse (exon9; P3): CCGTAGCTTGGTCAGTCCAT, for Actb, forward: GATCCACATCTGCTGGAAGG and reverse: AAGTGTGACGTTGACATCCG.

Flow cytometry

Cells were treated with an anti-CD16/32 monoclonal antibody (mAb) (clone: 93) (Biolegend; San Jose, CA, USA) for 30 min at 4°C in Hanks' balanced salt solution containing 2% FBS and 0.01% sodium azide, and then stained with antibodies described in Table 1 for 30 min at 4°C. For intracellular staining, cells were stimulated with 50 ng/ml PMA (Sigma; St. Louis, MO, USA), 500 ng/ml ionomycin (Sigma), and 2 μM monensin (Sigma) for 5 h. After staining surface antigens, cells were fixed and permeabilized with Foxp3/Transcription Factor Staining Buffer (eBioscience; San Diego, CA, USA) according to the manufacturer's instructions. The intracellular antigens were then stained with antibodies described Table 2 for 30 min at 4°C, followed by analysis with a FACSCanto II apparatus (BD Biosciences; San Jose, CA, USA) with FlowJo software (Tree Star; Ashland, OR, USA). Biotin-conjugated anti-CD40 mAb was stained with Pacific Blue-conjugated streptavidin (Invitrogen; Carlsbad, CA, USA). Dead cells were stained with 7-amino-actinomycin D (Sigma) or Aqua Dead Cell Stain Kit (Molecular Probes; Eugene, Oregon, USA).

Table 1

Antigen	**Label**	**Clone**	**Source**
B220	APC	RA3-6B2	Biolegend
B220	APC/Cy7	RA3-6B2	Biolegend
B220	PerCP/Cy5.5	RA3-6B2	eBioscience
CD117	Pacific Blue	2B8	Biolegend
CD11b	APC	M1/70	Biolegend
CD11b	PE	M1/70	Biolegend
CD11c	PE	HL3	BD Biosciences
CD19	APC	6D5	Biolegend
CD19	PerCP	6D5	Biolegend
CD3ε	APC	145-2C11	Biolegend
CD4	PE/Cy7	RM4-5	Biolegend
CD40	Biotin	3/23	Biolegend
CD40	APC	3/23	Biolegend
CD45	APC/Cy7	30-F11	Biolegend
CD45.1	Pacific Blue	A20	Biolegend
CD62L	Pacific Blue	MEL-14	Biolegend
CD8a	APC/Cy7	53-6.7	Biolegend
F4/80	APC	BM8	Biolegend
Foxp3	PE	FJK-16s	eBioscience
γ/δ TCR	FITC	GL3	eBioscience
IFNγ	Pacific Blue	XMG1.2	Biolegend
IL-17A	APC	TC11-18H10.1	Biolegend
IL-1R1	PE	JAMA-147	Biolegend
Ly6C	APC/Cy7	HK1.4	Biolegend
Ly6C	Pacific Blue	HK1.4	Biolegend
Ly6G	Pacific Blue	1A8	Biolegend
Ly6G	PE/Cy7	1A8	Biolegend
Phycoerythrin (PE)	Biotin	PE001	Biolegend
(Armenian Hamster IgG Isotype Ctrl)	PE	HTK888	Biolegend
(Rat IgG2a Isotype Ctrl)	APC	RTK2758	Biolegend

CIA

CIA was performed as previously described (47). CFA was prepared by mixing 1 mg heat-killed M. tuberculosis (H37Ra; Difco Laboratories; Detroit, MI, USA) with 1 ml IFA (Thermo Scientific; Waltham, MA, USA). 4 mg of chicken type II collagen (IIC) (Sigma) was dissolved in 1 ml of 10 mM acetic acid for overnight at 4°C. An emulsion was formed by combining CFA with an equal volume of IIC solution. Mice were immunized by subcutaneous injection with 200 μl emulsion at two different sites on each hind flank. Twenty days later, mice received the same immunization and 10 μg LPS (Sigma) administration intraperitoneally as a boost. Arthritis severity was scored for each limb with total score 12: 0 = normal, 1 = slight swelling and/or erythema, 2 = extensive swelling and/or erythema, 3 = ankhylosing change of the joint.

Histological assessment of arthritis

On day 40 of CIA, two hind limbs were fixed with 10% neutral-buffered formalin and were decalcified with 10% EDTA. They were embedded in paraffin, and slices were prepared. Sections were stained with hematoxylin and eosin. Four histological parameters, inflammation, pannus formation and cartilage/bone damage were scored for each limbs with total score 6. Inflammation: 0 = normal, 1 = few local infiltrates, 2 = broad local infiltrates and 3 = broad infiltrates invading the joint capsule. Pannus: 0 = normal, 1 = pannus formation at up to two sites, 2 = pannus formation at

up to four sites, 3 = pannus formation at more than four sites, one broad pannus formation count as two sites. Cartilage damage: 0 = normal, 1 = few loss of articular chondrocytes, 2 = cartilage degradation in one region, 3 = cartilage degradation in more than two region. Bone damage: 0 = normal, 1 = rough surface of talus, 2 = shallow loss of talus, 3 = deep loss of talus.

Measurement of mRNA levels in inflammatory joints

On day 40 of CIA, two hind limbs were homogenized in Sepasol-RNA I Super and RNA was purified according to the manufacture's instructions. The resulting RNAs were reverse-transcribed using a high capacity cDNA reverse transcription kit (Applied Biosystems; Carlsbad, CA, USA). Quantitative PCR (qPCR) was performed with the SYBR® Premix Ex Taq™ (TaKaRa; Shiga, Japan) using an iCycler system (Bio-Rad; Hercules, CA, USA). The content of mRNA was determined from the appropriate standard curve and normalized to the amount of *Gapdh* mRNA. The primer sets are shown in Table 2.

Table 2

Gene	Forward (5' to 3')	Reverse (5' to 3')
Col1a1	TGGCAACAAAGGAGACACTG	GGCTCCTCGTTTTCCTTCTT
Cxcl2	CACTGCGCCCAGACAGAAGTC	TCCTCCTTTCCAGGTCAGTTAGCC
Gapdh	TTCACCACCATGGAGAAGGC	GGCATGGACTGTGGTCATGA
Hprt	AGCTACTGTAATGATCAGTCAACG	AGAGGTCCTTTTCACCAGCA
Il1a	TCGGGAGGAGACGACTCTAA	TGTTTCTGGCAACTCCTTCA
Il1b	CAACCAACAAGTGATATTCTCCATG	GATCCACACTCTCCAGCTGCA
Il1r1	ACCTTCCCACAGCGGCTCCACATT	TTGTCAAGAAGCAGAGGTTTACAG
Il1r2	GATCCAGTCACAAGGGAGGA	CCAGGAGAACGTGGAAGAGA
Il1rap	AAGAACCAGGAGAGGAACTGG	GGGGTGACTTTCTTGATGCT
Il1rn	TAGACATGGTGCCTATTGACCT	TCGTGACTATAAGGGGCTCTTC
Il6	TAGTCCTTCCTACCCCAATTTCC	TTGGTCCTTAGCCACTCCTTC
Nos2	ACATCGACCCGTCCACAGTAT	CAGAGGGGTAGGCTTGTCTC
Prg4	GGCAAGTGCTGTGCAGATTA	ATTTGGGTGAGCGTTTGGTA
Ptgs2	CTACATCCTGACCCACTTCAAGG	GCCCTGGTGTAGTAGGAGAGGTT
Tnf	GCCTCCCTCTCATCAGTTCT	CACTTGGTGGTTTGCTACGA

Measurement of collagen-specific antibody concentrations

Sera were collected from the tail on day 0 and 40 of CIA. A total of 20 μg/ml IIC in PBS was coated on 96-well plate at 4°C overnight. Then the wells were blocked with 10% FBS in PBS at room temperature for 1 h. Next, diluted serum samples (5,000, 2,500, 500, 500 and 100-fold dilution for total IgG, IgG1, IgG2a, IgG2b and IgG3, respectively) were applied and incubated at room temperature for 1 h, followed by the addition of 0.8 μg/ml horseradish peroxidase-conjugated goat anti-mouse IgG (Jackson ImmunoResearch; West Grove, PA, USA) or 0.4 μg/ml alkaline phosphatase-conjugated anti-mouse IgG1, IgG2a, IgG2b and IgG3 (Santa Cruz; Dallas, TX, USA).

Then, 3,3',5,5'-Tetramethylbenzidine solutions (Dako; Carpinteria, California, USA) or p-nitrophenyl phosphate solutions (Sigma) were applied as the substrate and 1 N HCl or 1 N NaOH was added to stop color development. The absorbancy at 450 nm or 415nm was measured using a microplate reader (MTP-300; Corona Electric; Hitachinaka, Japan). The wells were washed with 0.05% Tween20 in PBS between each steps. The IgG antibody concentration was calculated using an anti-IIC polyclonal IgG standard with a known concentration. The anti-IIC polyclonal IgG was purified from pooled sera obtained from IIC-immunized mice. I used Protein G sepharose (GE healthcare; Waukesha, WI, USA) for prepurification and NHS-activated sepharose (GE healthcare) for affinity-based purification.

IIC-specific proliferation assay and cytokine titration

I immunized mice with IIC and CFA and harvested lymph nodes (LNs) at day 7 after immunization. Then, LN cells (5×10^5 cells/well in 96-well plate) were cultured in the absence or presence of 50 μg/ml heat-denatured IIC for 3 days, and labeled with [^{3}H]-thymidine (0.25 μCi/ml) (PerkinElmer; Boston, MA, USA) for 6 h. RPMI 1640 (Wako; Osaka, Japan) containing 10% FBS (GIBCO), 50 μM 2-mercaptoethanol (Gibco; Big Cabin, OK, USA), 100 U/ml penicillin (Gibco; Big Cabin, OK, USA) and 100 μg/ml streptomycin (Gibco; Big Cabin, OK, USA), so called R10 medium, was used as culture medium. Then, cells were harvested with a Micro 96 cell harvester (Skatron; Tranby,

Norway), and radioactivity was measured with Micro Beta (Pharmacia Biotech; Uppsala, Sweden).

To measure cytokine concentrations, I collected the culture supernatants from the culture for proliferation assay after 3 d and measured the concentration of IFN-γ, IL-17 and TNF with the mouse IFN-γ ELISA set (R&D; Minneapolis, MN, USA), mouse IL-17 ELISA set (R&D) and the mouse TNF-α ELISA MAX™ (Biolegend), respectively.

Myeloid cell preparation and culture

Bone marrow macrophages (BMMPs) were prepared from bone marrow cells (BMCs) as previously described (48). In brief, I seeded BMCs obtained from femurs and tibiae at 1×10^6 cells/ml in a 100-mm non-treated dish using R10 medium supplemented with 20 ng/ml recombinant mouse M-CSF (R&D). On day 3, non-adherent cells were discarded and re-cultured with another 10 ml of fresh medium. At day 7, non-adherent cells were discarded and adherent cells were collected by treating with 0.7 mM EDTA/PBS. For thioglycolate-elicited peritoneal macrophages (TGCMPs) preparation, mice were injected 1 ml of 4% thioglycolate (TGC) (Nissui; Tokyo, Japan) i.p. Peritoneal cells were collected at 3 days after TGC injection and cultured over night. After discarding nonadherent cells, adherent cells were collected by cell scraper as TGCMPs. Neutrophils ($Ly6G^+Ly6C^{int}$) and monocytes ($Ly6G^-Ly6C^{high}$) were sorted from BMCs by flow cytometry on a FACSAria apparatus (BD Biosciences) or MoFlo XPD IntelliSort II (Beckman Coulter; Brea, CA,

USA). Obtained myeloid cells were cultured in R10 medium containing stimulants described below.

In vitro neutrophil survival assay

For cell survival assay, neutrophils were cultured with either 10 ng/ml IL-1β (Peprotech; Rocky Hill, NJ, USA), IL-4 (Peprotech) or GM-CSF (Peprotech) for 48 h. Live cells ($7AAD^{-}AnnexinV^{-}$ [Biolegend]) were counted by flow cytometry. Survival ratio was calculated by dividing live cell number in each condition by cell number without any cytokines.

ROS generation assay

For ROS generation assay, neutrophils were cultured with 1mM luminol (Santa Cruz) plus either 100 ng/ml IL-1β or 50 ng/ml C5a (R&D). After stimulation, chemiluminescence was measure by the EnVision plate-reader (Perkin Elmer; Norwalk, CT, USA) at indicated time points.

Activation assay

For activation assay, neutrophils and monocytes were stimulated by 100 ng/ml IL-1β or 1 μg/ml Pam3CSK4 (Invivogen; San Diego, CA, USA). 15 h after stimulation, cells were collected and surface CD40 expression was examined by flow cytometry.

Cytokine production assay

For cytokine production assay, neutrophils and monocytes were treated with either IL-1β or LPS (Sigma), while BMMPs and TGCMPs were cultured with 10 ng/ml IL-1α (Peprotech), 10 ng/ml IL-1β or 1 ng/ml LPS. Cultured supernatants were collected at 20 h and the concentration of TNF and IL-6 was measured with the Mouse TNF-α ELISA MAX™ (Biolegend) and Mouse IL-6 ELISA MAX™ (Biolegend), respectively.

qPCR for macrophages and monocytes

For the measurement of mRNAs, cultured BMMPs and TGCMPs were collected at 3 h after the treatment with stimulants and total RNAs were purified using GenElute mammalian total RNA miniprep kit (Sigma). Similarly, mRNAs from monocytes were collected at 1 or 3 h after stimulation with 100 ng/ml IL-1β or 1 μg/ml LPS. qPCR was performed as described above and the content of mRNA was normalized to the amount of *Hprt* mRNA.

Western blotting

For Western blotting analysis, BMMPs were cultured for 8 h with normal RPMI 1640, and then stimulated by 5 ng/ml IL-1α plus 5 ng/ml IL-1β or 1 ng/ml LPS. Stimulated cell were lysed with

sample buffer (62.5 mM Tris-HCl, pH 6.8, 2% SDS, 5% glycerol, 0.003% bromophenol blue, 5% 2-ME, NaCl 61.7 mM, KCl 1.2 mM, Na_2HPO_4 4.5 mM, KH_2PO_4 0.8 mM) at various periods of time. The cell lysates were separated by SDS-PAGE using 12.5% polyacrylamide gel (Wako). Then, proteins were transferred onto polyvinyldifluoride membranes (BioRad Laboratories; Shinagawa, Japan) in wet condition. The membranes were blocked by 2% polyvinylpyrrolidone (Sigma) / 2% BSA (Sigma) / TBST for 1 h at room temperature. After that, membranes were incubated with primary antibodies for overnight at 4°C, and then with horseradish peroxidase-conjugated secondary antibodies for 1 h at room temperature. Used antibodies are listed in Table 3. Signals were developed by ECL detection system (GE Healthcare). Chemiluminescence was measure by LAS 4000 (Fujifilm Life Science; Tokyo, Japan).

Table 3

Antigen	**Host**	**Dilution**	**Clone**	**Source**
P-JNK	Rabbit	1:1000	81E11	CST
JNK	Mouse	1:1250	252355	R&D
P-p38	Rabbit	1:1000	3D7	CST
p38	Rabbit	1:1000	(Polyclone)	CST
IκBα	Mouse	1:1000	44D4	CST
β-actin	Mouse	1:20000	AC-74	Sigma
Rabbit IgG	Goat	1:5000	(Polyclone)	Jackson
Mouse IgG	Goat	1:5000	(Polyclone)	Jackson

Peritonitis

For the analysis of EGFP expressing cells, WT and *Il1r2*$^{+/-}$ mice were injected 1 ml of 4% TGC i.p. Peritoneal cells were collected at 15 h after TGC injection. For *in vivo* neutrophil survival assay, BMCs were isolated from WT (CD45.1) and *Il1r2*$^{-/-}$ (CD45.2) mice, mixed 1:1 ratio and resuspended in PBS. Total 1×10^7 BMCs were transferred i.v. into irradiated (5.5 Gy twice, 3 h apart) *Rag2*$^{-/-}$ mice. Four weeks later, these mice were injected 10 ng IL-1α i.p. Peritoneal cells and BMCs were collected at 6 h after IL-1α injection.

Fibroblast-like synovial cell (FLSC) preparation and culture

I prepared FLSCs according to Chou et al. (49). After ankle was removed, it was digested in 1 mg/ml collagenase (Wako), 2 mg/ml dispase (Gibco) and 10% FBS in DMEM (Gibco) for 1 h at 37°C with a tube rotator. Then, cells were suspended in DMEM containing 10% FBS, 100 U/ml penicillin and 100 μg/ml streptomycin, and were incubated with Clophosome (FormuMax Scientific; Palo Alto, CA, USA) for 24 h to remove contaminated macrophages. FLSCs were stimulated with IL-1α, IL-1β, TNFα (Peprotech), IL-17A (R&D) and PGE_2 (Nacalai) for 20 h. Cultured supernatants were collected at 20 h and the concentration of CCL2 and IL-6 was measured with the Mouse CCL2/JE/MCP-1 DuoSet (R&D) and Mouse IL-6 ELISA MAX™ (Biolegend), respectively.

Statistical analysis

P values were calculated using Mann-Whitney *U*-test for clinical and histological score of CIA, χ^2 test for incidence of CIA and two-tailed unpaired student's *t*-test for all other experiments. *P* value < 0.05 was defined as significant.

III-4. Results

Generation of Il1r2$^{-/-}$ mice

Il1r2$^{-/-}$ mice were generated by replacing the exon 2, 3 and 4 of the *Il1r2* gene with the *EGFP* gene and the neomycin resistant gene using homologous recombination techniques (Fig. 4A). Homologous recombination was confirmed by genomic Southern blot hybridization analysis (Fig. 4B). *Il1r2* deficiency was verified by RT-PCR using the RNA from bone marrows. I could not detect the PCR product from the exon 3 to exon 9. The PCR product from exon 5 to exon 9 was also not detected, indicating that there was no truncated mRNA from the targeted gene (Fig. 4C).

When *Il1r2*$^{+/-}$ mice were intercrossed, *Il1r2*$^{-/-}$ mice were born at the expected Mendelian ratio. They were fertile and showed no obvious phenotypic abnormalities under specific pathogen-free conditions (data not shown). The content of T cells, B cells plasmacytoid DCs, conventional DCs, migratory DCs, monocytes and neutrophils in the LNs, spleen, thymus and bone marrow in *Il1r2*$^{-/-}$ mice was normal as analyzed by flow cytometry (Fig. 5).

In WT mice, *Il1r2* mRNA expression was detected in the bone marrow, pancreas and lymphoid organs including Peyer's patch, LNs, and the thymus (Fig. 6). I also analyzed the expression of *Il1r2* through the expression of EGFP in *Il1r2*$^{+/-}$ mice, in which *EGFP* gene was inserted into just after the *Il1r2* translation start site in the exon 2. High EGFP expression was observed in neutrophils (Fig. 7). Low levels of EGFP expression were detected in macrophages and

monocytes from TGC-treated mice, although the expression was very low under physiological conditions. The expression was not detected in T cells or B cells. The EGFP expression level was consistent with the *Il1r2* mRNA level determined by qPCR (Fig. 8B). *Il1r2* expression in WT BMMPs was confirmed by using *Il1r2*$^{-/-}$ BMMPs as negative control (Fig. 8E). Like *Il1r2, Il1rn* and *Il1rap* mRNA were highly expressed in neutrophils and modestly in other types of cells (Fig. 8C and D). On the other hand, high levels of *Il1r1* mRNA expression were observed in FLSCs, but only low in other cells (Fig. 8A).

Il1r2$^{-/-}$ *mice show increased susceptibility to CIA*

Because it was suggested that IL-1R2 is involved in the pathogenesis or progression of RA (33-35), I examined the susceptibility of *Il1r2*$^{-/-}$ mice to CIA. *Il1r2*$^{-/-}$ mice showed higher clinical scores and incidence (Fig. 9). Infiltration of polymorphonuclear leukocytes, pannus formation, erosion of cartilage and bone destruction were more severe in arthritic joints of *Il1r2*$^{-/-}$ mice than WT mice (Fig. 10). These results suggest that IL-1R2 negatively controls the development of arthritis.

Inflammatory mediator production, but not antibody production and T cell proliferative responses, is enhanced in Il1r2$^{-/-}$ *mice after CIA induction*

It is well known that both humoral and cell-mediated immunity are involved in the development of

CIA (50, 51). To elucidate the mechanism for the exacerbation of CIA in *Il1r2*$^{-/-}$ mice, I first analyzed anti-IIC IgG concentration in sera. No significant differences were found between WT mice and *Il1r2*$^{-/-}$ mice (Fig. 11A). The levels of anti-IIC IgGs in each IgG subclass also did not differ between WT and *Il1r2*$^{-/-}$ mice (Fig. 11B). Next, I examined IIC-specific recall T cell responses; inguinal LN cells were harvested 7 days after immunization and the cells were incubated for 3 days with or without IIC. Proliferative response against IIC of *Il1r2*$^{-/-}$ LN cells was similar to WT cells (Fig. 11C). Consistent with the proliferative response, cytokine production such as IFN-γ, IL-17 and TNF was normal in LN cells from *Il1r2*$^{-/-}$ mice upon stimulation with IIC (Fig. 11D-F). Furthermore, the number of total LN cells, B cells, $CD4^+$ and $CD8^+$ T cells, IFN-γ^+ $CD4^+$ and $CD8^+$ T cells, IL-17^+ $CD4^+$ T cells, and $Foxp3^+$ $CD4^+$ T cells was normal in *Il1r2*$^{-/-}$ mice at day 7 after immunization (Fig. 11G). Interestingly, I found that the expression of *Il6*, *Cxcl2*, *Nos2* and *Il1b* mRNAs, which are produced in macrophages and fibroblasts (52-55), in inflammatory joints was strongly up-regulated in *Il1r2*$^{-/-}$ mice (Fig. 12).

Il1r2$^{-/-}$ *neutrophils show normal phenotype*

IIC-specific T cells and antibodies are important for the development of arthritis by recruiting neutrophils and monocytes/macrophages, which enhance inflammation by producing cytokines, chemokines, nitric oxide and chemical mediators. In addition, joint resident FLSCs are also

involved in the development of inflammation (56). Because antibody production and T cell priming were normal in *Il1r2*$^{-/-}$ mice, I next examined the effect of IL-1R2 deficiency on these cells.

Since neutrophils highly expressed *Il1r2* and a previous report suggested involvement of IL-1R2 in neutrophil survival (17), I analyzed the effects of IL-1 on neutrophils. I found that neutrophil survival did not change upon stimulation with IL-1β in *Il1r2*$^{-/-}$ neutrophils (Fig. 13A). IL-6 production also did not change by the treatment with IL-1β both in WT and *Il1r2*$^{-/-}$ neutrophils (Fig. 13B). In contrast, GM-CSF and LPS prolonged neutrophil survival and induced cytokine production in both WT and *Il1r2*$^{-/-}$ neutrophils. Although IL-4 is suggested to induce *Il1r1* and *Il1r2* mRNA in neutrophils (17), IL-4 or IL-1β plus IL-4 did not affect the survival of both WT and *Il1r2*$^{-/-}$ neutrophils (Fig. 13A). And also, IL-1β failed to induce ROS generation from both WT and *Il1r2*$^{-/-}$ neutrophils, in contrast to C5a (Fig. 13C). Furthermore, Although TLR2 ligand Pam3CSK4 up-regulate CD11b and down-regulate CD62L, IL-1β could not alter adhesion molecule expression on both WT and *Il1r2*$^{-/-}$ neutrophils (Fig. 13D).

I also examined the effect of IL-1R2 deficiency on neutrophil survival *in vivo*. Peritonitis was induced by i.p. IL-1α injection to CD45.1^{+} WT and CD45.2^{+} *Il1r2*$^{-/-}$ bone marrow chimeras, and 6 h after injection, infiltration of neutrophils and monocytes into peritoneal cavity was examined. As shown in Fig. 14A, infiltration of neutrophil and monocyte was clearly observed. However, WT and *Il1r2*$^{-/-}$ ratio did not change in peritoneal cavity and bone marrow, suggesting

comparable survival between WT and *Il1r2*$^{-/-}$ neutrophils in these mice (Fig. 14B).

Excess cytokine production in Il1r2$^{-/-}$ *macrophages was observed upon stimulation with IL-1*

Next, I examined inflammatory mediator production from FLSCs upon treatment with IL-1 or TNF. FLSCs were prepared as described Materials and Methods. The percentage of contaminated macrophages in the FLSC preparation was below 1% as determined by flow cytometry using anti-CD45 mAb (Fig. 15A). Messenger RNAs for Proteoglycan 4 (*Prg4*) or lubricin, which is a component of synovial fluid, and α1 type1 collagen (*Col1a1*), which is the major component of type 1 collagen, were highly expressed in FLSCs (Fig. 15B). I found that the production of IL-6 and CCL2 was normal in *Il1r2*$^{-/-}$ FLSCs (Fig. 16).

On the other hand, monocytes from both WT and *Il1r2*$^{-/-}$ mice did not respond to IL-1 to produce TNF or IL-6 like neutrophils, while these cells produced those cytokines to similar levels in response to LPS (Fig. 17). Although we detected slight up-regulation of *Tnf*, *Il1b* and *Cxcl2* mRNA upon IL-1 stimulation, no difference between WT and *Il1r2*$^{-/-}$ monocytes was observed (Fig. 18). Similarly, cell surface expression of CD40 was marginally up-regulated by the treatment with IL-1, but its expression levels were comparable between WT and *Il1r2*$^{-/-}$ monocytes (Fig. 19).

In contrast, significantly higher amounts of TNF and IL-6 were produced in *Il1r2*$^{-/-}$ BMMPs and TGCMPs compared to WT cells in response to IL-1α or IL-1β, but not LPS (Fig. 20).

qPCR revealed that mRNA expression of *Il1a*, *Il1b*, *Cxcl2*, *Nos2,* which encodes iNOS, and *Ptgs2,* which encodes COX-2, was also enhanced in *Il1r2*$^{-/-}$ BMMPs and TGCMPs (Fig. 21). I prepared cell lysate from IL-1 or LPS stimulated BMMPs to check the phosphorylation of MAPKs and the degradation of IκBα by western blotting. The phosphorylation of JNK and p38 as well as the degradation of IκBα were enhanced in *Il1r2*$^{-/-}$ BMMPs upon IL-1 stimulation but not LPS (Fig. 22). These results suggest that IL-1R2 negatively regulates IL-1 signaling in monocytes and macrophages, but not in other cells including neutrophils and fibroblasts.

III-5. Discussion

IL-1R2 is considered to be a decoy receptor for IL-1α and IL-1β, and many reports support this concept *in vitro* (17-20). Negative regulatory function of IL-1R2 against IL-1 signaling is also suggested in *Il1r2*-transgenic mice which are designed to express IL-1R2 in keratinocytes (21). However, the physiological as well as the pathological roles of endogenous IL-1R2 have not been elucidated completely. Here, I have first shown that IL-1R2 is functional in monocytes and macrophages as a negative regulator of IL-1 and suppresses CIA.

Il1r2$^{-/-}$ mice were born healthy and breed normally. However, I found that the development of CIA was enhanced in *Il1r2*$^{-/-}$ mice. The severity score and incidence of arthritis were increased. Anti-IIC concentrations in the serum, IIC-specific T cell proliferative responses, and cytokine production in LN cells upon stimulation with IIC, were normal in *Il1r2*$^{-/-}$ mice, suggesting that *Il1r2* is not involved in the control of T cell priming and production of Ag-specific antibodies. I showed, however, that the expression of mRNAs for inflammatory mediators such as IL-6, CXCL2, NOS2 and IL-1β, which are important for the development of arthritis (57-60), was up-regulated in the joint of *Il1r2*$^{-/-}$ mice. Furthermore, I found that cytokine and inflammatory mediator production, including IL-6, CXCL2, NOS2 and IL-1β, upon stimulation with IL-1α and IL-1β were greatly enhanced in macrophages, but not in FLSCs or monocytes, from *Il1r2*$^{-/-}$ mice compared with that from WT mice, suggesting that increased inflammatory mediators in *Il1r2*$^{-/-}$

mouse joints are derived from macrophages. Consistent with this notion, it was reported that macrophage depletion results in the suppression of CIA associated with down-regulation of these inflammatory mediators (61). In addition, enhanced activation by IL-1 was observed in *Il1r2*$^{-/-}$ monocytes, and it may contribute to local T cell activation. Thus, these observations suggest that IL-1R2 regulates the development of arthritis by suppressing IL-1 activity on macrophages and monocytes.

I found that IL-1R2 is most prominently expressed in neutrophils among T cells, B cells, monocytes, BMMPs and FLSCs, consistent with a recent report (62). However, in contrast to macrophages, I did not detect any functional abnormality of *Il1r2*$^{-/-}$ neutrophils. The neutrophil content in the bone marrow was similar between WT and *Il1r2*$^{-/-}$ mice. The survival after treatment with IL-1β, IL-4, or both, did not change between WT and *Il1r2*$^{-/-}$ neutrophils. IL-6 production after treatment with IL-1α or IL-1β also did not change. ROS production was not induced by IL-1 both from WT and *Il1r2*$^{-/-}$ neutrophils. Furthermore, the content of *Il1r2*$^{-/-}$ neutrophils, monocytes, macrophages and B cells in peritoneal cavity, blood, and BM were similar to that of WT after induction of peritonitis in mixed BM chimera mice. Consistent with my notion, Prince et al. demonstrated that IL-1 is not involved in neutrophil survival, cell adhesion molecule expression and cytokine production (63). Although it was reported that IL-1 prolongs neutrophil survival (17), Prince et al. showed that neutrophils purified by percoll gradient method, that was used by the

previous report (13), were contaminated with other types of cells and neutrophils were indirectly activated by IL-1 through these contaminated cells. Regarding the reason why *Il1r2*$^{-/-}$ neutrophils are refractory to IL-1 stimulation, I first thought that this is because IL-1Ra is highly expressed in neutrophils, as shown in Fig. 2B. However, I found that this is not the case, because neutrophils from *Il1rn* and *Il1r2* double deficient mice still did not respond to IL-1 (Fig. 23). Therefore, it is conceivable that either IL-1R1 expression on cell surface is too low to respond to IL-1, or some signaling molecules are missing, or negative regulations are working in the signal transduction in neutrophils. Consistent with the first possibility, IL-1R1 expression was not detected on neutrophils, although the mRNAs for IL-1R1 and IL-1RAcP were clearly detected. Unfortunately, I also failed to detect expression of IL-1R1 on macrophages to which I could clearly observe the effects of IL-1. IL-1R1 expression on macrophages and neutrophils was not detected even after amplification using biotin-conjugated anti-PE antibody and after stimulation with GM-CSF, IFN-γ and IL-23 (Fig. 24). Because I could easily detect cell surface IL-1R1 expression on peritoneal CD62L^{-} γ/δ T cells from WT mice, but not from *Il1r1*$^{-/-}$ mice as described before (36), the expression levels of IL-1R1 on neutrophils and macrophages are much lower than that on these cells.

I found that *Il1rn*$^{-/-}$*Il1r2*$^{-/-}$ neutrophils produced higher levels of TNF than WT when cells were treated with LPS. Interestingly, *Il1rn*$^{-/-}$*Il1r2*$^{-/-}$ mice chronically suffered from skin inflammation and were severely emaciated (Ikarashi *et al*. manuscript in preparation). Therefore, I

think that *Il1rn*$^{-/-}$*Il1r2*$^{-/-}$ neutrophils are constitutively activated due to chronic inflammation in the skin, and easily produce TNF upon stimulation with LPS. Another possibility is that IL-1R2 suppresses TLR4 signaling to induce TNF in collaboration with IL-1Ra. Clearly, further investigation is needed to distinguish these possibilities and to elucidate very unique cell-type-specific IL-1R2 action mechanism.

Nonetheless, high expression of IL-1R2 in neutrophils may have some physiological and/or pathological roles. In fact, it was demonstrated that neutrophils scavenge IL-1β through IL-1R2 (64) and both human and mouse neutrophils cleave IL-1R2 to release extracellular domain of IL-1R2 (62, 65). Because a IL-1R2-expressing T cell line can neutralize IL-1 activity through IL-1R2-mediated internalization of IL-1β, but less efficiently through binding of soluble IL-1R2 to IL-1 (66), I examined the IL-1 neutralizing capacity of neutrophils in two models. Co-culture of WT or *Il1r2*$^{-/-}$ neutrophils with *Il1r2*$^{-/-}$ macrophages did not affect IL-1β-induced IL-6 production in macrophages (Fig. 25). Furthermore, preincubation of 2×10^6 neutrophils with 5 pg/ml IL-1β failed to inactivate the IL-1β activity, although 10^4 IL-1R2-transfected T cells neutralized 10 pg/ml IL-1β in the previous report (66) (Fig. 26). More improved co-culture condition may need to solve this problem. Neutrophil specific *Il1r2* deficient mice may help us to elucidate the roles of IL-1R2 in neutrophils.

Horai et al. previously reported that *Il1rn*$^{-/-}$ mice spontaneously develop autoimmune

arthritis on the BALB/c background (24). In contrast to *Il1rn*$^{-/-}$ mice, *Il1r2*$^{-/-}$ mice did not develop autoimmunity both on the BALB/c and C57BL/6 background. This difference between *Il1rn*$^{-/-}$ and *Il1r2*$^{-/-}$ mouse phenotypes could be explained by the difference of target cells; IL-1Ra can inhibit IL-1R1 on all cell types whereas IL-1R2 can only compete with IL-1R1 on macrophages. Deficient mice for other type IL-1 receptor signal regulators such as ST2 and SIGIRR also do not develop arthritis (67, 68). These observations suggest that IL-1Ra has the strongest inhibitory activity among endogenous IL-1 inhibitors.

In summary, I showed that IL-1R2 plays a regulatory role in the progression of collagen-induced arthritis through the inhibition of IL-1 action on macrophages. This inhibitory action of IL-1R2 is strictly cell-type specific, unlike IL-1Ra. These observations may provide a clue to use IL-1R2 for the treatment of inflammatory diseases.

III-6. Figures

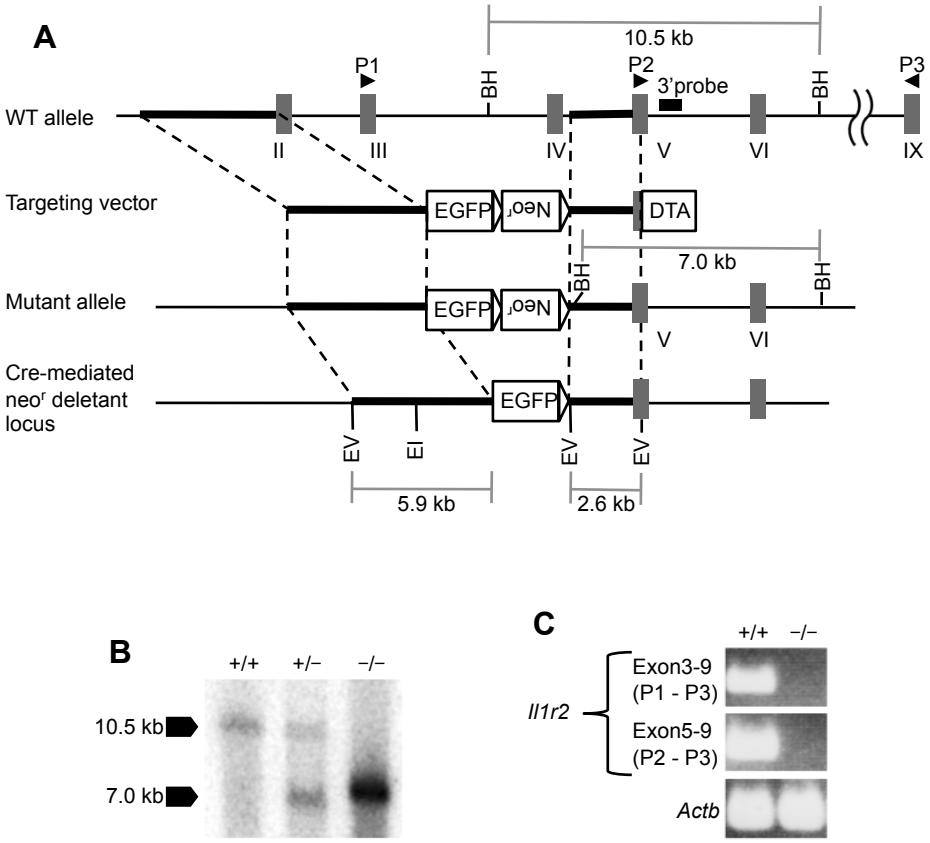

FIGURE 4. Generation of *Il1r2*$^{-/-}$ mice.
(A) Structure of the mouse *Il1r2* locus (WT locus), the IL-1R2 targeting construct (Targeting vector), and the predicted mutated gene before (Mutant locus) and after neomycin resistance gene (neo^r) deletion (Cre-mediated neo^r deletant locus). Bold lines indicate arms used for homologous recombination. Gray boxes with roman numbers represent the exons of the *Il1r2* gene and its number, respectively. Exon 2, 3 and 4 of the *Il1r2* gene were replaced with the *EGFP* gene and the loxP flanked *neo*^{r} gene. A *DTA* gene was bound to the 3′ end of the targeting vector for negative selection. (B) Southern blot analysis of the ES cells. The WT (10.5 kb) and targeted band (7.0 kb) were detected in Southern blot analysis using the BamHI (BH) digested DNA from ES cells and a 3'probe shown in (A). (C) RT-PCR analysis of the *Il1r2* mRNA from bone marrow cells of WT and *Il1r2*$^{-/-}$ mice. Arrowheads, P1-3, in (A) indicate positions of PCR primers.

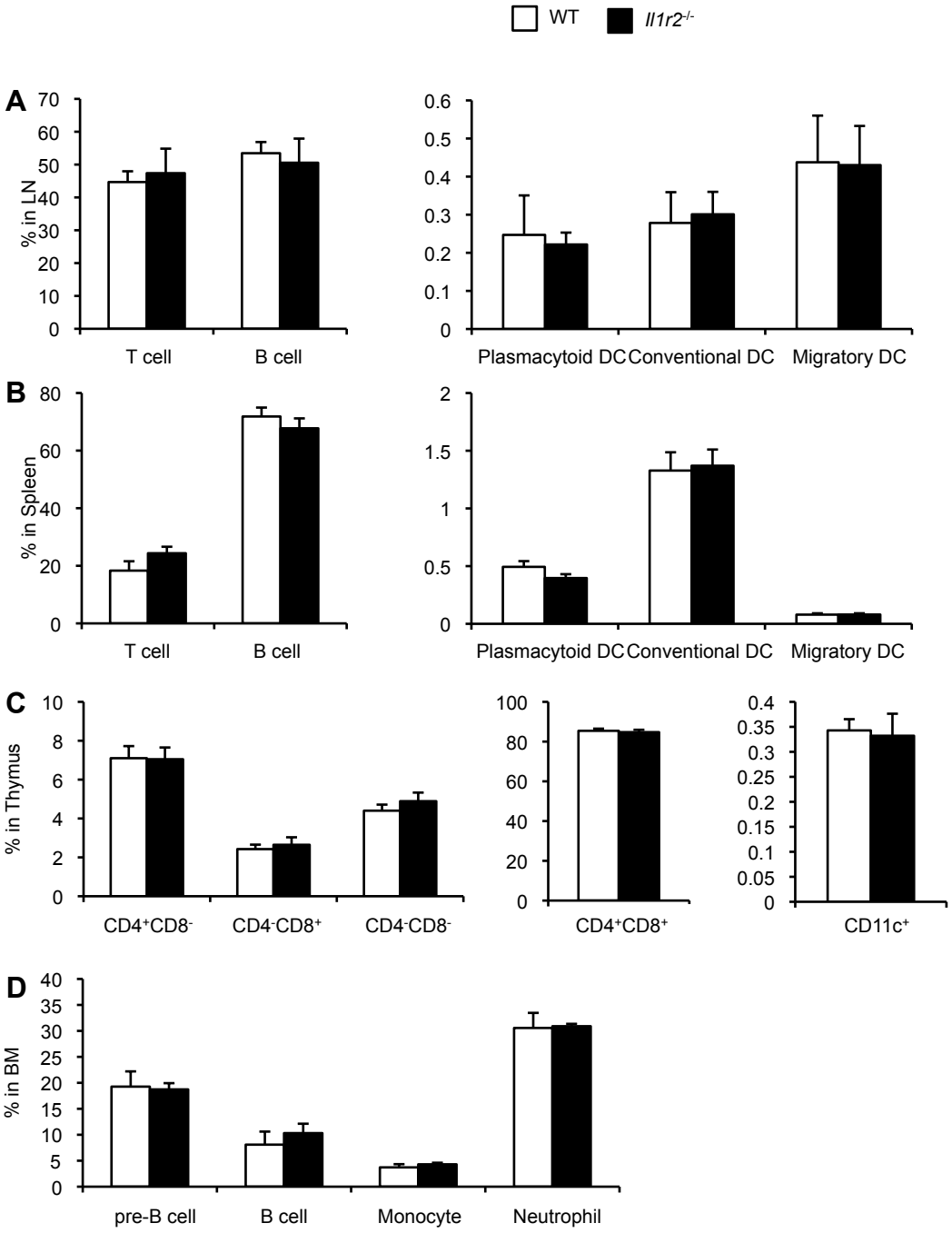

FIGURE 5. Normal leukocyte population in immune organs.
(A) LN cells and (B) spleen cells from WT or *Il1r2*$^{-/-}$ mice (n=5 each) were analyzed for the populations of T cells (CD3^{+}B220^{-}), B cells (CD19^{+}B220^{-}), plasmacytoid DC (CD3^{-}CD19^{-}B220^{+}CD11c^{int}, conventional DC (CD3^{-}CD19^{-}B220^{-}CD11c^{high}CD40^{int}) and migratory DC (CD3^{-}CD19^{-}B220^{-}CD11c^{int}CD40^{high}). (C) Thymocytes from WT or *Il1r2*$^{-/-}$ mice (n=6 each) were analyzed for the populations of CD4^{+}CD8^{-}, CD4^{-}CD8^{+}, CD4^{-}CD8^{-}, CD4^{+}CD8^{+} and CD11c^{+}. (D) Bone marrow cells from WT or *Il1r2*$^{-/-}$ mice (n=3 each) were analyzed for the populations of pre-B cell (CD117^{-}B220^{int}), B cell (CD117^{-}B220^{high}), Monocyte (CD117^{-}CD11b^{+}Ly6C^{high}Ly6G^{-}) and Neutrophil (CD117^{-}CD11b^{+}Ly6C^{int}Ly6G^{+}). Data are the mean ± s.d.

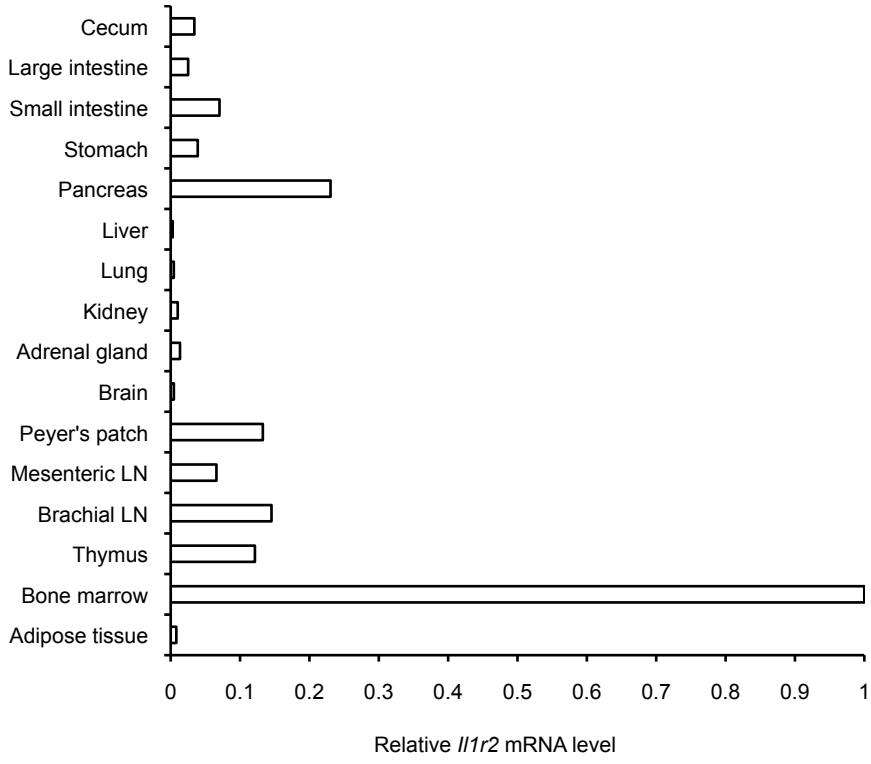

FIGURE 6. Tissue specificity of *Il1r2* mRNA expression.
Il1r2 mRNA expression was determined by quantitative PCR in tissues from WT mice.

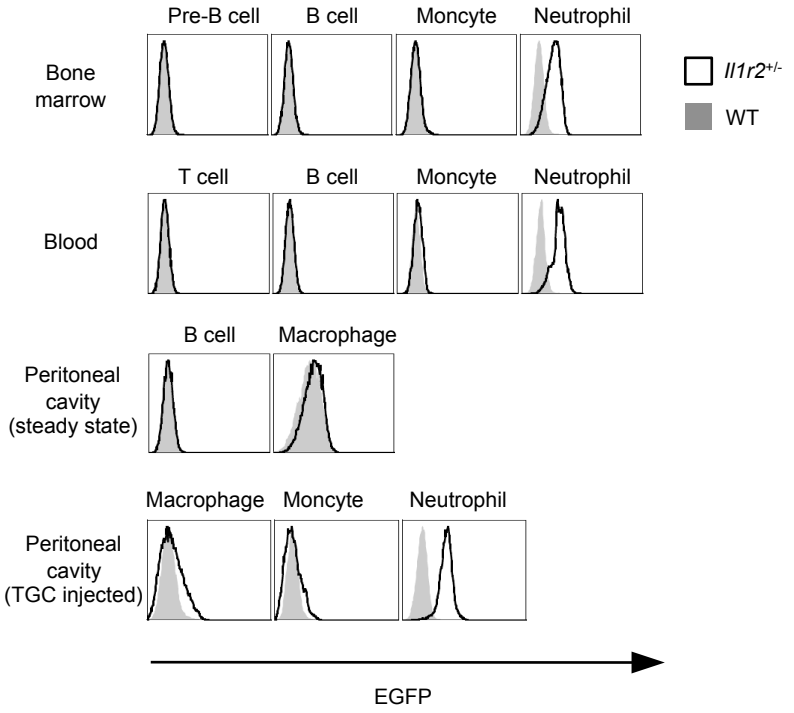

FIGURE 7. EGFP expression in various cell types.
EGFP expression in pre-B cells, B cells, T cells, monocytes, macrophages, and neutrophils from bone marrow, blood and peritoneal cavity of WT (shaded histograms) and *Il1r2*$^{+/-}$ (open histograms) mice was analyzed by flow cytometry. Peritoneal B cells, macrophages, monocytes, and neutrophils were collected before and after induction of peritonitis with TGC.

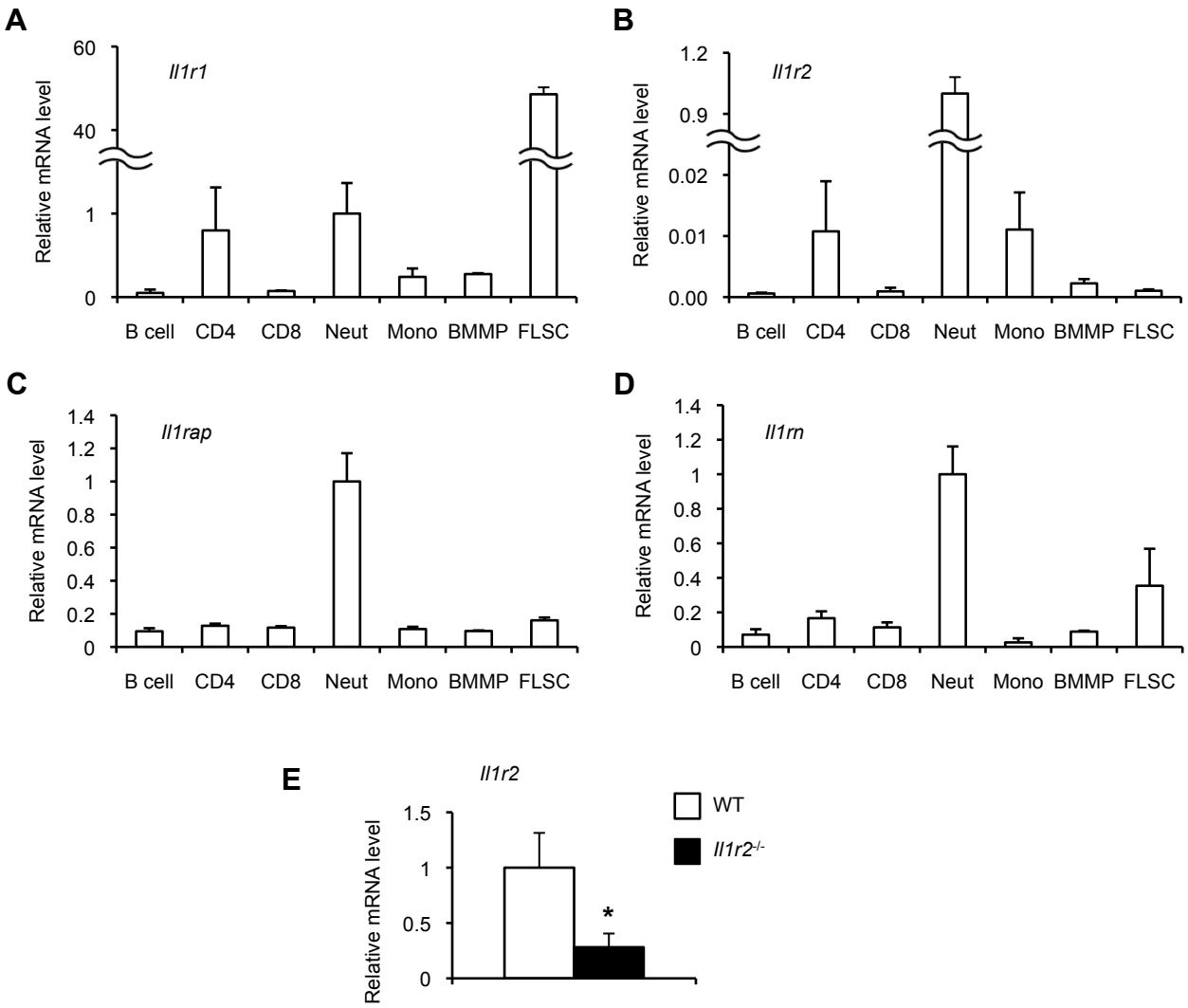

FIGURE 8. IL-1 family gene expression in various cell types. (A-D) The expression of *Il1r1*, *Il1r2*, *Il1rap* and *Il1rn* mRNA was analyzed by quantitative PCR in different types of cells from WT mice. The content of mRNA was normalized to the amount of *Hprt* mRNA. (E) The expression of *Il1r2* mRNA was analyzed by quantitative PCR in BMMPs from WT and *Il1r2*$^{-/-}$ mice. Data are the mean ± s.d. of triplicates and are representative of two independent experiments. **P* < 0.05 by the two-tailed unpaired student's *t*-test.

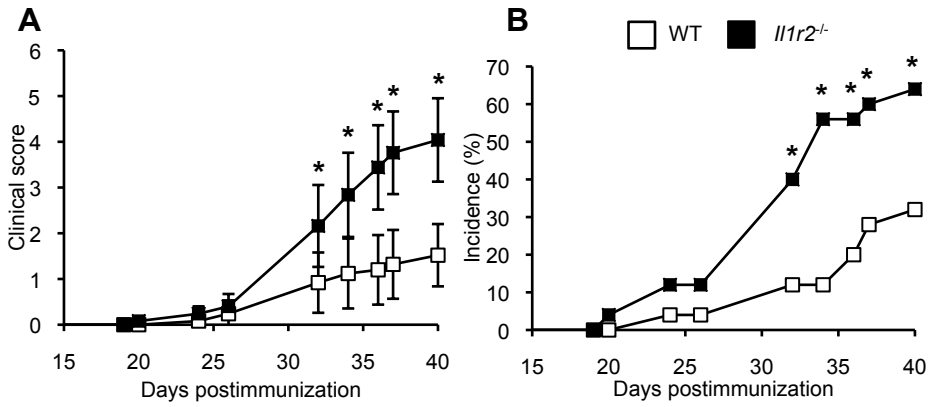

FIGURE 9. Development of CIA is exacerbated in *Il1r2*$^{-/-}$ mice. (A, B) WT mice (n=25) and *Il1r2*$^{-/-}$ mice (n=25) were immunized with 400 mg chicken IIC emulsified with CFA intradermally at two different sites on each hind flank on day 0 and 20. Clinical score (A) and incidence (B) of arthritis are shown. Data are the mean ± s.e.m. Data are combined from three independent experiments with similar results (A and B). *$P < 0.05$ by the Mann-Whitney *U*-test (A) or χ^2 test (B).

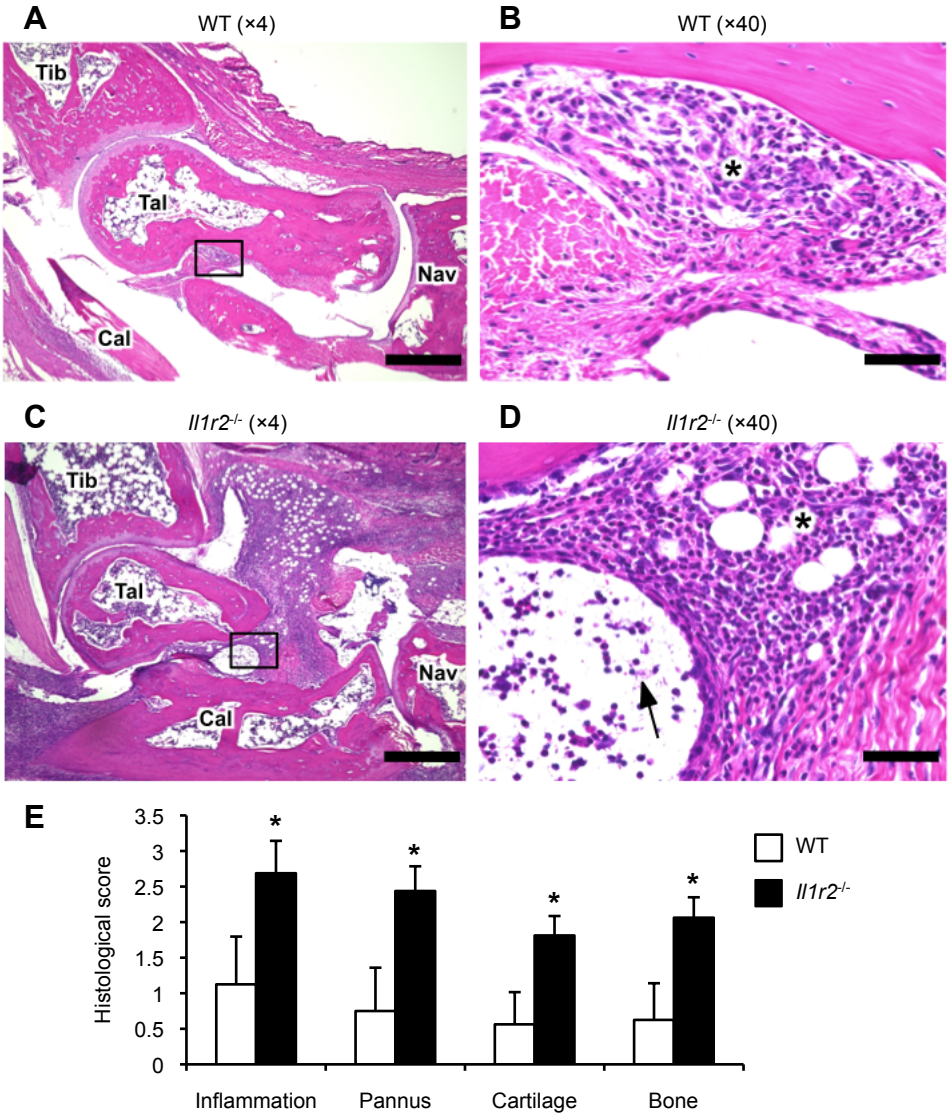

FIGURE 10. Histological analysis of inflamed joint
(A-D) Representative sections of the hind limbs of WT (A and B) and *Il1r2*$^{-/-}$ (C and D) mice at day 40 after immunization were stained with hematoxylin and eosin. Tib, tibia; Tal, talus; Cal, calcaneus; Nav, navicular. The asterisks denote synovitis and the arrow indicates joint exudate. Images are magnified ×4 (A and C) and ×40 (B and D, square frames in A and C respectively). Scale bars are 500 mm (A and C) and 50 mm (B and D). (E) Four histological parameters, including inflammation, pannus formation, cartilage destruction, and bone damage, were assessed from sections of WT mice (n=16) and *Il1r2*$^{-/-}$ mice (n=16). Data are the mean ± s.e.m. Data are combined from two independent experiments with similar results (E). *$P < 0.05$ by the Mann-Whitney *U*-test (E).

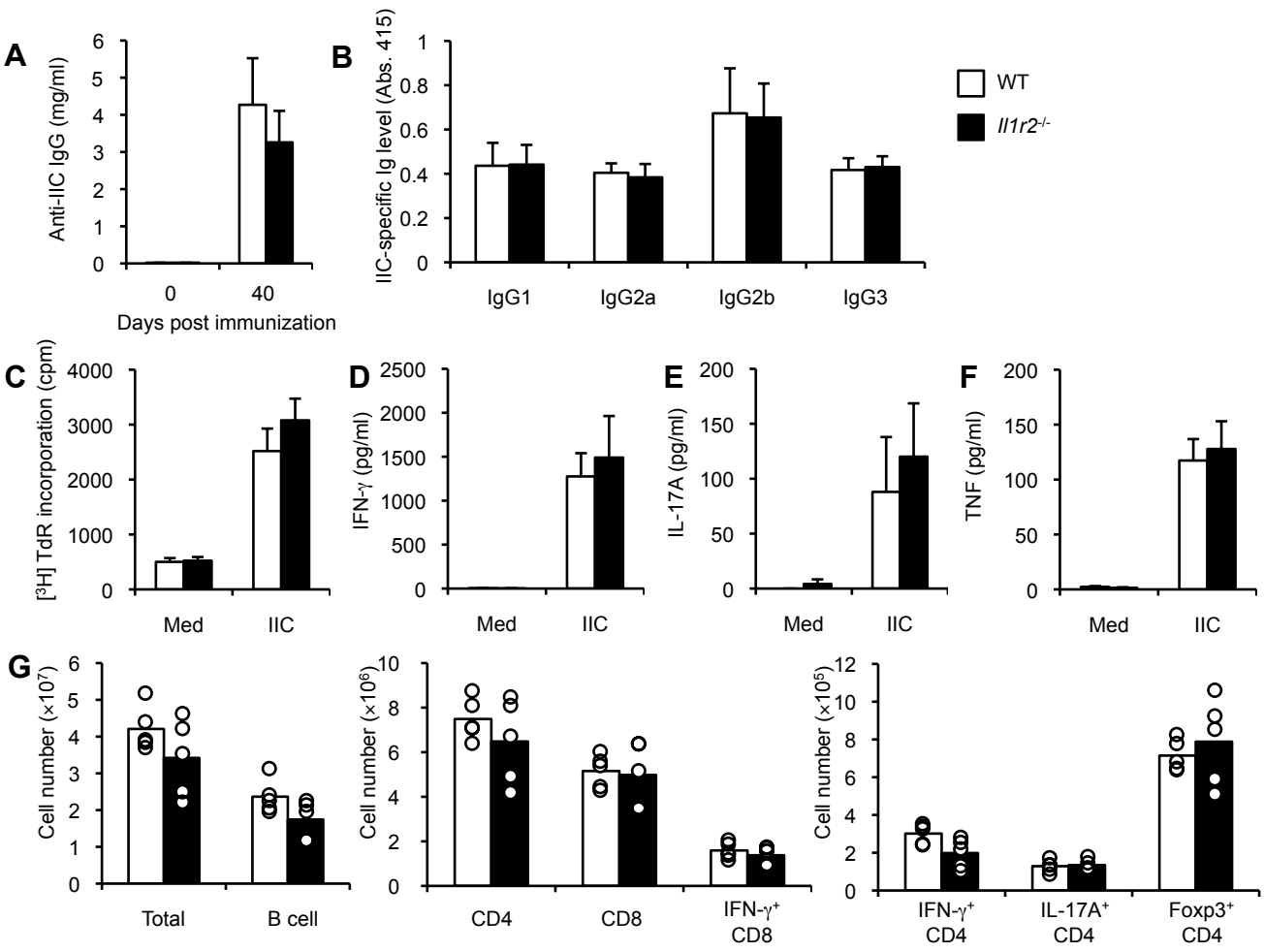

FIGURE 11. Antibody production and T cell responses are normal in *Il1r2*$^{-/-}$ mice upon induction of CIA .

(A and B) Anti-IIC antibody titer in sera. Sera of WT mice (n=8) and *Il1r2*$^{-/-}$ mice (n=8) were collected after induction of CIA, and anti-IIC IgG levels were measured by ELISA. (C-F) Inguinal LNs were isolated on the day 7 from IIC immunized WT mice (n=4) and *Il1r2*$^{-/-}$ mice (n=3). Single cells were prepared and incubated for 72 h in the absence or presence of IIC. T cell proliferative response was determined by [^{3}H] thymidine (TdR) incorporation (C). Concentrations of IFN-g (D), IL-17 (E) and TNF (F) in the culture supernatant were measured by ELISA. (G) Cell numbers of the indicated T cell and B cell subsets in inguinal LNs were determined by flow cytometry on day 7 after immunization. WT mice (n=5) and *Il1r2*$^{-/-}$ mice (n=5). Each circles represent individual mice. Data are the mean ± s.d. (A-F) of each group and are representative of two (A and G) or five (C-F) independent experiments.

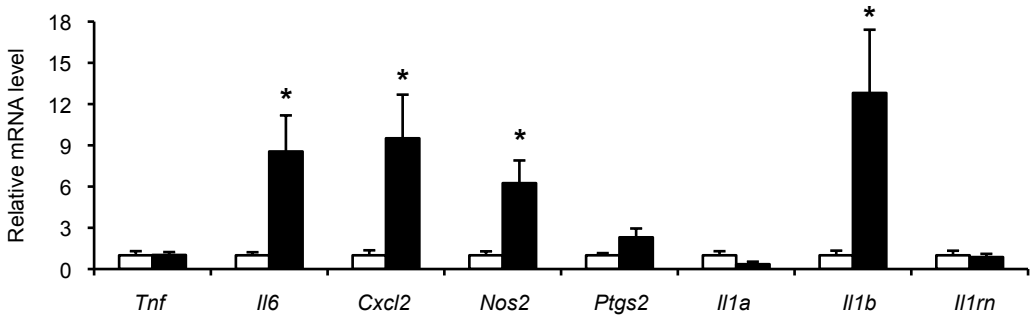

FIGURE 12. Inflammatory mediator production is enhanced in *Il1r2*$^{-/-}$ mice upon induction of CIA.
The mRNA levels of inflammatory mediators. RNA was purified from paws of WT mice (n=8) and *Il1r2*$^{-/-}$ mice (n=9) on the day 40 after CIA induction, and mRNA levels were determined by quantitative PCR. Data are the mean ± s.e.m. of each group and are representative of two independent experiments. *$P < 0.05$ by the two-tailed unpaired student's *t*-test.

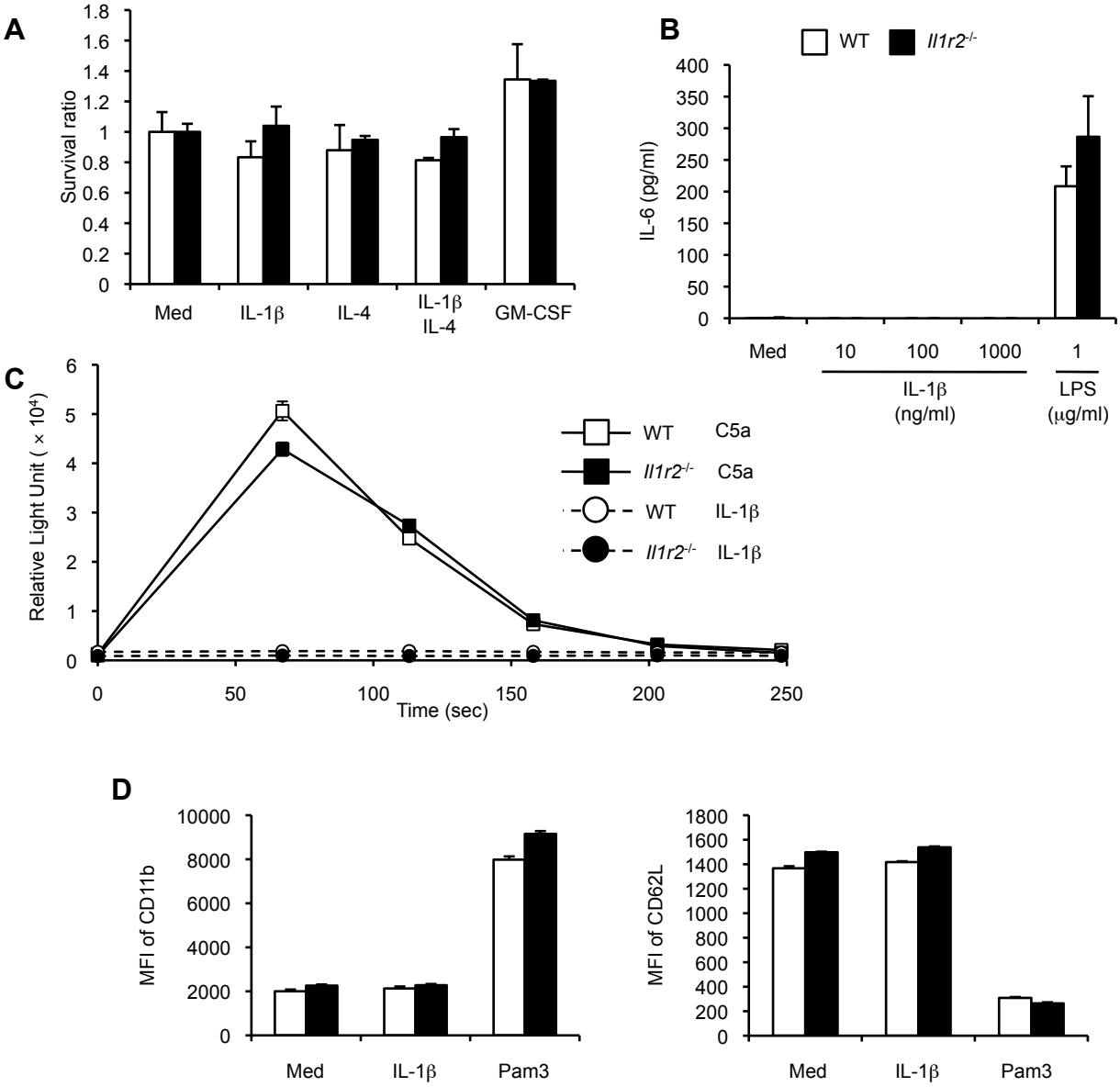

FIGURE 13. The response of *Il1r2*$^{-/-}$ neutrophils to IL-1 is normal *in vitro*. (A-C) Neutrophils from WT and *Il1r2*$^{-/-}$ mice were treated with indicated cytokines (10 ng/ml) and survival ratio was measured by flow cytometry after 48 h culture (A). IL-6 production was measured by ELISA at 20 h after treatment with IL-1β or LPS (B). ROS generation was measured as chemiluminescence by the luminometer at indicated time points after IL-1β or C5a stimulation (C). CD11b and CD40 expression was examined by flowcytometry 15 h after treatment with IL-1β or Pam3CSK4. Data are the mean ± s.d. of triplicates and are representative of two (A, C and D) or four (B) independent experiments.

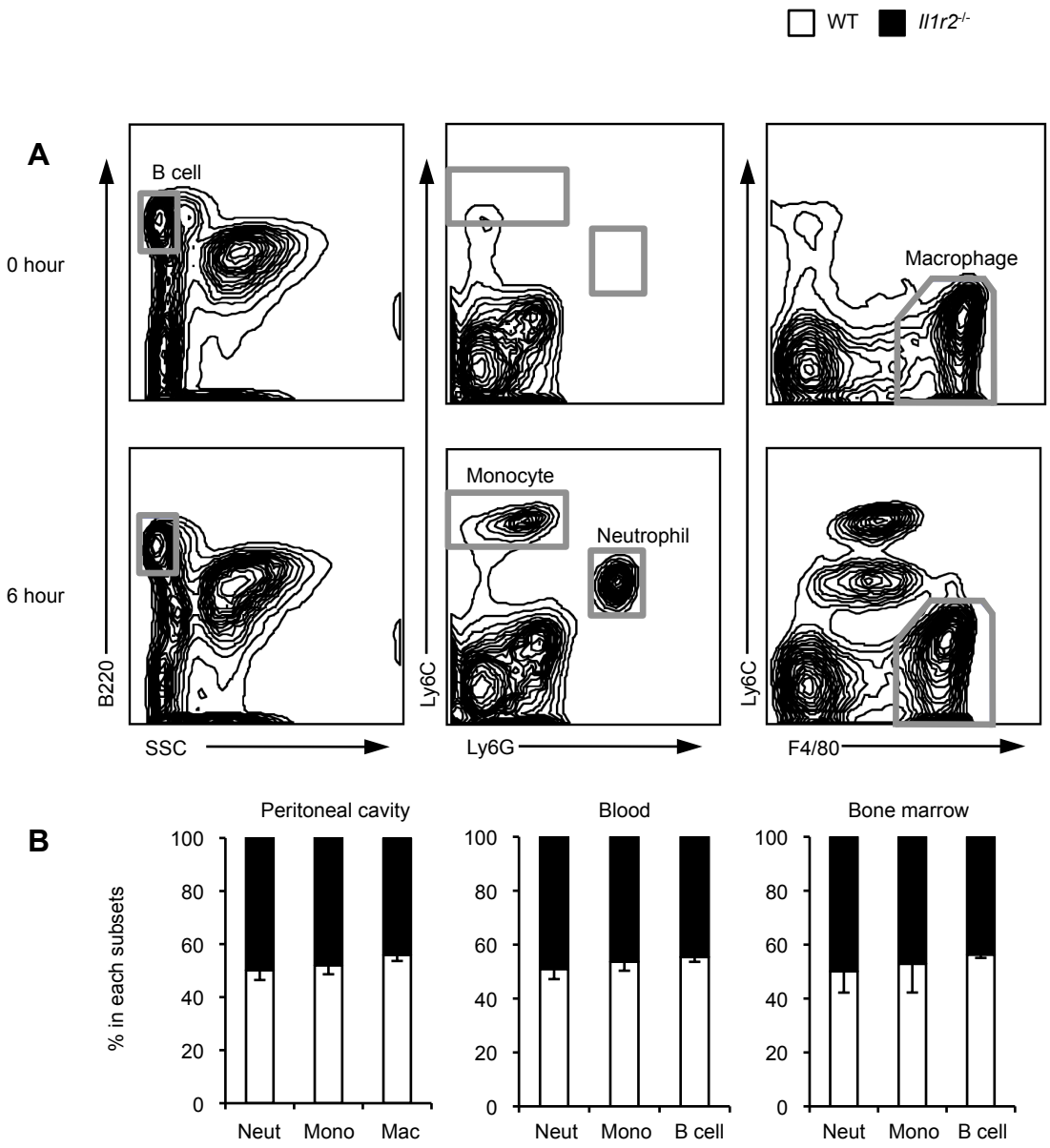

FIGURE 14. Normal *Il1r2*$^{-/-}$ neutrophil accumulation during peritonitis. A mixture of CD45.1^{+} WT and CD45.2^{+} *Il1r2*$^{-/-}$ BM cells were transferred into irradiated *Rag2*$^{-/-}$ mice and these BM chimeras were injected by IL-1a to induce peritonitis. After 6 h, neutrophil and monocyte infiltration into the peritoneal cavity were examined (A). The content of neutrophils (Neut), Monocytes (Mono), macrophages (Mac) and B cells of each genotype was determined by allelic forms of CD45 antigen in the peritoneal cavity and BM (B). Data are the mean ± s.d. of four mice, and are representative of two independent experiments.

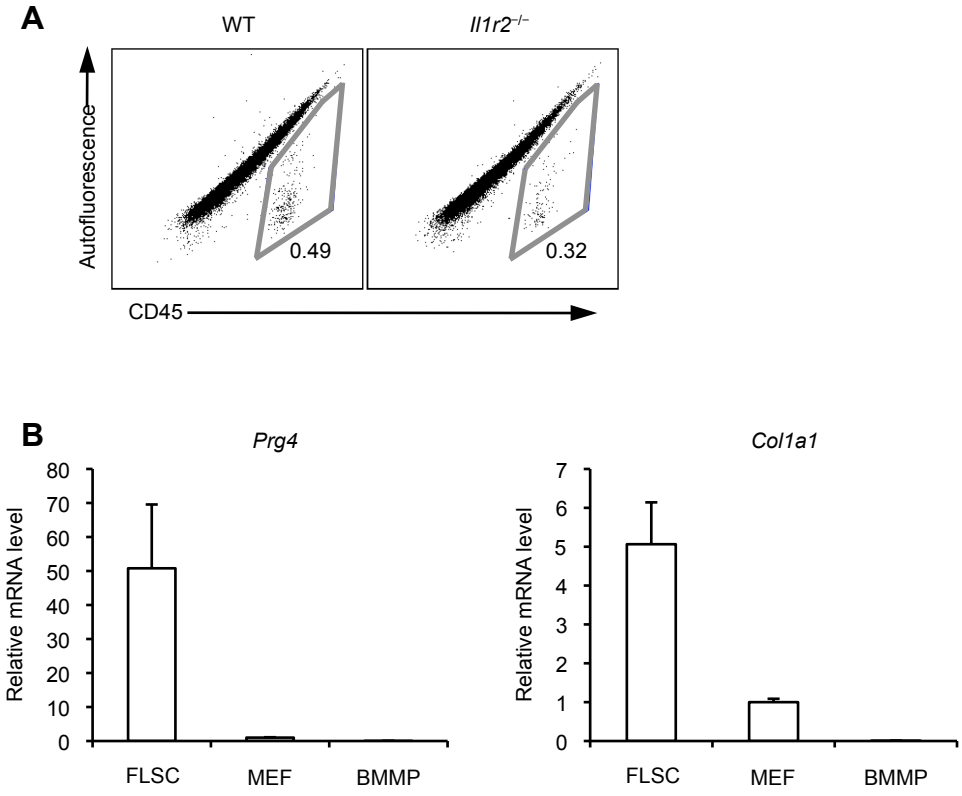

FIGURE 15. FLSC preparation.
(A) Flow cytometric analysis of FLSCs. Percentage of contaminated leukocytes in prepareted FLSC was less than 1%. (B) *Prg4* and *Col1a1* mRNA production were analyzed by quantitative PCR in FLSCs. Mouse embryonic fibroblasts (MEF) and bone marrow derived macrophages (BMMP) were used as a non-synovial fibroblast and non-fibroblast control, respectively. Data are the mean ± s.d. of triplicates.

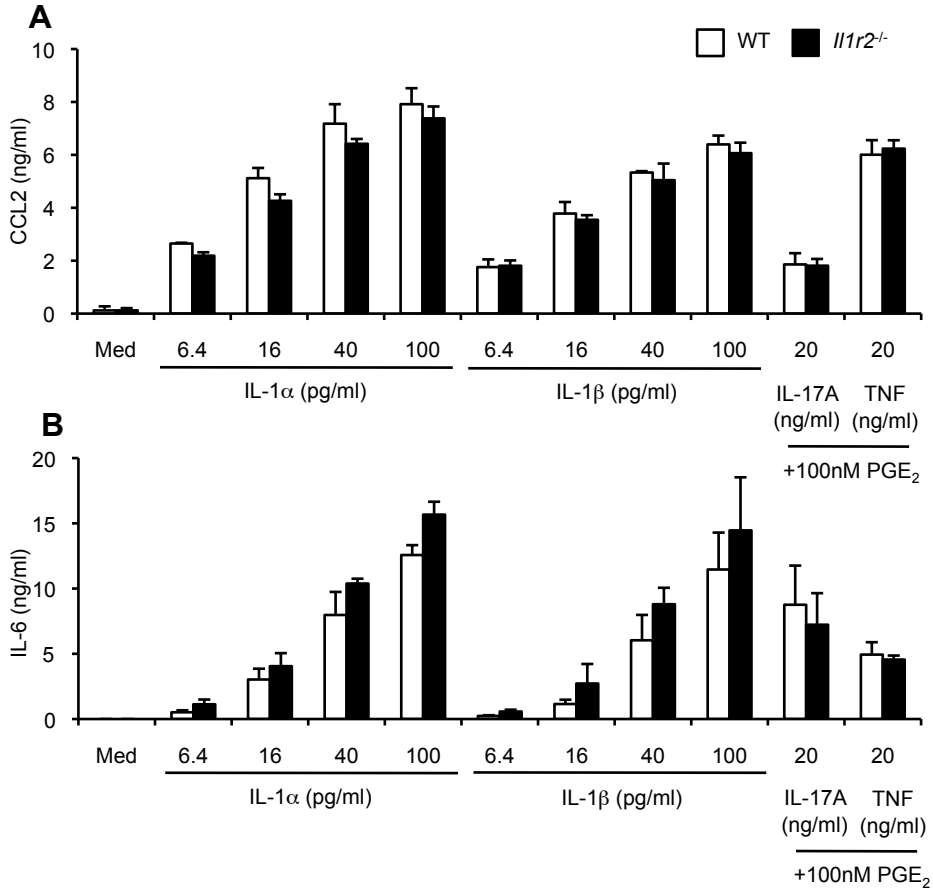

FIGURE 16. Normal inflammatory mediator production in *Il1r2*$^{-/-}$ FLSCs

(A, B) FLSCs from WT and *Il1r2*$^{-/-}$ mice were stimulated with cytokines as indicated. The concentrations of IL-6 and CCL2 in the culture supernatant were measured by ELISA. No significant difference was observed. Data are the mean ± s.d. of triplicate cultures and are representative of three independent experiments.

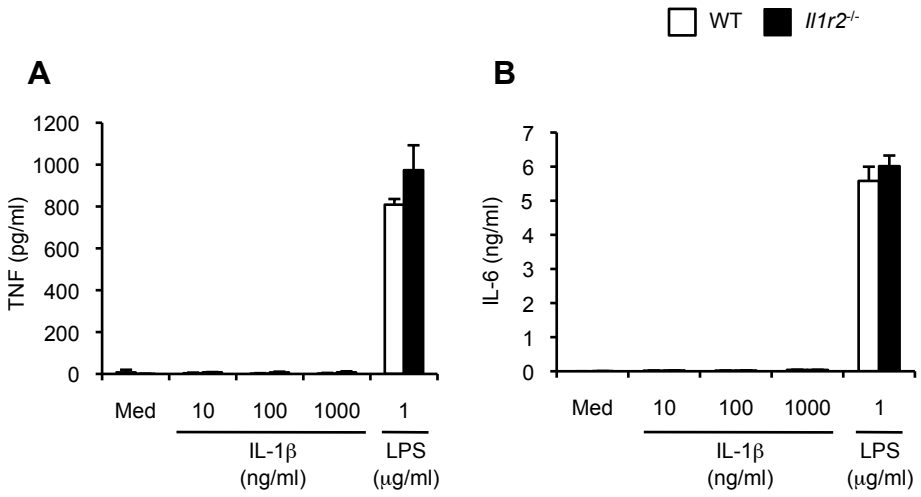

FIGURE 17. Monocytes did not produce TNF and IL-6 upon IL-1 stimulation.
Monocytes from WT and *Il1r2*$^{-/-}$ mice were stimulated with indicated concentrations of IL-1β or LPS, and the concentrations of TNF (A) and IL-6 (B) were measured by ELISA. Data are the mean ± s.d. of triplicate cultures and are representative of four independent experiments.

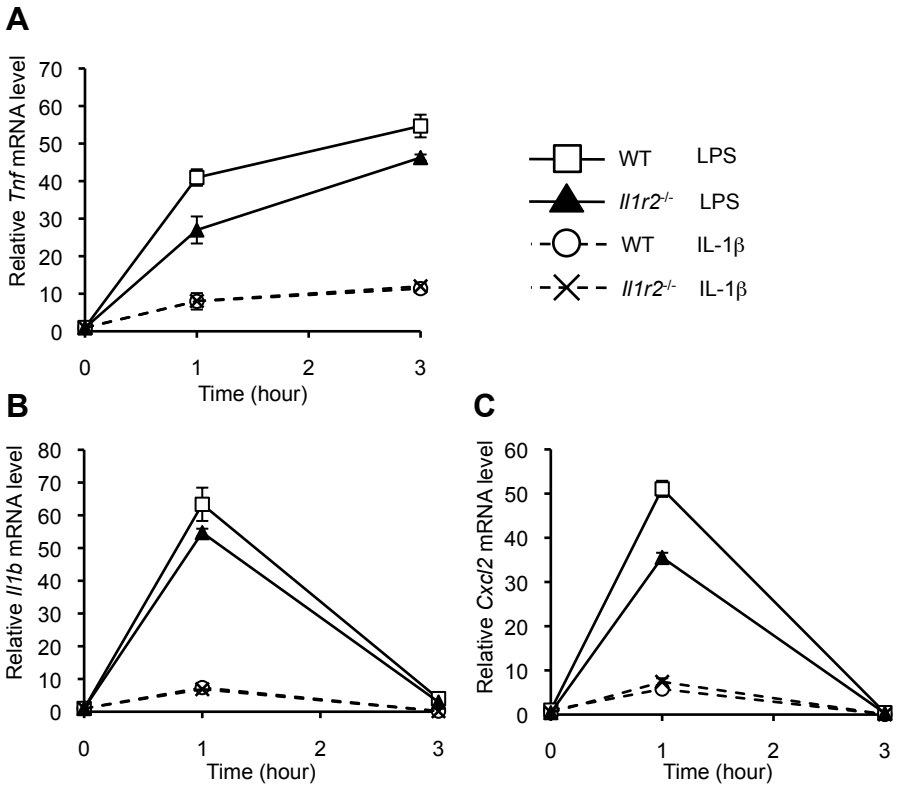

FIGURE 18. Normal mRNA induction of inflammatory mediator in *Il1r2*$^{-/-}$ monocytes.
Monocytes from WT and *Il1r2*$^{-/-}$ mice were stimulated with 100 ng/ml of IL-1β or 1 μg/ml of LPS, and the mRNA level of *Tnf* (A), *Il1b* (B) and *Cxcl2* (C) were measured by qPCR. Data are the mean ± s.d. of triplicate.

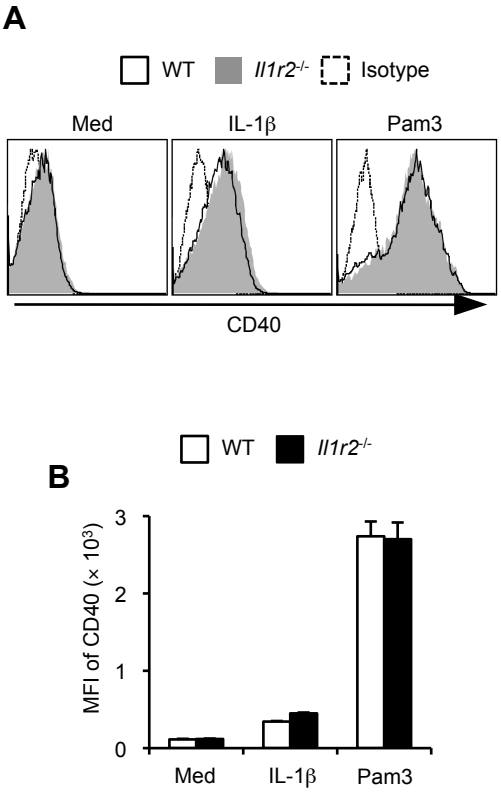

FIGURE 19. Normal CD40 expression of *Il1r2*$^{-/-}$ monocytes upon IL-1 stimulation.
Monocytes from WT and *Il1r2*$^{-/-}$ mice were stimulated with 100 ng/ml of IL-1β or 1 μg/ml of Pam3CSK4 (Pam3), and the surface CD40 expression was analyzed by flow cytometry. Representative histogram and the MFI levels of CD40 are shown in (A) and (B), respectively. Data are the mean ± s.d. of triplicate cultures and are representative of two independent experiments. *$P < 0.05$ by the two-tailed unpaired student's *t*-test.

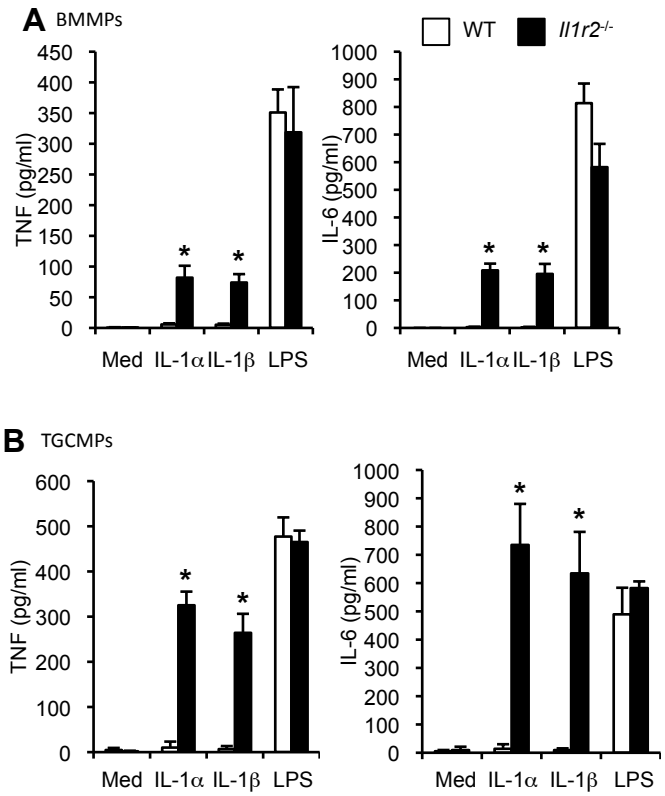

FIGURE 20. TNF and IL-6 production is increased in *Il1r2*$^{-/-}$ macrophages. BMMPs (A) and TGCMPs (B) from WT and *Il1r2*$^{-/-}$ mice were stimulated with either 10 ng/ml IL-1α, 10 ng/ml IL-1β or 1 ng/ml LPS, and the concentrations of TNF and IL-6 in the culture supernatant were measured by ELISA. Data are the mean ± s.d. of triplicates and are representative of two (A) independent experiments. *$P < 0.05$ by the two-tailed unpaired student's *t*-test.

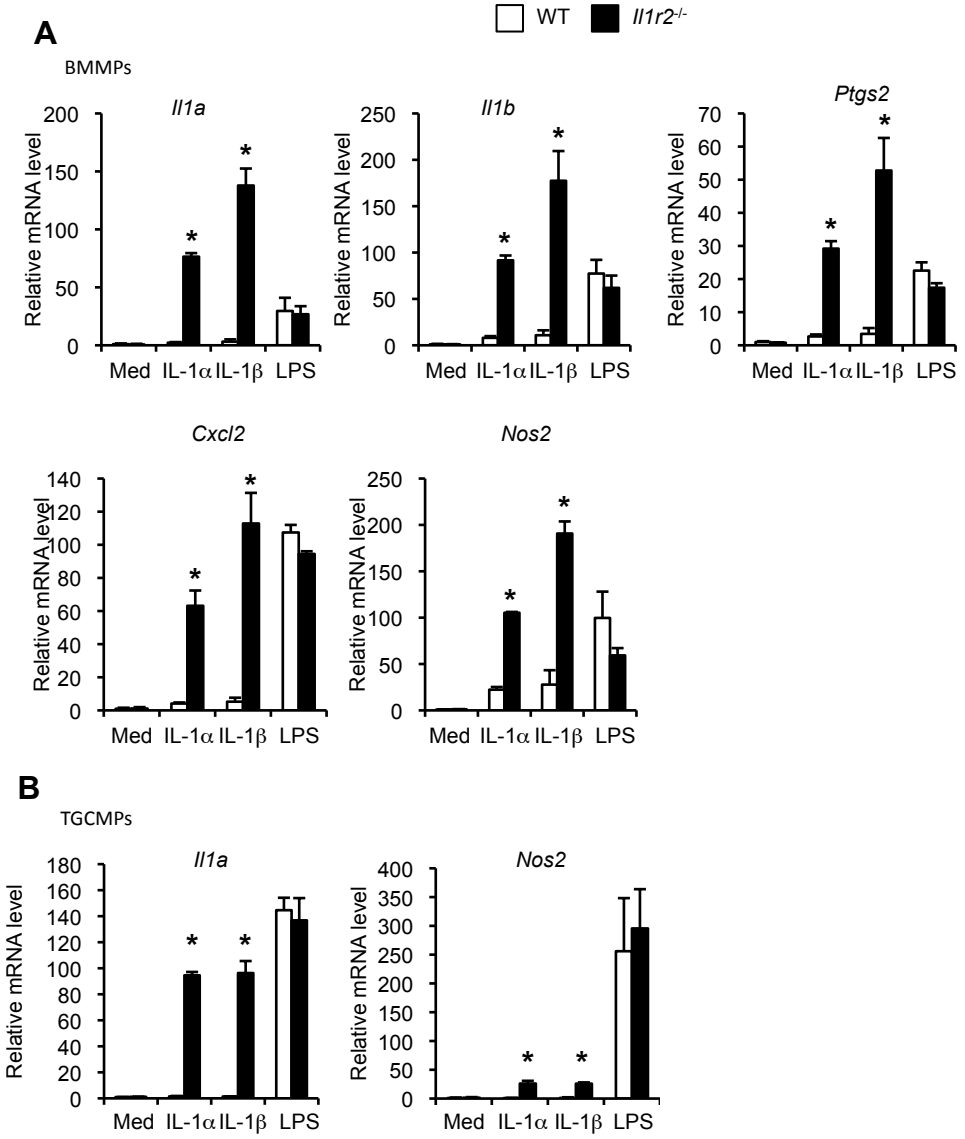

FIGURE 21. Inflammatory mediator production is increased in *Il1r2*$^{-/-}$ macrophages.
BMMPs (A) and TGCMPs (B) from WT and *Il1r2*$^{-/-}$ mice were stimulated with either 10 ng/ml IL-1α, 10 ng/ml IL-1β or 1 ng/ml LPS, and the mRNA levels of *Il1a, Il1b, Cxcl2, Nos2*, and *Ptgs2* gene were determined by quantitative PCR. Data are the mean ± s.d. of triplicates and are representative of two (A) independent experiments. *$P < 0.05$ by the two-tailed unpaired student's *t*-test.

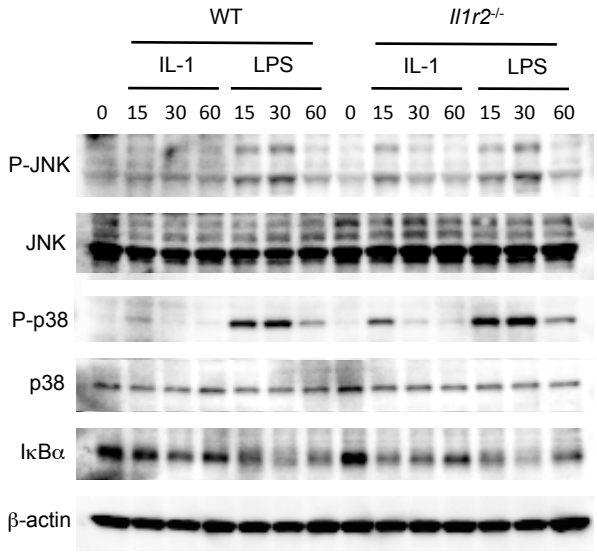

FIGURE 22. IL-1 signal is enhanced in *Il1r2*$^{-/-}$ macrophages. Phosphorylation of JNK and p38 as well as degradation of IκBα were examined by western blotting analysis with WT and *Il1r2*$^{-/-}$ BMMPs 0, 15, 30, and 60 min after stimulation with IL-1 or LPS.

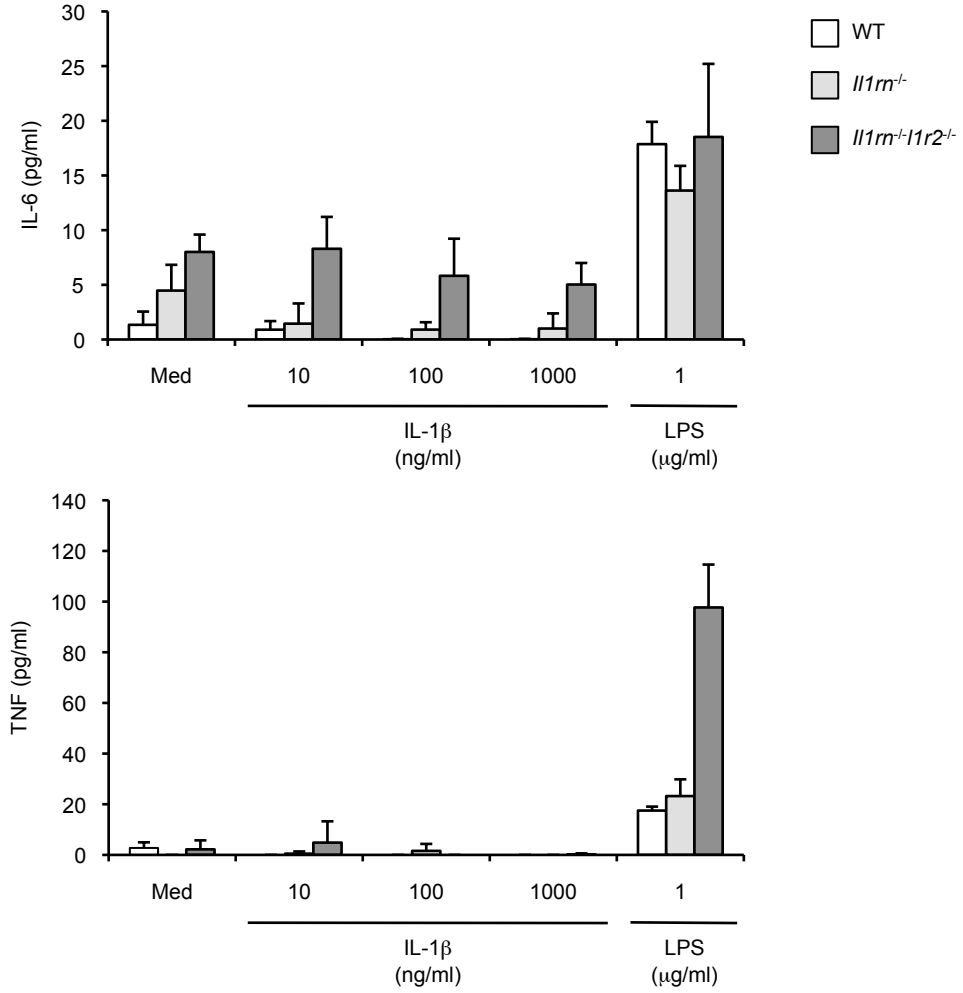

FIGURE 23. *Il1rn*$^{-/-}$*Il1r2*$^{-/-}$ neutrophils do not respond to IL-1. Neutrophils from WT, *Il1rn*$^{-/-}$ and *Il1rn*$^{-/-}$*Il1r2*$^{-/-}$ mice were treated with indicated stimuli. IL-6 and TNF production were measured by ELISA at 20 h after treatment. Data are the mean ± s.d. of triplicates.

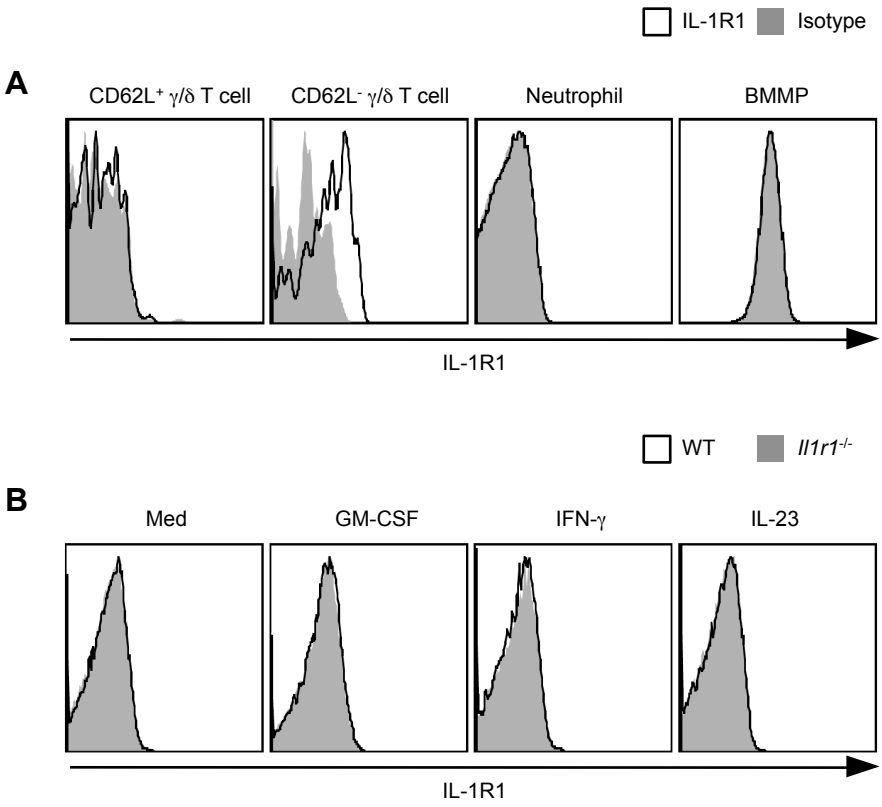

FIGURE 24. IL-1R1 expression is not detected on neutrophil surface. (A) γ/δ T cells were collected from peritoneal cavity and gated on γ/δ TCR^+CD62L^+ or γ/δ TCR^+CD62L^-. Neutrophils were collected from bone marrow and gated on $Ly6C^{int}Ly6G^+$. BMMP were differentiated from BMC and gated on $F4/80^+$. These cells were stained with PE-conjugated anti-IL-1R1 antibody or isotype control, followed by biotin-conjugated anti-PE antibody and PE-conjugated streptavidin for enhancement of fluorescence intensity. (B) BMCs were stimulated with 10 ng/ml GM-CSF, 20 ng/ml IFN-g or 10 ng/ml IL-23 for 24 h. Then, cells were prepared for FCM. Histograms show IL-1R1 expression in neutrophils gated on $Ly6G^+$.

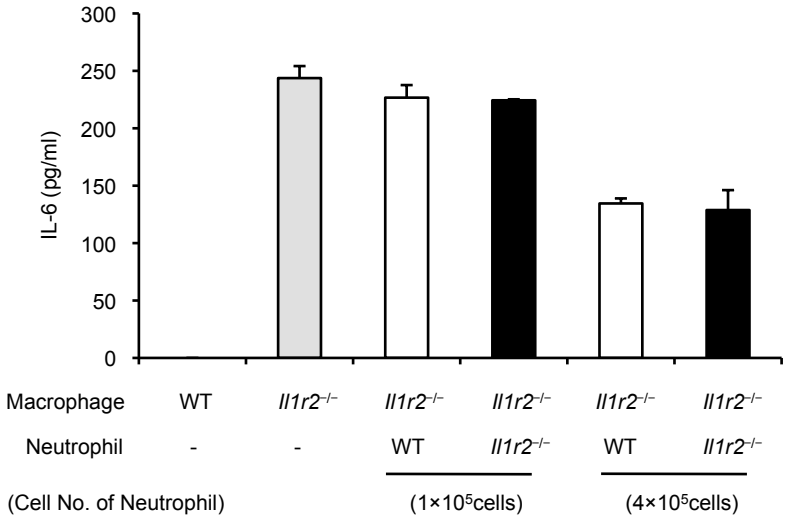

FIGURE 25. IL-1R2 expressed by neutrophils does not compete with IL-1R1 on macrophages in trans.
BMMPs were co-cultured with indicated number of neutrophils and stimulated with 10 ng/ml IL-1β. The levels of IL-6 in supernatant were measured by ELISA. Data are the mean ± s.d. of triplicates.

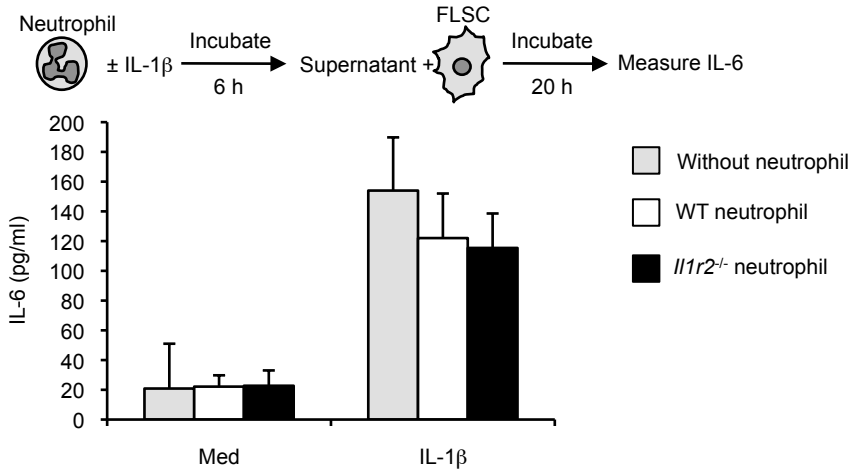

FIGURE 26. Neutrophils do not neutralize IL-1 activity. Neutrophils (2 x 10^6) were cultured with 5 pg/ml IL-1β for 6 h. Then, the supernatant was collected for subsequent stimulation of FLSCs. The levels of IL-6 in supernatant were measured by ELISA. Data are the mean ± s.d. of triplicates.

IV

Interleukin-1 receptor type 2 as a new Th17 differentiation regulator

IV-1. Abstract

Th17 differentiation is regulated by various cell intrinsic and extrinsic mechanisms. IL-1 is one of such factors, which promote Th17 differentiation. In this study, I investigated the roles of IL-1R2 in Th17 differentiation, since Th17 expresses IL-1R2. Contrary to my prospect, Th17 differentiation was impaired in *Il1r2*$^{-/-}$ T cells. The same result was observed, even when IL-1 signal was cancelled by IL-1Ra. On the other hands, differentiation of Th1, Th2 and Treg was normal in *Il1r2*$^{-/-}$ T cells. Several reports showed that intracellular IL-1R2 controls transcription in collaboration with IL-1α. *Il1a*$^{-/-}$ T cells also had less Th17 differentiation capacity. *Rorc* and *Ifr4* expression were normal in *Il1r2*$^{-/-}$ T cells during Th17 differentiation, suggesting direct *Il17a* transcription control by IL-1α/IL-1R2. I tried to examine Th17 differentiation in *Il1r2*$^{-/-}$ and *Il1a*$^{-/-}$ T cells *in vivo*. However, normal Th17 differentiation was observed in experimental autoimmune encephalomyelitis (EAE)-induced mice. Thus, although IL-1R2 and IL-1α clearly control Th17 differentiation *in vitro*, the molecular mechanisms and *in vivo* functions remain to be elucidated.

IV-2. Introduction

Differentiation of Th17

Helper T cells are classified into Th1, Th2, Th17 and Treg by cytokine, surface marker and transcription factor what they express (69). Th1 cells secrete IFNγ to promote cellular immunity. Th2 cells secrete IL-4 to promote humoral immunity. Treg cells secrete IL-10 and expresses CTLA-4 to suppress immune response. Th17 derived cytokines, such as IL-17A, IL-17F, IL-21 and IL-22, play important roles in host defense against bacteria and fungi, and also in development of inflammatory diseases (70). Mechanisms of Th17 differentiation have been energetically investigated. $CD4^+$ T cells differentiate into Th17 cells under TGFβ and IL-6/IL-21 stimulation in both mouse (71-75) and human (76-78). On the other hands, IL-1 (79), IL-7 (80) and IL-23 (81) promote maintenance, but not commitment, of Th17. Many transcription factor are involved in Th17 differentiation (82). RORγ and its splicing variant RORγt are recognized as master regulator of Th17 (83). In addition, STAT3 (84), IRF4 (85), RORα (86), AHR (87-90), IκBζ (91), Batf (92), c-Rel, RelA/p65 (93), RUNX1 (94) and HIF-1α (95) are essential, but not sufficient, for Th17 differentiation. In contrast, Foxp3 (96), STAT5 (97), T-bet (98), IRF8 (99), NFIL3 (100) and Gfi1 (101) negatively control Th17 differentiation.

Experimental autoimmune encephalomyelitis (EAE)

Multiple sclerosis (MS) is an autoimmune disease affecting approximately 0.1% of people in North Europe, North America and South Australia, but 0.04% people in Asia and Africa. MS is characterized by chronic inflammation of central nervous systems accompanied by demyelination that causes multiple neurological disorders. EAE is the most widely used mouse model for MS. To induce EAE, mice are immunized with peptides of myelin oligodendrocyte glycoprotein (MOG), which is a component of myelin (102). In these mice, MOG-specific T cells differentiate into Th17 cells, which express chemokine receptor CCR6 in the higher level than other T cell subsets. These Th17 cells migrate into spinal cord and brain through the fifth lumbar spinal cord, where CCL20, the ligand for CCR6, is highly expressed (103). Migrated Th17 cells recognize self-MOG to induce inflammation, which causes the demyelination in spinal cord and brain.

Intracellular function of IL-1α

IL-1α localizes in nuclei and its localization depends on nuclear localization sequence (NLS) in its N-terminal region (104). Many studies suggest IL-1R1 independent intracellular function of IL-1α (105). Maier et al. found that overexpression of IL-1α in human endothelial cell line resulted in impaired proliferation as well as enhanced PAI-1 and collagenase expression (106). These results were not observed when C-terminal region of IL-1α was overexpressed, although C-terminal region of IL-1α is sufficient to induce IL-1 signal through IL-1R1. Moreover, addition of IL-1Ra could not

cancel the effect of IL-1α overexpression, suggesting that IL-1α controls proliferation and gene expression in IL-1R1 independent manner. Although IL-1α itself does not have DNA binding domain, IL-1α fused to DNA binding domain of GAL4 can activate transcription (107). N-terminal region of IL-1α binds to histone acetyltransferase complex to promote transcription (108).

Intracellular function of IL-1R2

It is suggested that IL-1R2 also has intracellular roles by few reports. Kawaguchi et al. demonstrate that IL-1R2 and IL-1α co-localize in nuclei of fibroblasts from systemic sclerosis patients but not from healthy controls (109). IL-1R2 binds to C-terminal region of IL-1α. Knock down of *Il1r2* resulted in down regulation of IL-6 and procollagen type I production. Same as this report, Chang et al. show that overexpression of IL1R2 in human urothelial cell line induces mRNA transcription of IL-6 and collagen type I and knock down of IL1A cancels it (110).

Purpose of study in chapter 2

Since IL-1 maintenances Th17, I thought that IL-1R2 might suppress Th17 differentiation. From open access microarray data, I found that IL1R2 expression increases during Th17 differentiation (111). In Chapter 2, I tried to explore the roles of IL-1R2 in Th17 differentiation. Here, I show that IL-1R2 and IL-1α control Th17 differentiation at least *in vitro*.

IV-3. Materials and Methods

T cell purification

For $CD4^+$ T cells purification, pooled lymph nodes (LNs) and spleen cells were labeled with anti-mouse CD4 microbeads and sorted by auto MACS Pro Separator according to the manufacturer's directions (Miltenyi Biotec; Bergisch Gladbach, Germany).

For $CD4^+$ naïve T cells and Treg purification, pooled lymph nodes (LNs) and spleen cells were incubated with antibodies cocktail (Table 4) and then labeled with anti-biotin microbeads and biotin-labeled cell were removed by auto MACS Pro Separator. Naïve T cells ($CD4^+CD62L^+CD25^-$) and Treg ($CD4^+CD25^+$) were purified from remaining cells by flow cytometry on a MoFlo XPD IntelliSort II.

Table 4

Antigen	**Label**	**Clone**	**Source**
TER119	Biotin	TER119	BD Pharmingen
CD8α	Biotin	53-6.7	Biolegend
CD11b	Biotin	M1/70	Biolegend
CD25	Biotin	PC61	Biolegend
CD49b	Biotin	DX5	Biolegend
B220	Biotin	RA3-6B2	Biolegend
γδTCR	Biotin	GL3	BD Pharmingen
CD4	PE/Cy7	GK1.5	Biolegend
CD62L	Pacific Blue	MEL-14	Biolegend
CD25	APC	3C7	Biolegend

Helper T cell differentiation

Purified $CD4^+$ T cells or naïve $CD4^+$ T cells were cultured in the condition described in Table 5 and 6. For Th2 differentiation, naïve $CD4^+$ T cells were cultured in 1^{st} round condition for 5 d and then subcultured in fresh 2^{nd} round condition for 2 d. X-VIVO 20 medium was purchase from Lonza (Basel, Switzerland).

Table 5

	Th17	Th17	Treg
Cell	$CD4^+$	Naïve $CD4^+$	Naïve $CD4^+$
Medium	R10	X VIVO 20	X VIVO 20
Culture	3 d	5 d	5 d
αCD3 (clone 145-2C11; Biolegend)	4 μg/ml	4 μg/ml	2 μg/ml
αCD28 (clone 37.51; Biolegend)	1 μg/ml	1 μg/ml	1 μg/ml
αIFNγ (clone XMG1.2; Biolegend)	1 μg/ml	1 μg/ml	1 μg/ml
Murine IL-23 (R&D)	10 ng/ml	-	-
Murine IL-6 (Peprotech)	20 ng/ml	40 ng/ml	-
Human TGFβ (Peprotech)	5 ng/ml	3 ng/ml	3 ng/ml

Table 6

	Th1	Th2 1^{st} round	Th2 2^{nd} round
Cell	Naïve $CD4^+$	Naïve $CD4^+$	Naïve $CD4^+$
Medium	R10	R10	R10
Culture	5 days	5 days	2 days
αCD3 (clone 145-2C11; Biolegend)	2 μg/ml	1 μg/ml	-
αCD28 (clone 37.51; Biolegend)	1 μg/ml	1 μg/ml	-
αIFNγ (clone XMG1.2; Biolegend)	-	10 μg/ml	10 μg/ml
αIL-4 (clone 11B11; Biolegend)	1 μg/ml	-	-
Murine IL-12 (Peprotech)	30 ng/ml	-	-
Murine IL-4 (Peprotech)	-	30 ng/ml	-
Murine IL-2 (Peprotech)	10 ng/ml	-	30 ng/ml

qPCR

For the measurement of mRNAs, cultured T cells were collected and total RNAs were purified using GenElute mammalian total RNA miniprep kit. qPCR was performed as described in Chapter 1 and the content of mRNA was normalized to the amount of *Gapdh* mRNA. The primer sets are shown in Table 7.

Table 7

Gene	**Forward (5' to 3')**	**Reverse (5' to 3')**
Foxp3	CCCATCCCCAGGAGTCTTG	ACCATGACTAGGGGCACTGTA
Gapdh	TTCACCACCATGGAGAAGGC	GGCATGGACTGTGGTCATGA
Gata3	CTCGGCCATTCGTACATGGAA	GGATACCTCTGCACCGTAGC
Il17a	CTCCAGAAGGCCCTCAGACTAC	GGGTCTTCATTGCGGTGG
Il17f	TGCTACTGTTGATGTTGGGAC	AATGCCCTGGTTTTGGTTGAA
Il1a	TCGGGAGGAGACGACTCTAA	TGTTTCTGGCAACTCCTTCA
Il1r2	GATCCAGTCACAAGGGAGGA	CCAGGAGAACGTGGAAGAGA
Il21	GCCAGATCGCCTCCTGATTA	CATGCTCACAGTGCCCCTTT
Il22	TGACGACCAGAACATCCAGA	AGCTTCTTCTCGCTCAGACG
Il23r	CATTGCACTGCTGAATGTCC	TTCCAGGTGCATGTCATGTT
Irf4	TCCTCTGGATGGCTCCAGATGG	CACCAAAGCACAGAGTCACCTG
Rorc	AGCAGTGTAATGTGGCCTAC	GCACTTCTGCATGTAGACTG
Tbx21	AGCAAGGACGGCGAATGTT	GGGTGGACATATAAGCGGTTC

Flow cytometry

Flow cytometry was performed as described in Chapter 1. Used antibodies are listed in Table 8.

Table 8

Antigen	Label	Clone	Source
CD3ε	APC/Cy7	145-2C11	Biolegend
CD4	APC	RM4-5	Biolegend
CD4	PE/Cy7	RM4-5	Biolegend
CD4	Brilliant Violet 510	RM4-5	Biolegend
CD45.1	Pacific Blue	A20	Biolegend
CD45.2	FITC	104	Biolegend
Foxp3	PE	FJK-16s	eBioscience
IFNγ	FITC	XNG1.2	Biolegend
IFNγ	Pacific Blue	XNG1.2	Biolegend
IFNγ	APC	XNG1.2	Biolegend
IL-17A	Pacific Blue	TC11-18H10.1	Biolegend
IL-17A	APC	TC11-18H10.1	Biolegend
IL-17A	PE/Cy7	TC11-18H10.1	Biolegend
IL-4	APC	11B11	Biolegend
RORγ(t)	PE	B2D	eBioscience

EAE in CD4$^+$ T cell-reconstituted mice

CD4$^+$ T cells were collected from 2D2 mice (Jackson Laboratory; Bar Harbor, ME, USA) or *Il1r2*$^{-/-}$2D2 mice as described above and resuspended in PBS. 2 × 10^6 of these CD4$^+$ T cells were transferred i.v. into *Rag2*$^{-/-}$ or *Rag2*$^{-/-}$*Il1r2*$^{-/-}$ mice. 24 h later, these mice were immunized on day 0 with 50 μl each of MOG/CFA emulsion at left fore-flank and right hind-flank subcutaneously. Immunized emulsion was prepared by mixing 1 ml of PBS containing 2 mg of MOG35-55 peptide with 1 ml of CFA containing 2 mg of heat-killed M. tuberculosis H37Ra. On day 0 and 8, 50 ng of pertussis toxin (PTx) (List Biological Laboratories, Inc; Campbell, CA, USA) was injected

intraperitoneally. On day 7, mice were immunized with 50 μl each of MOG/CFA emulsion at right fore-flank and left hind-flank subcutaneously. Clinical severity was scored for each body parts with total score 9. Limbs: 1 = hind limb paresis, 2 = one hind limb paralyzed, 3 = both hind limbs paralyzed, 4 = fore limbs paralyzed. Tail: 1 = partially paralyzed tail, 2 = paralyzed stiff tail, 3 = paralyzed limp tail. Trunk: 1 = partially paralyzed abdominal muscle, 2 = paralyzed abdominal muscle. When mice died, they were scored 10.

Bone marrow chimera mice

BMCs were isolated from WT (CD45.1) and *Il1r2*$^{-/-}$ or *Il1a*$^{-/-}$ (CD45.2) mice, mixed 1:1 ratio and resuspended in PBS. Total 1 × 10^7 BMCs were transferred i.v. into irradiated (5.5 Gy twice, 3 h apart) *Rag2*$^{-/-}$ or *Rag2*$^{-/-}$*Il1r2*$^{-/-}$ mice. Four weeks later, these mice were used for naïve $CD4^+$ T cell purification or EAE. For EAE, bone marrow chimera mice were immunized on day 0 with 50 μl each of MOG/CFA emulsion at left fore-flank and right hind-flank subcutaneously. Immunized emulsion was prepared by mixing 1 ml of PBS containing 2 mg of MOG35-55 peptide with 1 ml of CFA containing 5 mg of heat-killed M. tuberculosis H37Ra. On day 0 and 2, 200 ng of PTx was injected intraperitoneally. On day 7, mice were immunized with 50 μl each of MOG/CFA emulsion at right fore-flank and left hind-flank subcutaneously. On day 19, mice were perfused by PBS, and then draining LNs and spinal cord were collected for flowcytometry analysis. For single cell

preparation from spinal cord, organs were digested in type VIII collagenase (Sigma) for 30 min at 37°C followed by final 20 mM EDTA for 10 min at room temperature. Digested organs were suspended in 30% percoll (Sigma) and mounted on 70% percoll for separation of mononuclear cells by centrifuge at 850 G for 20 min at 20°C.

Statistical analysis

P values were calculated using two-tailed unpaired student's *t*-test for all experiments. *P* value < 0.05 was defined as significant.

IV-4. Results

Helper T cell highly expresses Il1r2

First, I determined the *Il1r2* expression in each helper T cell subsets by qPCR. Naïve $CD4^+$ T cell was sorted by flowcytometer and differentiated to Th1, Th2 and Th17. $CD4^+CD25^+$ was sorted as Treg. Exact helper T cell sampling was confirmed by *Tbx21*, *Gata3*, *Rorc* and *Foxp3* expression which are master regulator of Th1, Th2, Th17 and Treg respectively. I found that *Il1r2* was highly expressed in each helper T cell subsets but not in naïve $CD4^+$ T cell (Fig. 27).

Impaired Th17 differentiation in $Il1r2^{-/-}$ $CD4^+$ T cell independent of IL-1 signal

To investigate the roles of IL-1R2 during Th17 differentiation, purified $CD4^+$ T cell were cultured in Th17 differentiation condition which contains αCD3 antibody, αCD28 antibody, recombinant IL-6, recombinant TGFβ and recombinant IL-23. Endogenous IL-1 must existed in this condition, since Th17 differentiation of $Il1r1^{-/-}$ T cell was impaired (Fig. 28). Contrary to my expectation, Th17 differentiation of $Il1r2^{-/-}$ T cell was also impaired. When IL-1β was added to this culture condition, Th17 differentiation of WT T cell was enhanced but $Il1r1^{-/-}$ T cell was not. Although Th17 differentiation of $Il1r2^{-/-}$ T cell was also enhanced by IL-1β addition, its differentiation capacity was still lower than WT. To clarify whether impaired Th17 differentiation depend on IL-1 signal or not, IL-1Ra was added to Th17 differentiation condition. No difference of Th17

differentiation capacity between WT and *Il1r1*$^{-/-}$ T cells indicated that addition of IL-1Ra nearly completely blocked the IL-1 signal. In this condition, Th17 differentiation of *Il1r2*$^{-/-}$ T cell was still lower than WT. Thus, impaired Th17 differentiation of *Il1r2*$^{-/-}$ T cell did not depend on IL-1 signal. qPCR analysis revealed that other Th17 related genes, such as *Il17f, Il22* and *Il23r*, also down-regulated in *Il1r2*$^{-/-}$ T cell, although *Il21* expression was similar between WT and *Il1r2*$^{-/-}$ T cell (Fig. 29).

Same results were obtained, when purified naïve CD4^{+} T cell were used for Th17 differentiation assay (Fig. 30). Although Foxp3^{+} Treg cells arose together during Th17 differentiation, cell number of Foxp3^{+} was similar between WT and *Il1r2*$^{-/-}$ T cells. It suggested that less % of IL-17A^{+} cell in *Il1r2*$^{-/-}$ T cells was not due to expansion of non-Th17 lineages.

In contrast, when naïve CD4^{+} T cell were cultured in Th1, Th2 and Treg differentiation condition, normal differentiation was observed in *Il1r2*$^{-/-}$ T cells (Fig. 31).

IL-1R2 expressed by T cell controls Th17 differentiation

To determine which IL-1R2 expressing cells are responsible for promoting Th17 differentiation, I generated the mixed bone marrow chimera mice. 1 : 1 mixture of WT (CD45.1) and *Il1r2*$^{-/-}$ (CD45.2) bone marrow cells were used as donor and irradiated *Rag2*$^{-/-}$ or *Rag2*$^{-/-}$*Il1r2*$^{-/-}$ mice were used as recipient. Naïve CD4^{+} T cells were purified from the mixed bone marrow chimera mice and

cultured in both Th17 and Treg differentiation condition. No significant difference of Th17 differentiation between *Rag2*$^{-/-}$ and *Rag2*$^{-/-}$*Il1r2*$^{-/-}$ derived WT T cells suggested that IL-1R2 expressed by non-hematopoietic cells were not involved in Th17 differentiation (Fig. 32). Impaired Th17 differentiation in *Il1r2*$^{-/-}$ T cells compared to WT T cells purified from same mice indicated that IL-1R2 expressed by T cell is responsible for promoting Th17 differentiation. Under Treg differentiation condition, no difference was observed in the frequency of Foxp3^{+} cells.

Impaired Th17 differentiation in Il1a$^{-/-}$ *CD4*$^{+}$ *T cell*

Since IL-1R2 was thought to control Th17 differentiation independent of IL-1 signal, it was suggested that IL-1R2 works intracellularly collaborating with IL-1α. If so, Th17 differentiation of *Il1a*$^{-/-}$ T cell must decline. Consist with my prediction, naïve CD4^{+} T cell purified from *Il1a*$^{-/-}$ mice has impaired Th17 differentiation capacity (Fig. 33). And also, I found that *Il1a* expression of Th17 was higher than that of naïve T cell (Fig. 27).

Normal Rorc expression in *Il1r2*$^{-/-}$ *CD4*$^{+}$ *T cell*

Previous reports demonstrated that IL-1α enhances the transcription via interacting with histone acetyltransferase (HAT). Since IL-1α does not have DNA binding domain, it is suggested that IL-1α recruits HAT to promoter region through other DNA binding transcription factors (Fig. 34A).

IL-6 induces *Il17a* transcription through the three transcription factor cascade; STAT3, IRF4 and RORγ(t) (Fig. 34B). I examined the mRNA level of *Irf4*, *Rorc* and *Il17a* to unveil which transcription factor interact with IL-1α. I found that only mRNA level of *Il17a*, but not *Irf4* and *Rorc*, was decreased in *Il1r2*$^{-/-}$ CD4^{+} T cell (Fig. 35). Normal RORγ(t) expression was also confirmed by flowcytometry (Fig. 36).Thus it was suggested that IL-1α interact with RORγ(t) to control *Il17a* transcription. This idea is consist with the data of Fig. 27, because *Rorc*$^{-/-}$ T cell shows same phenotype; down-regulation of *Il17a*, *Il17f*, *Il22* and *Il23r* but not *Il21* (75). At the same time, I also found that mRNA level of *Il1r2* and *Il1a* increased during Th17 differentiation (Fig. 35). It indicated that IL-1R2-IL-1α system is needed for sustain *Il17a* transcription at late phase of Th17 differentiation.

Normal development of EAE in CD4^{+} *T cell-specific Il1r2*$^{-/-}$ *mice*

Next, I attempted to analyze the pathogenicity of *Il1r2*$^{-/-}$ CD4^{+} T cells using Th17-dependent autoimmune model; EAE. It was demanded to generate CD4^{+} T cell-specific *Il1r2*$^{-/-}$ mice to separate the intracellular function of IL-1R2 in CD4^{+} T cells from the decoy receptor function in other cell types especially in macrophages. Although transfer of CD4^{+} T cells into *Rag*$^{-/-}$ mice can achieve this purpose, this method induces colitis in these mice due to proliferation of CD4^{+} T cells in response to commensal gut microbiota-derived antigens (112). Not to induce colitis, I used CD4^{+}

T cells collected from 2D2 mice; TCR-transgenic mice which recognize MOG (113). As expected, when 2D2 $CD4^+$ T cells were transferred, *Il1r2*$^{-/-}$*Rag*$^{-/-}$ mice developed severer EAE than *Rag*$^{-/-}$ mice (Fig. 37). It was probably because IL-1 signal was enhanced in *Il1r2*$^{-/-}$*Rag*$^{-/-}$ macrophages. Unexpectedly, there were no difference in clinical scores between 2D2 $CD4^+$ T cells transferred *Rag*$^{-/-}$ mice and *Il1r2*$^{-/-}$2D2 $CD4^+$ T cells transferred *Rag*$^{-/-}$ mice.

Normal Th17 differentiation of Il1r2$^{-/-}$ *and Il1a*$^{-/-}$ *T cell during EAE*

There were two possible causes for normal EAE development in $CD4^+$ T cell-specific *Il1r2*$^{-/-}$ mice: (i) the reduction level of Th17-related genes in *Il1r2*$^{-/-}$ $CD4^+$ T cell is not sufficient to alleviate EAE, and (ii) Th17 differentiation of *Il1r2*$^{-/-}$ T cell was not impaired *in vivo*. Although I had already found that Th17 differentiation was not affected by IL-1R2 deficiency during CIA (Chapter 1), I thought that inhibition of IL-1 signal by myeloid cell derived IL-1R2 offset the effect of IL-1R2 in Th17 differentiation. For this reason, I need the experimental system which can evaluate the roles of IL-1R2 only in T cells. To this end, I induced EAE, an IL-17A dependent disease model, in mixed bone marrow chimera mice with 50% of WT and 50% of knockout bone marrow cells. In contrast to my anticipation, Th17 as well as Th1 and Treg differentiation was similar between WT and *Il1r2*$^{-/-}$ T cells in LN and CNS of EAE induced mice (Fig. 38). Likewise, *Il1a*$^{-/-}$ T cells also have normal helper T cell differentiation capacity during EAE (Fig. 39).

IV-5. Discussion

The two facts implant in me the idea that IL-1R2 suppresses Th17 differentiation: (i) IL-1 promotes Th17 differentiation and (ii) IL-1R2 is highly expressed by Th17. Though, I found that *Il1r2*$^{-/-}$ CD4^{+} T cells have less capacity to differentiate to Th17 in IL-1R1 signal independent fashion. It was due to lack of IL-1R2 in T cell. Since *Il1a*$^{-/-}$ CD4^{+} T cells were also hard to differentiate to Th17, it seemed that IL-1R2 and IL-1α collaborate to enhance Th17 differentiation. No difference of RORγ(t) expression between WT and *Il1r2*$^{-/-}$ Th17 suggested that IL-1R2 and IL-1α directly controlled the *Il17a* transcription. However, impaired Th17 differentiation in *Il1r2*$^{-/-}$ and *Il1a*$^{-/-}$ CD4^{+} T cell was not observed during EAE.

The discrepancy in roles of IL-1R2 in Th17 differentiation between *in vitro* and *in vivo* may be explained by following points. First, Th17 differentiation might be saturated *in vivo* on day 19 of EAE. Generally, EAE starts to develop on day 10 and its severity peaks at day 20. Impaired Th17 differentiation of *Il1r2*$^{-/-}$ and *Il1a*$^{-/-}$ CD4^{+} T cell may be observed at earlier time points. Second, the involvement of IL-1R2 and IL-1α in Th17 differentiation is too subtle to be detected *in vivo*. Third, other factors, which are absent *in vitro* culture condition, may cancel the effect of IL-1R2 and IL-1α. Fourth, *in vitro* generated Th17 and *in vivo* generated Th17 have different features such as expression and localization of IL-1R2 and IL-1α.

The molecular mechanisms how IL-1R2 and IL-1α control Th17 differentiation remain unclear. ChIP assay using anti-IL-1α antibody will reveal the genes controlled by IL-1α. Transcription factors which bind to IL-1α can be explored by mass spectrometry after immunoprecipitation using anti-IL-1α antibody. There are few clues to predict the molecular role of IL-1R2 in transcription. IL-1R2 protects IL-1α from cleavage by calpain, the proteolytic enzyme which processes IL-1α to N-terminal peptide and C-terminal peptide (22). Full length IL-1α has more efficient transcription activity than N-terminal peptide of IL-1α (107). Altogether, it seems that IL-1R2 increases the amount of full length IL-1α which has effective transcription activity. Although calpain inhibition during Th17 differentiation *in vitro* does not affect the production level of IL-17A (114), this report does not conflict to my hypothesis because of existence of various calpain target other than IL-1α. It is unclear why full length IL-1α has more efficient transcription activity. Nuclear localization of IL-1α is not affected by IL-1R2 (109). Consist with this, Full length IL-1α and N-terminal peptide of IL-1α have similar nuclear localization capacity (115). Conversely, two reports shows that full length IL-1α has less nuclear localization capacity than N-terminal peptide of IL-1α (106, 116). IL-1R2 may stabilize IL-1α-HAT complex. Conceivably, IL-1R2 might regulate Th17 differentiation in IL-1α independent manner.

Although the role of IL-1R2 and IL-1α in Th17 differentiation has few meaning in physiological condition, it is interesting that cytokine and its receptor act as transcriptional regulator.

Previous reports showed that several cytokines play roles intracellularly. IL-33, one of the IL-1 family genes, also has NLS in its N-terminal region and localizes to nuclei (117). IL-33 interacts with NF-κB to prevent its binding to DNA, which results in down-regulation of NF-κB dependent transcription (118). HMGB is originally recognized as a transcriptional modulator (119), but now it is well known that HMGB induce inflammation through various receptors (120). IL-1α, IL-33 and HMGB are classified into damage-associated molecular patterns (DAMPs), since they share the feature; they localize in nuclei not to be secreted at steady state and are released upon necrosis.

In this study, I found the intracellular role of IL-1α/IL-1R2 in Th17 differentiation. I need further study to reveal the importance of intracellular role of IL-1α/IL-1R2 under physiological condition as well as the molecular mechanism how IL-1α/IL-1R2 controls transcription.

IV. Figures

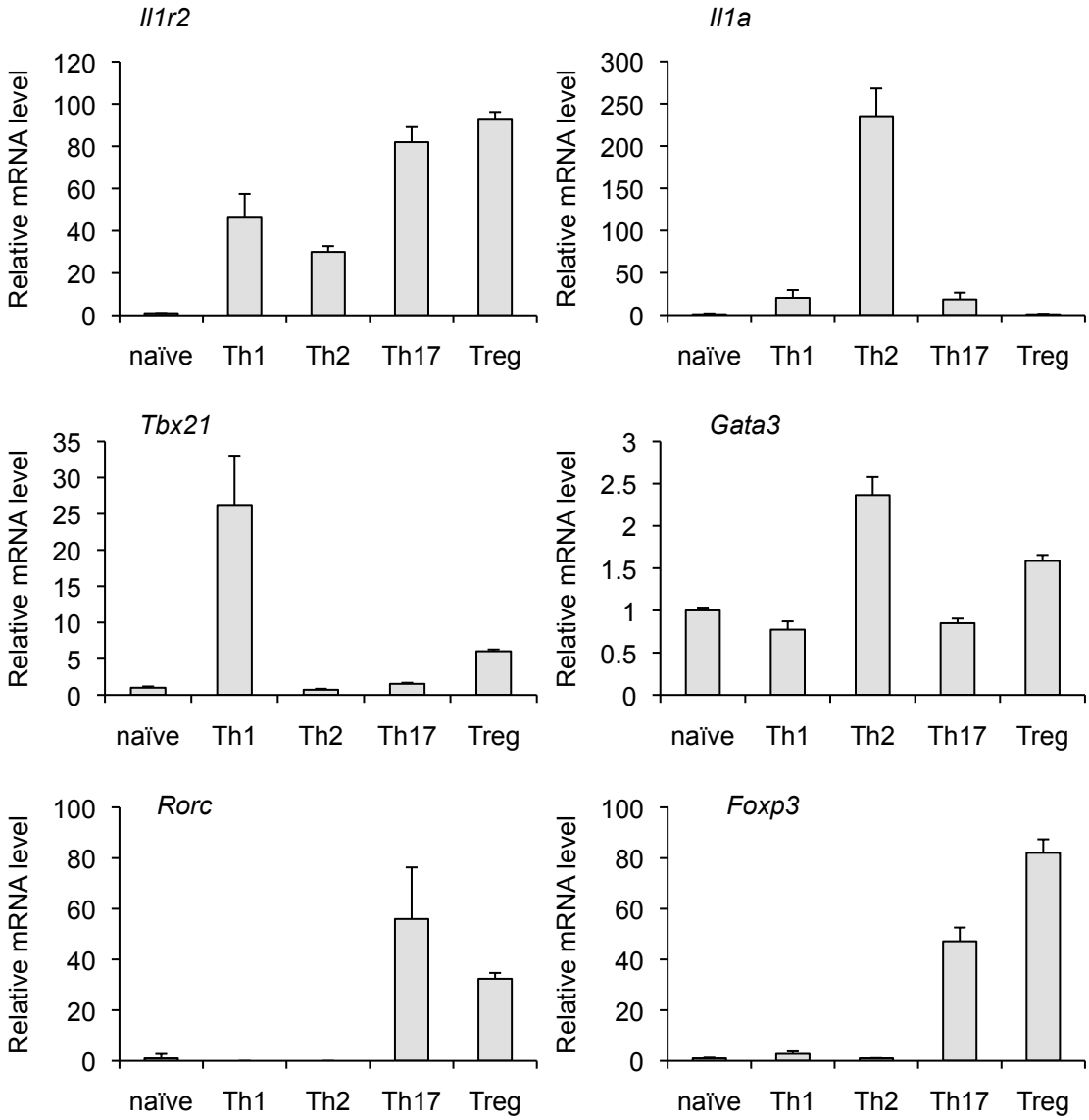

FIGURE 27. The *Il1r2* and *Il1a* expression in each T cell subsets. mRNA were extracted from sorted naïve CD4+ T cell and Treg as well as differentiated Th1, Th2 and Th17. The expression of *Il1r2*, *Il1a, Tbx21, Gata3, Rorc* and *Foxp3* mRNA was analyzed by quantitative PCR. Data are the mean ± s.d. of triplicates.

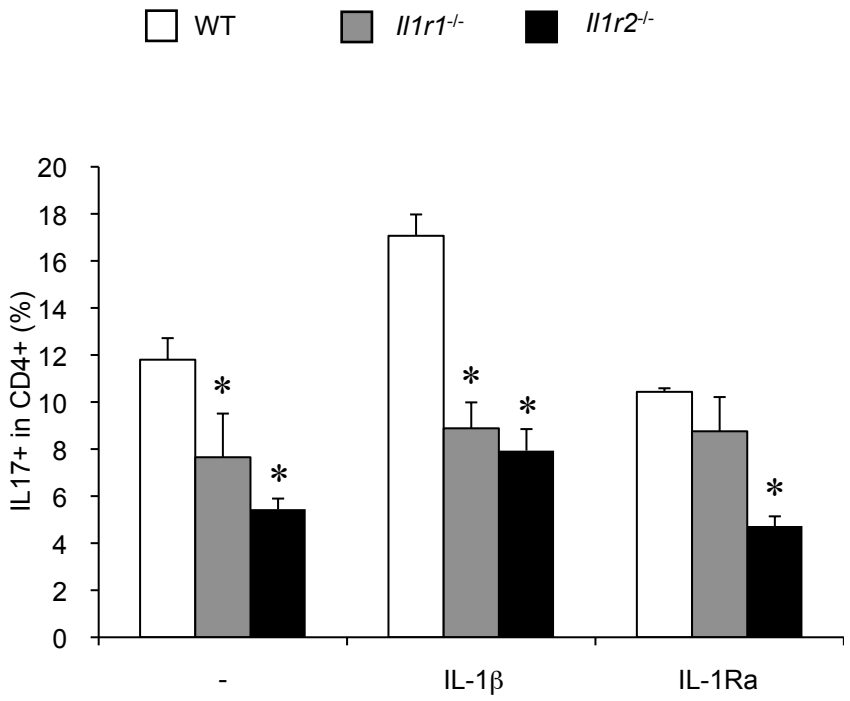

FIGURE 28. Impaired Th17 differentiation of *Il1r2*$^{-/-}$ CD4^{+} T cell. CD4^{+} T cells were purified from WT, *Il1r1*$^{-/-}$ or *Il1r2*$^{-/-}$ mice. Purified cells were cultured in Th17 differentiation condition with or without IL-1β or IL-1Ra. % of IL-17A^{+} cell was measured by flowcytometry on day 3. Data are the mean ± s.d. of triplicates. *$P < 0.05$ by the two-tailed unpaired student's *t*-test compared to WT in the same condition.

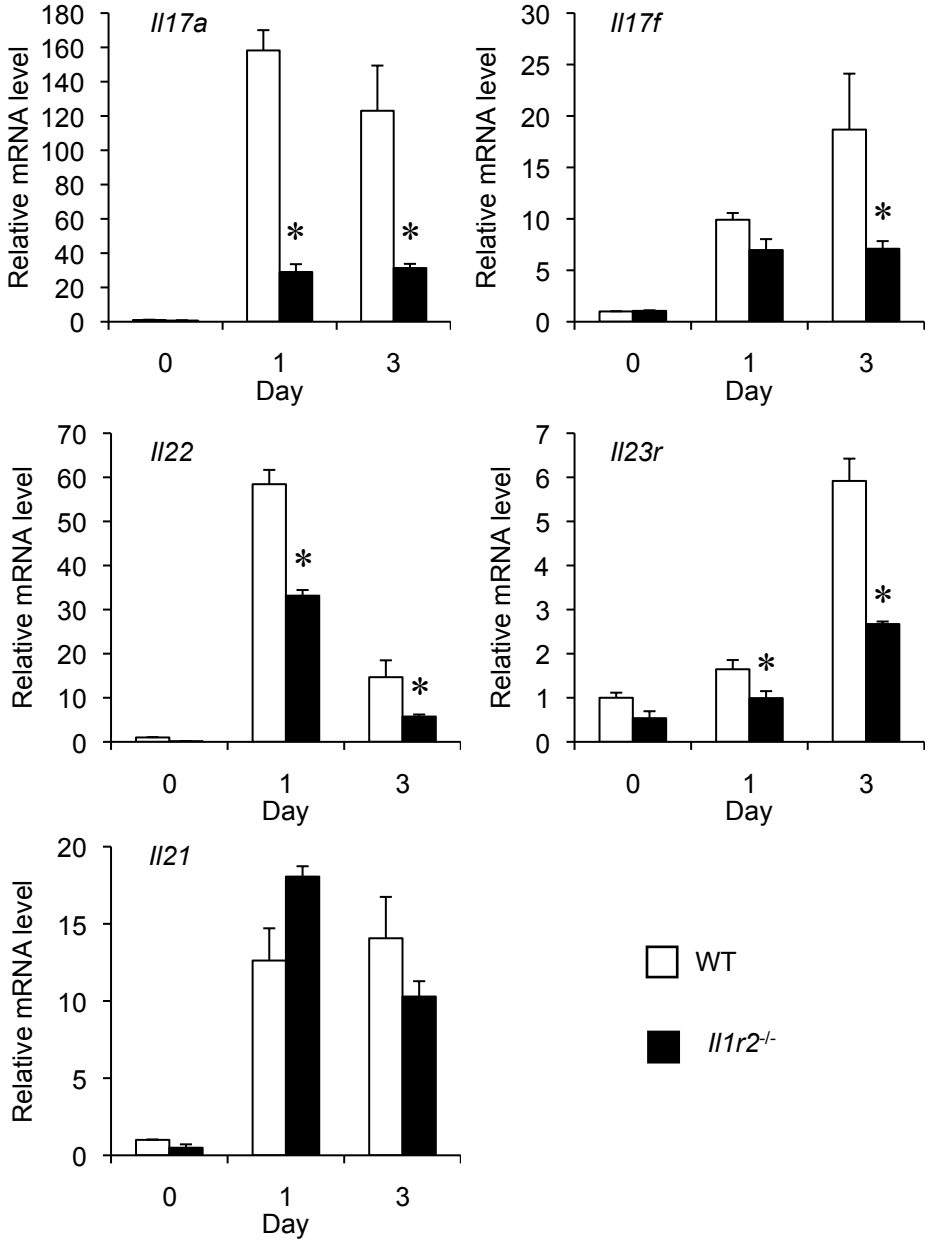

FIGURE 29. Th17 related Gene expression during Th17 differentiation.
$CD4^+$ T cells were purified from WT or *Il1r2*$^{-/-}$ mice. Purified cells were cultured in Th17 differentiation condition. RNA was extracted on day 0, 1 and 3. The amount of mRNA was measured by qPCR. Data are the mean ± s.d. of triplicates. **P* < 0.05 by the two-tailed unpaired student's *t*-test.

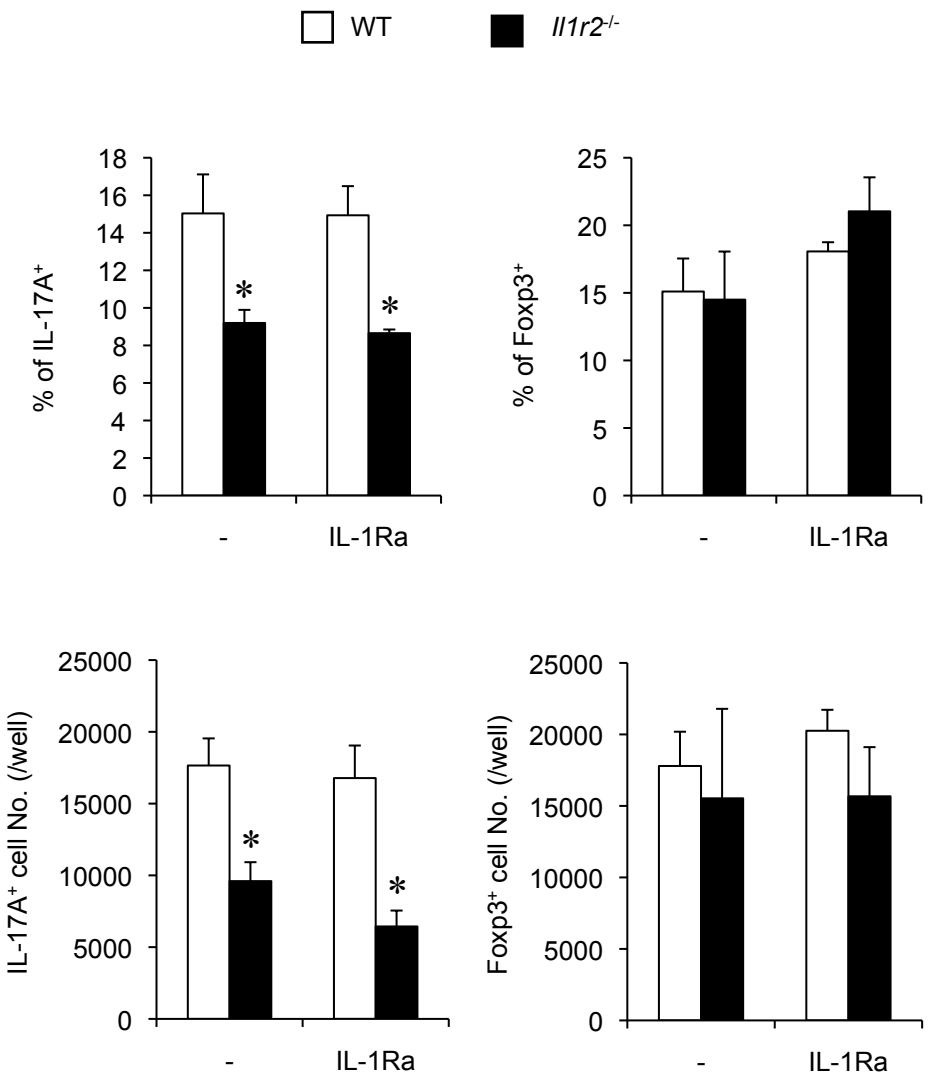

FIGURE 30. Impaired Th17 differentiation of *Il1r2*$^{-/-}$ naïve CD4^{+} T cell.

Naïve CD4^{+} T cells were purified from WT, *Il1r1*$^{-/-}$ and *Il1r2*$^{-/-}$ mice. Purified cells were cultured in Th17 differentiation condition with or without or IL-1Ra. % and number of IL-17A^{+} cell were measured by flowcytometry on day 5. Data are the mean ± s.d. of triplicates. *P < 0.05 by the two-tailed unpaired student's t-test.

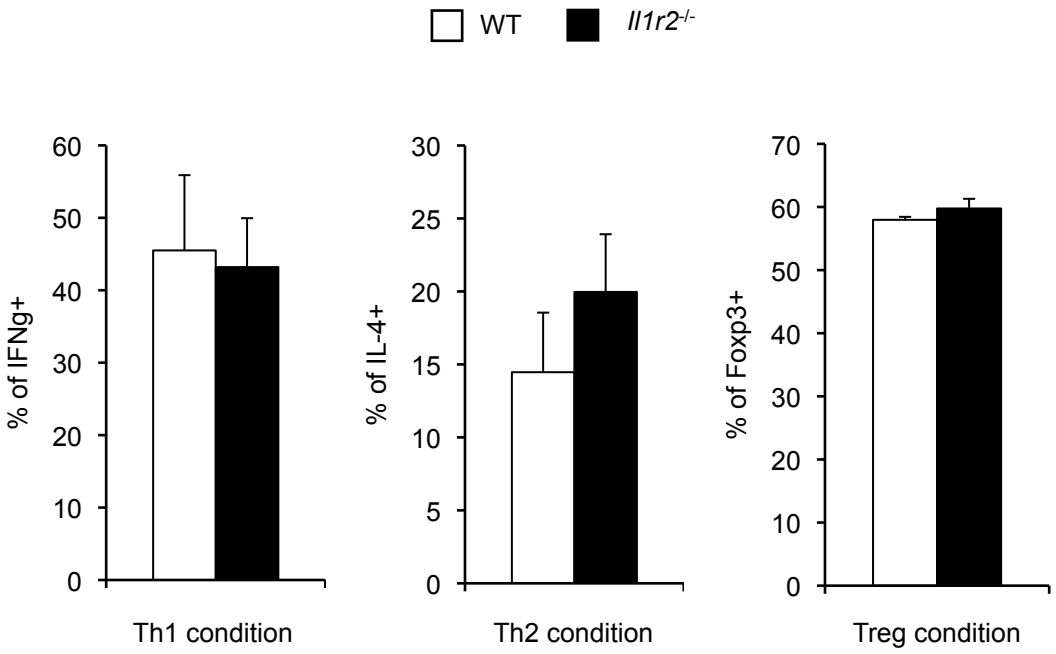

FIGURE 31. Normal Th1, Th2 and Treg differentiation of naïve *Il1r2*$^{-/-}$ CD4^{+} T cell.
Naïve CD4^{+} T cells were purified from WT, *Il1r1*$^{-/-}$ and *Il1r2*$^{-/-}$ mice. Purified cells were cultured in Th1, Th2 or Treg differentiation condition with or without or IL-1Ra. % of IL-17A^{+} cell was measured by flowcytometry.. Data are the mean ± s.d. of triplicates.

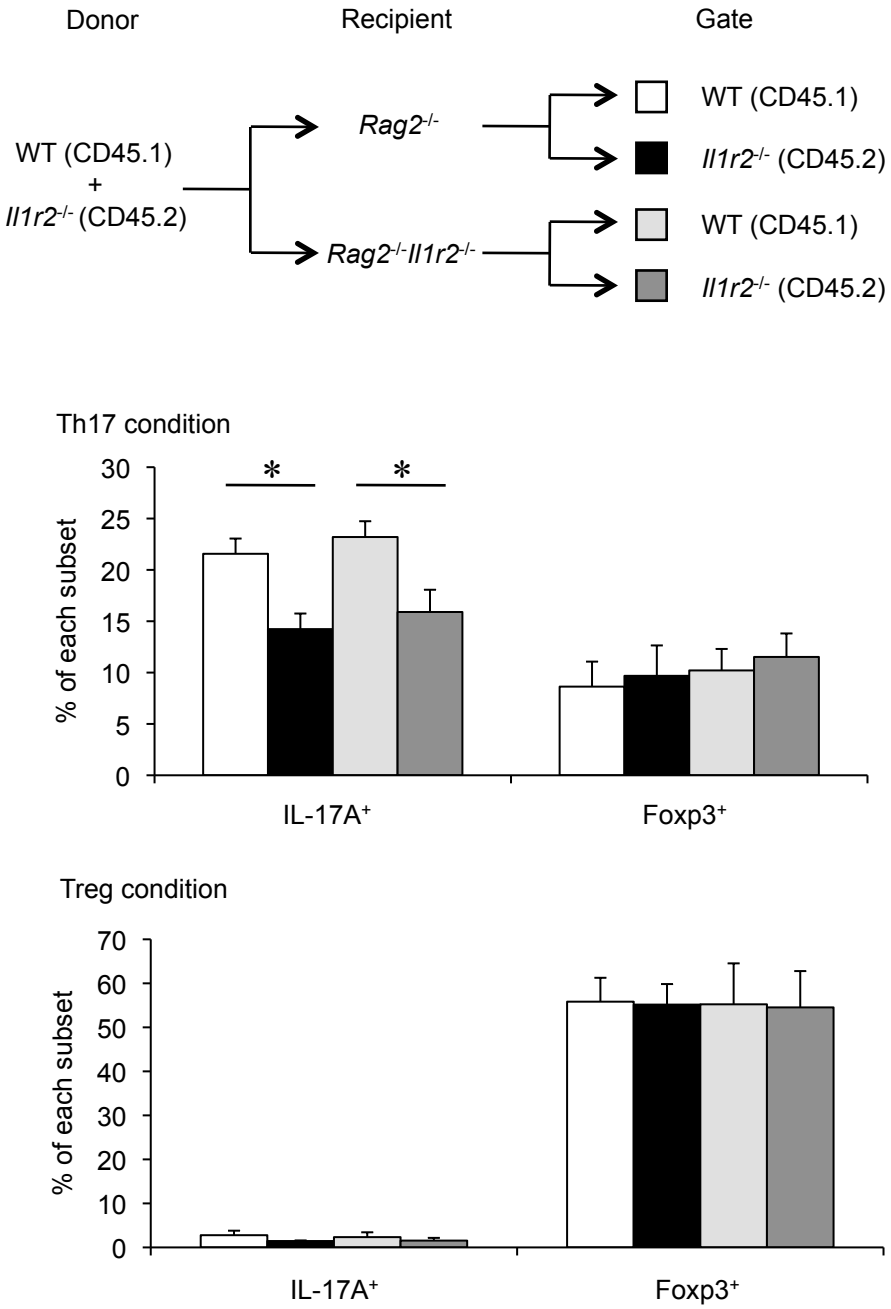

FIGURE 32. IL-1R2 expressed by T cell controlled the Th17 differentiation. Naïve CD4$^+$ T cells were purified from mixed bone marrow chimera mice. Purified cells were cultured in Th17 or Treg differentiation condition. % of IL-17A$^+$ or Foxp3$^+$ cell in WT or *Il1r2*$^{-/-}$ T cell were measured by flowcytometry on day 5. Data are the mean ± s.d. of triplicates. *$P < 0.05$ by the two-tailed unpaired student's *t*-test.

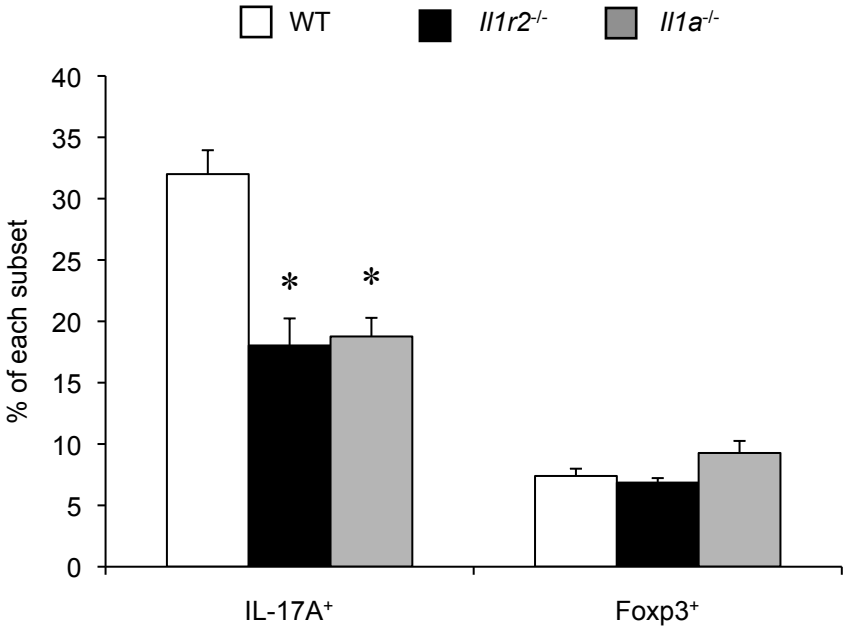

FIGURE 33. Impaired Th17 differentiation of *Il1a*$^{-/-}$ naïve CD4^{+} T cell. Naïve CD4^{+} T cells were purified from WT, *Il1r2*$^{-/-}$ or *Il1a*$^{-/-}$ mice. Purified cells were cultured in Th17 differentiation condition. % of IL-17A^{+} cell were measured by flowcytometry on day 5. Data are the mean ± s.d. of triplicates. *$P < 0.05$ by the two-tailed unpaired student's *t*-test.

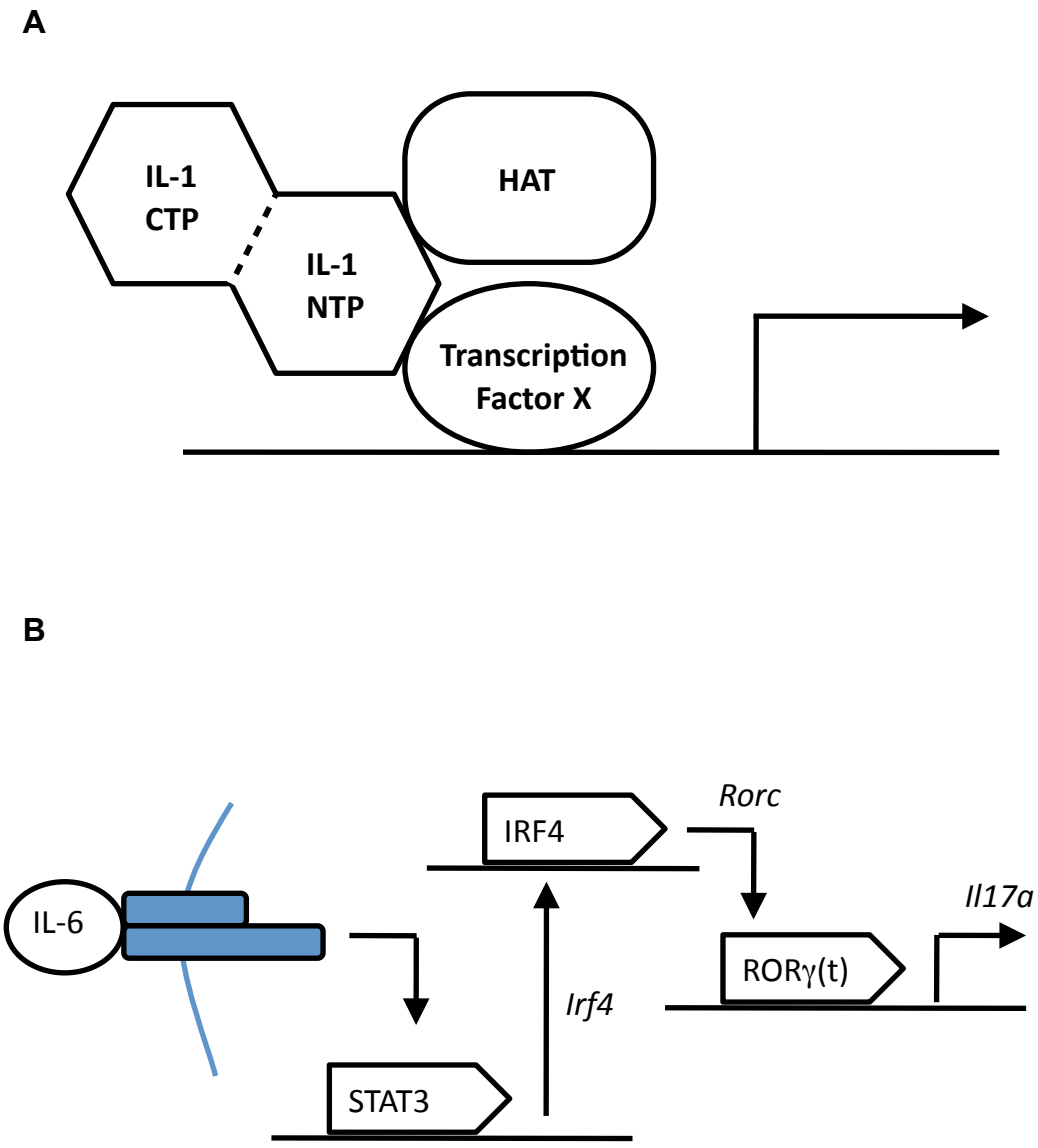

FIGURE 34. Schematic model IL-1α dependent *Il17a* transcription. (A) IL-1α recruit HAT via its N-terminal peptide (NTP). IL-1α transcription specificity may be assumed by binding to other transcription factor. (B) IL-6 activates STAT3 to induce *Irf4* transcription. And then IRF4 up-regulates RORγ(t) which induces *Il17a* transcription.

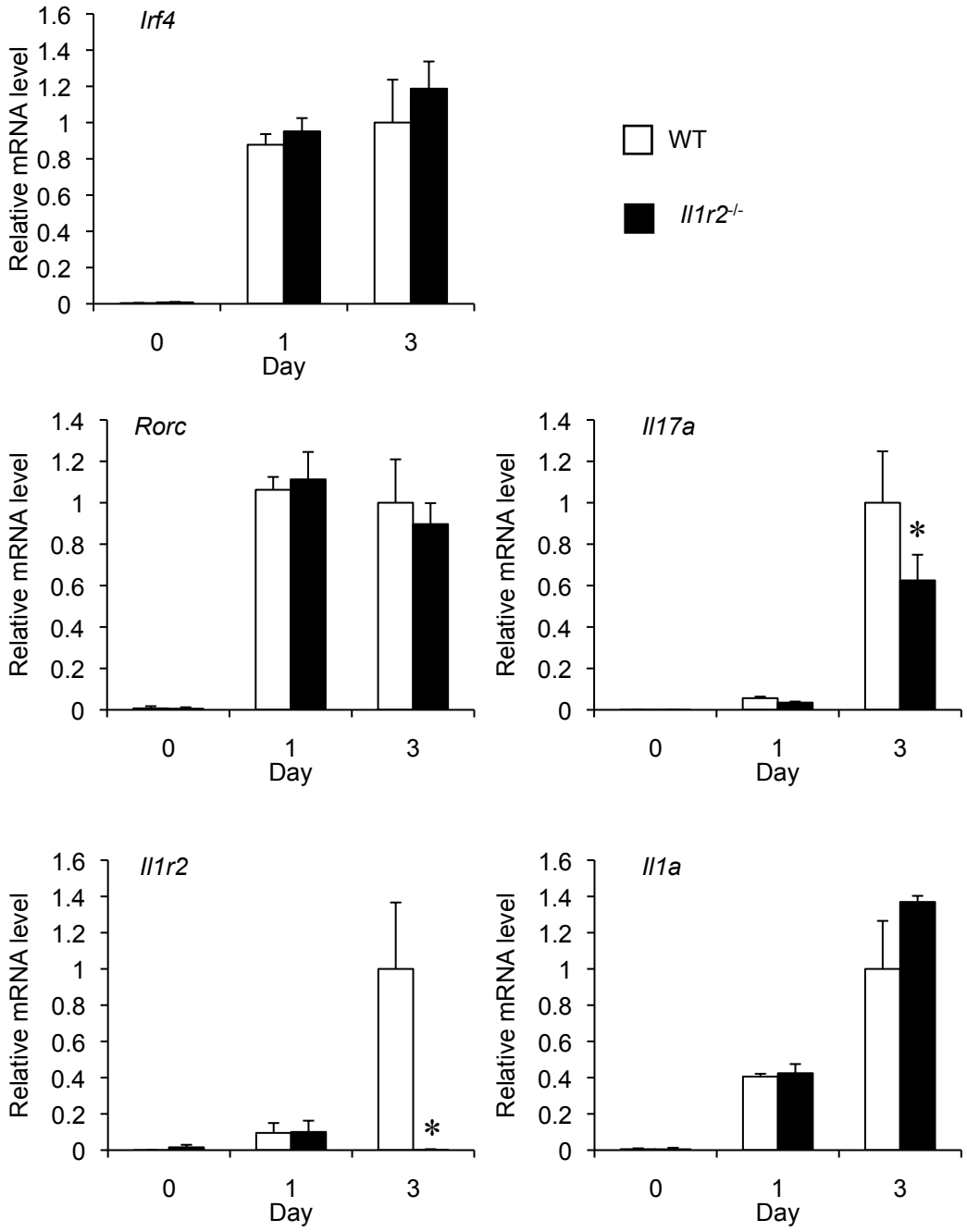

FIGURE 35. Expression of transcription factor during Th17 differentiation.
Naïve $CD4^+$ T cells were purified from WT or *Il1r2*$^{-/-}$ mice. Purified cells were cultured in Th17 differentiation condition. RNA was extracted on day 0, 1 and 3. The amount of mRNA was measured by qPCR. Data are the mean ± s.d. of triplicates. **P* < 0.05 by the two-tailed unpaired student's *t*-test.

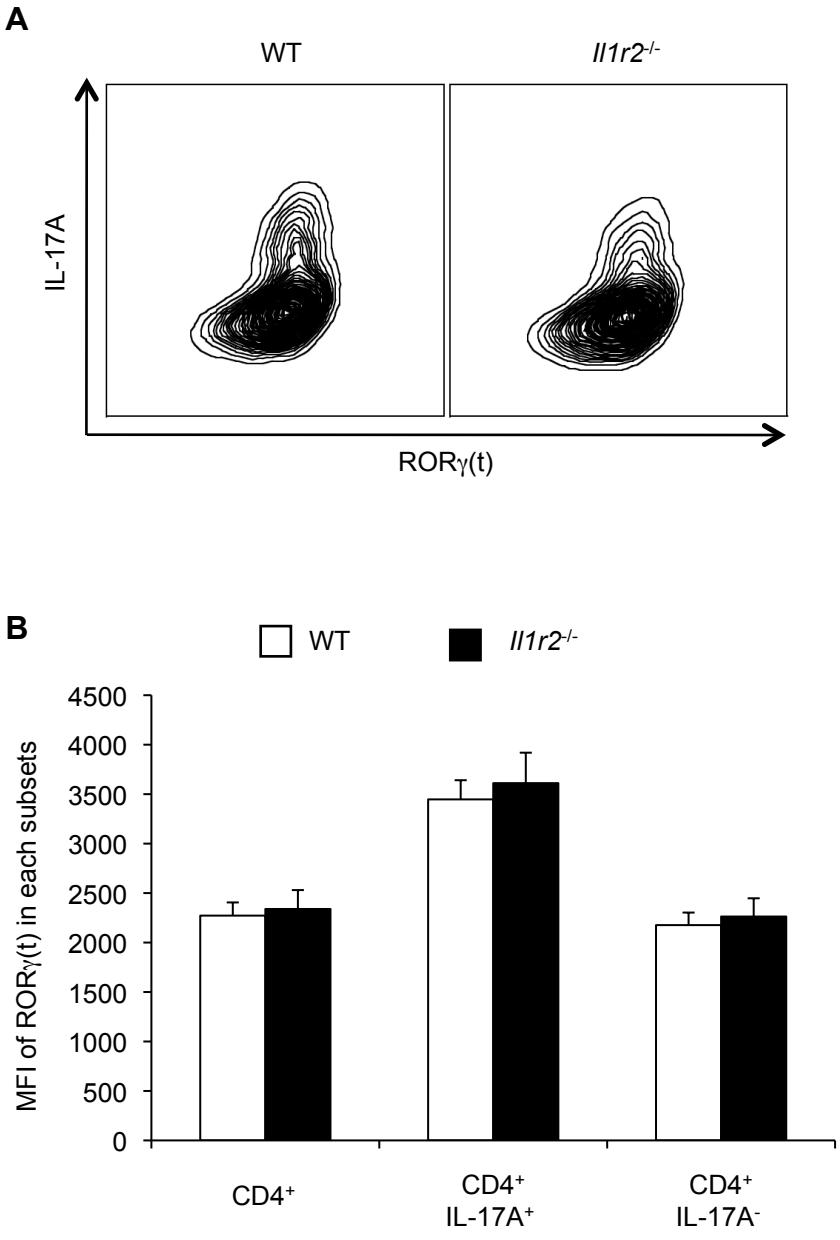

FIGURE 36. Normal Rorc expression in *Il1r2*$^{-/-}$ T cell.
Naïve CD4^{+} T cells were purified from WT and *Il1r2*$^{-/-}$ mice. Purified cells were cultured in Th17 differentiation. MFI of RORγ(t) was measured by flowcytometry on day 5. Representative counter plots and the MFI levels are shown in (A) and (B), respectively. Data are the mean ± s.d. of triplicates.

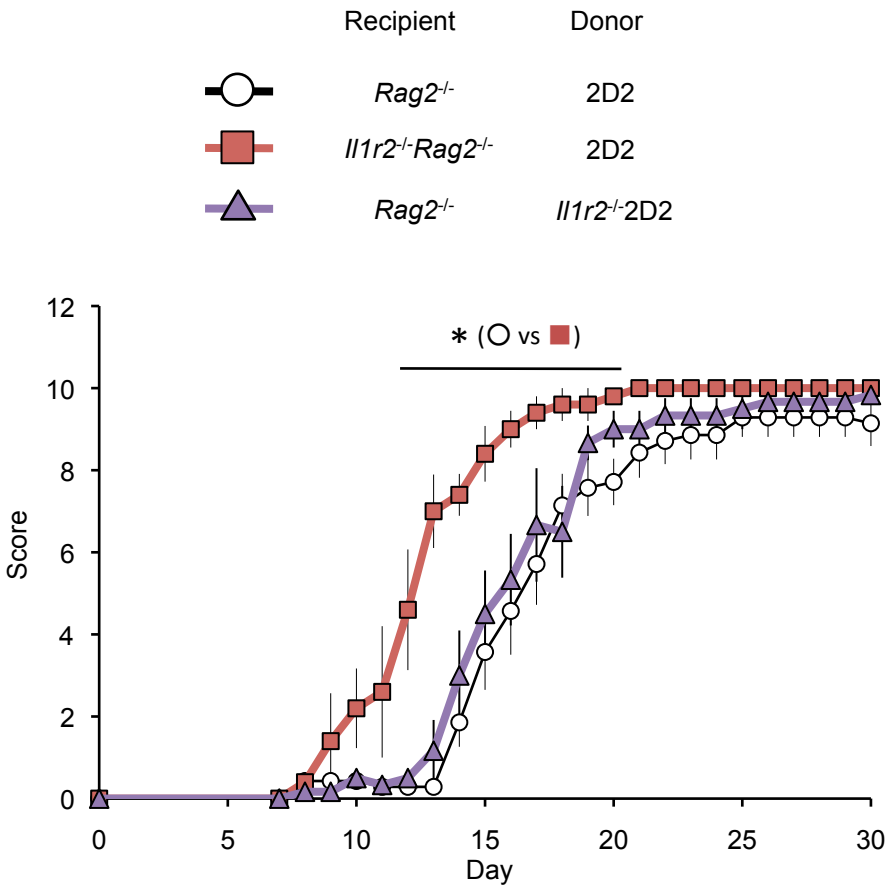

FIGURE 37. Normal development of EAE in CD4$^+$ T cell-specific *Il1r2*$^{-/-}$ mice.
CD4$^+$ T cells collected from 2D2 or *Il1r2*$^{-/-}$2D2 mice were transferred into *Rag2*$^{-/-}$ or *Rag2*$^{-/-}$*Il1r2*$^{-/-}$ mice. These mice were immunized with MOG peptide to induce EAE and scored for clinical severity.

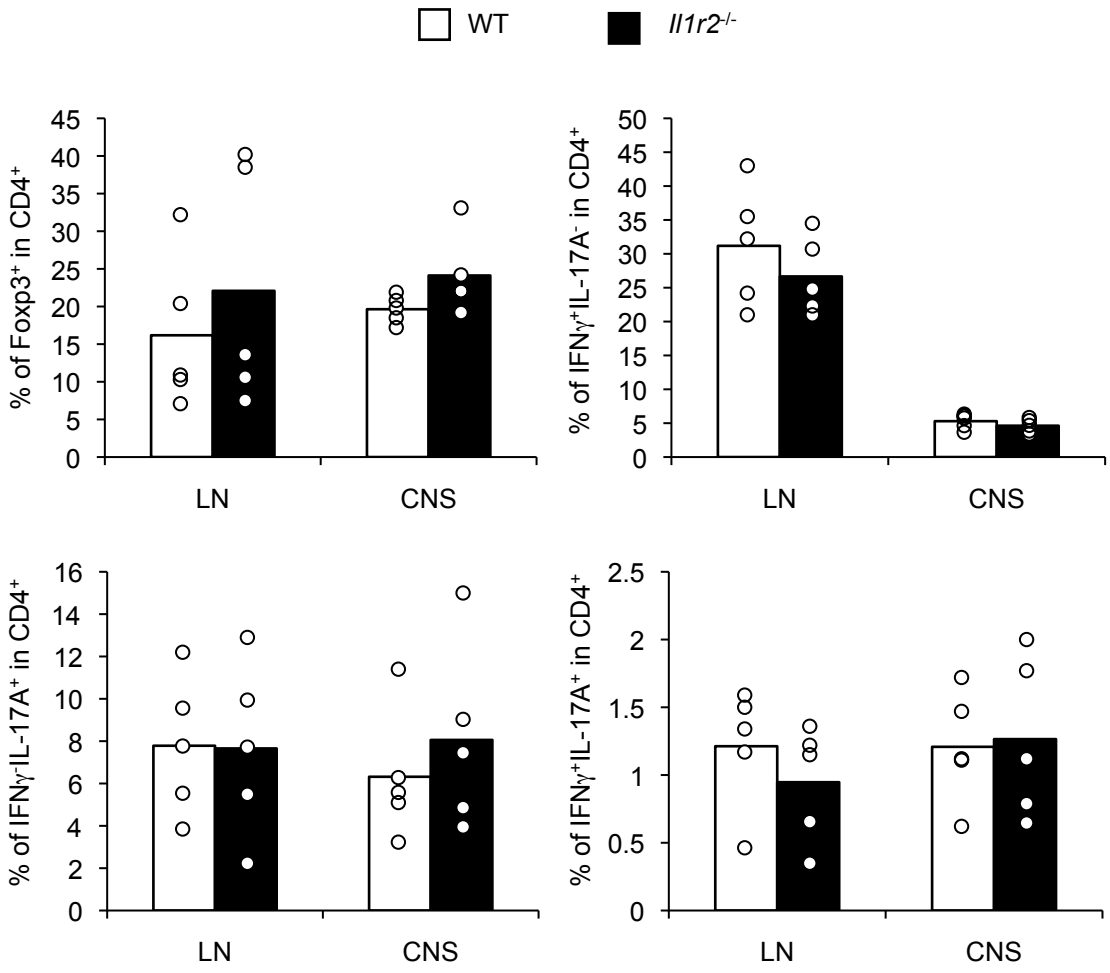

FIGURE 38. Normal helper T cell differentiation of *Il1r2*$^{-/-}$ T cell during EAE.
Mixed bone marrow chimera mice were immunized with MOG peptide to induce EAE. On day 19 of EAE, % of helper T cell subsets in LN and CNS were measured by flowcytometry. Each circles represent individual mice.

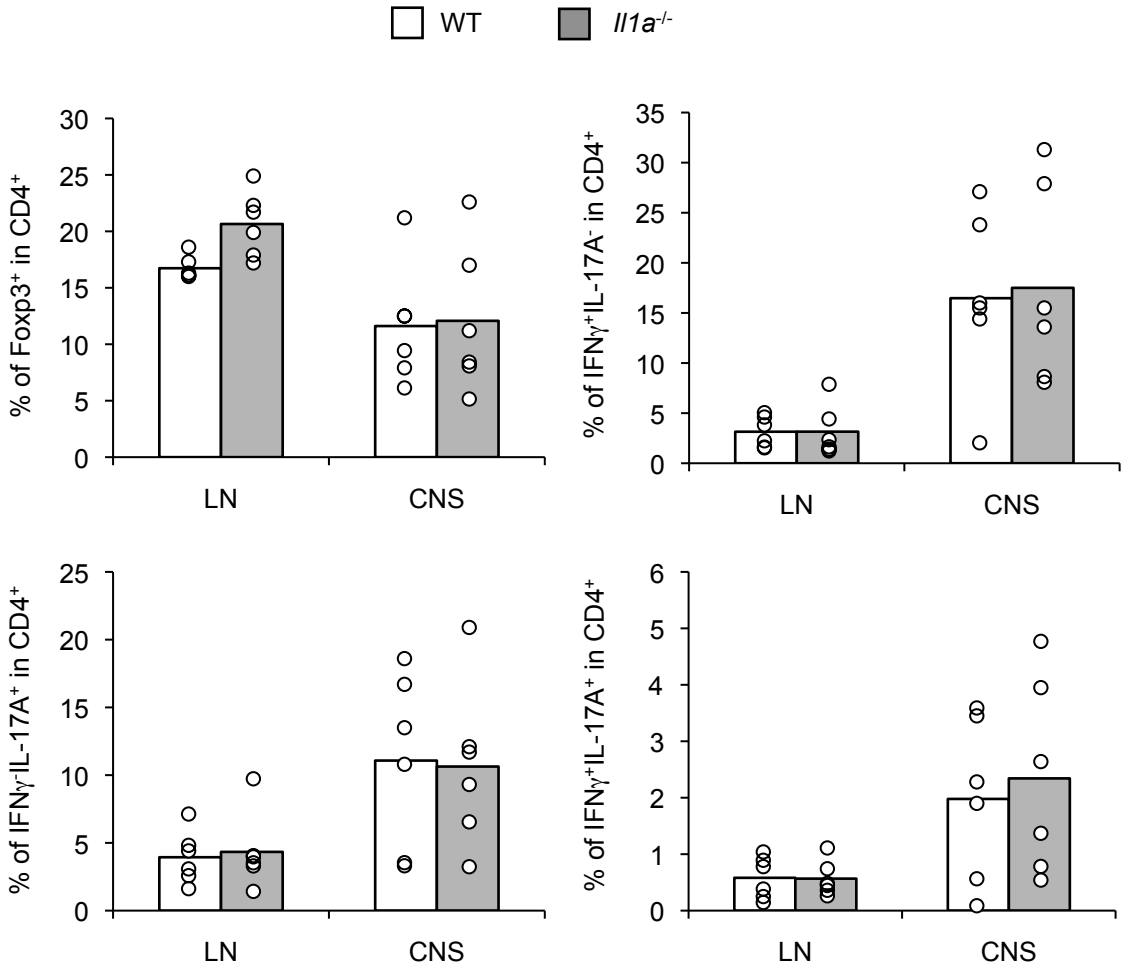

FIGURE 39. Normal helper T cell differentiation of *Il1a*$^{-/-}$ T cell during EAE.
Mixed bone marrow chimera mice were immunized with MOG peptide to induce EAE. On day 19 of EAE, % of helper T cell subsets in LN and CNS were measured by flowcytometry. Each circles represent individual mice.

V. Conclusion

In this report, I analyzed the *in vivo* roles of IL-1R2 using *Il1r2*$^{-/-}$ mice for the first time.

In chapter III, I demonstrated that IL-1R2 suppresses CIA by inhibiting IL-1 signal on macrophages. These results have re-confirmed the important roles of IL-1 in the development of arthritis. Also, the results clearly show that IL-1R2 is an important regulator of IL-1 function *in vivo* as a macrophage-specific decoy receptor. However, the roles of IL-1R2 in neutrophils still remain unclear, and further studies are needed.

In chapter IV, I showed that IL-1R2 promotes Th17 differentiation in a IL-1R1 signal independent manner. Although intracellular roles of IL-1α are reported by dozens of groups, that of IL-1R2 is reported by only few groups. My results strongly indicate that IL-1R2 has additional functional roles other than a decoy receptor for IL-1. The elucidation of the molecular mechanisms of Th17 cell differentiation by IL-1α/IL-1R2 as well as physiological and pathogenic roles of intracellular IL-1α/IL-1R2 should be very important not only to understand complex functional roles of IL-1 in our body but also to develop new therapeutics for inflammatory and autoimmune diseases.

VI. Reference

1. Dinarello CA. Immunological and Inflammatory Functions of the Interleukin-1 Family. Annual Review of Immunology. 2009;27:519-50.

2. Sims JE, Smith DE. The IL-1 family: regulators of immunity. Nature Reviews Immunology. 2010;10(2):89-102.

3. Zhu WQ, London NR, Gibson CC, Davis CT, Tong ZZ, Sorensen LK, et al. Interleukin receptor activates a MYD88-ARNO-ARF6 cascade to disrupt vascular stability. Nature. 2012;492(7428):252-5.

4. Dinarello CA. Infection, fever, and exogenous and endogenous pyrogens: some concepts have changed. Journal of Endotoxin Research. 2004;10(4):201-22.

5. Horai R, Asano M, Sudo K, Kanuka H, Suzuki M, Nishihara M, et al. Production of mice deficient in genes for interleukin (IL)-1 alpha, IL-1 beta, IL-1 alpha/beta, and IL-1 receptor antagonist shows that IL-1 beta is crucial in turpentine-induced fever development and glucocorticoid secretion. Journal of Experimental Medicine. 1998;187(9):1463-75.

6. Kagiwada K, Chida D, Sakatani T, Asano M, Nambu A, Kakuta S, et al. Interleukin (IL)-6, but not IL-1, induction in the brain downstream of cyclooxygenase-2 is essential for the induction of febrile response against peripheral IL-1 alpha. Endocrinology. 2004;145(11):5044-8.

7. Lichtman AH, Chin J, Schmidt JA, Abbas AK. ROLE OF INTERLEUKIN-1 IN THE ACTIVATION OF LYMPHOCYTES-T. Proceedings of the National Academy of Sciences of the United States of America. 1988;85(24):9699-703.

8. Nakae S, Asano M, Horai R, Sakaguchi N, Iwakura Y. IL-1 enhances T cell-dependent antibody production through induction of CD40 ligand and OX40 on T cells. Journal of Immunology. 2001;167(1):90-7.

9. Lee YM, Fujikado N, Manaka H, Yasuda H, Iwakura Y. IL-1 plays an important role in the bone metabolism under physiological conditions. International Immunology. 2010;22(10):805-16.

10. Joosten LAB, Helsen MMA, Saxne T, van de Loo FAJ, Heinegard D, van den Berg WB. IL-1 alpha beta blockade prevents cartilage and bone destruction in murine type II collagen-induced arthritis, whereas TNF-alpha blockade only ameliorates joint inflammation. Journal of Immunology. 1999;163(9):5049-55.

11. Matsuki T, Horai R, Sudo K, Iwakura Y. IL-1 plays an important role in lipid metabolism by regulating insulin levels under physiological conditions. Journal of Experimental Medicine. 2003;198(6):877-88.

12. Chida D, Hashimoto O, Kuwahara M, Sagara H, Osaka T, Tsubone H, et al.

Increased fat : carbohydrate oxidation ratio in Il1ra(-/-) mice on a high-fat diet is associated with increased sympathetic tone. Diabetologia. 2008;51(9):1698-706.
13. Garg AD, Nowis D, Golab J, Vandenabeele P, Krysko DV, Agostinis P. Immunogenic cell death, DAMPs and anticancer therapeutics: An emerging amalgamation. Biochimica Et Biophysica Acta-Reviews on Cancer. 2010;1805(1):53-71.
14. Afonina IS, Tynan GA, Logue SE, Cullen SP, Bots M, Luethi AU, et al. Granzyme B-Dependent Proteolysis Acts as a Switch to Enhance the Proinflammatory Activity of IL-1 alpha. Molecular Cell. 2011;44(2):265-78.
15. Maltez VI, Miao EA. NAIP inflammasomes give the NOD to bacterial ligands. Trends in Immunology. 2014;35(11):503-4.
16. Guma M, Ronacher L, Liu-Bryan R, Takai S, Karin M, Corr M. Caspase 1-Independent Activation of Interleukin-1 beta in Neutrophil-Predominant Inflammation. Arthritis and Rheumatism. 2009;60(12):3642-50.
17. Colotta F, Re F, Muzio M, Bertini R, Polentarutti N, Sironi M, et al. INTERLEUKIN-1 TYPE-II RECEPTOR - A DECOY TARGET FOR IL-1 THAT IS REGULATED BY IL-4. Science. 1993;261(5120):472-5.
18. Re F, Sironi M, Muzio M, Matteucci C, Introna M, Orlando S, et al. Inhibition of interleukin-1 responsiveness by type II receptor gene transfer: A surface "receptor" with anti-interleukin-1 function. Journal of Experimental Medicine. 1996;183(4):1841-50.
19. Neumann D, Kollewe C, Martin MU, Boraschi D. The membrane form of the type IIIL-1 receptor accounts for inhibitory function. Journal of Immunology. 2000;165(6):3350-7.
20. Yamaki M, Sugiura K, Muro Y, Shimoyama Y, Tomita Y. Epidermal growth factor receptor tyrosine kinase inhibitors induce CCL2 and CCL5 via reduction in IL-1R2 in keratinocytes. Experimental Dermatology. 2010;19(8):730-5.
21. Rauschmayr T, Groves RW, Kupper TS. Keratinocyte expression of the type 2 interleukin 1 receptor mediates local and specific inhibition of interleukin 1-mediated inflammation. Proceedings of the National Academy of Sciences of the United States of America. 1997;94(11):5814-9.
22. Zheng Y, Humphry M, Maguire JJ, Bennett MR, Clarke MCH. Intracellular Interleukin-1 Receptor 2 Binding Prevents Cleavage and Activity of Interleukin-1 alpha, Controlling Necrosis-Induced Sterile Inflammation. Immunity. 2013;38(2):285-95.
23. Kuhn P-H, Marjaux E, Imhof A, De Strooper B, Haass C, Lichtenthaler SF. Regulated intramembrane proteolysis of the interleukin-1 receptor II by alpha-, beta-,

and gamma-secretase. Journal of Biological Chemistry. 2007;282(16):11982-95.
24. Horai R, Saijo S, Tanioka M, Nakae S, Sudo K, Okahara A, et al. Development of chronic inflammatory arthropathy resembling rheumatoid arthritis in interleukin 1 receptor antagonist-deficient mice. Journal of Experimental Medicine. 2000;191(2):313-20.
25. Nakajima A, Matsuki T, Komine M, Asahina A, Horai R, Nakae S, et al. TNF, but Not IL-6 and IL-17, Is Crucial for the Development of T Cell-Independent Psoriasis-Like Dermatitis in Il1rn(-/-) Mice. Journal of Immunology. 2010;185(3):1887-93.
26. Qin JZ, Qian YC, Yao JH, Grace C, Li XX. SIGIRR inhibits interleukin-1 receptor- and toll-like receptor 4-mediated signaling through different mechanisms. Journal of Biological Chemistry. 2005;280(26):25233-41.
27. Brint EK, Xu DM, Liu HY, Dunne A, McKenzie ANJ, O'Neill LAJ, et al. ST2 is an inhibitor of interleukin 1 receptor and Toll-like receptor 4 signaling and maintains endotoxin tolerance. Nature Immunology. 2004;5(4):373-9.
28. Kondo T, Kawai T, Akira S. Dissecting negative regulation of Toll-like receptor signaling. Trends in Immunology. 2012;33(9):449-58.
29. Dinarello CA. Interleukin-1 in the pathogenesis and treatment of inflammatory diseases. Blood. 2011;117(14):3720-32.
30. Chae JJ, Komarow HD, Cheng J, Wood G, Raben N, Liu PP, et al. Targeted disruption of pyrin, the FMF protein, causes heightened sensitivity to endotoxin and a defect in macrophage apoptosis. Molecular Cell. 2003;11(3):591-604.
31. Iwakura Y. Roles of IL-1 in the development of rheumatoid arthritis: consideration from mouse models. Cytokine & Growth Factor Reviews. 2002;13(4-5):341-55.
32. Furst DE. Anakinra: Review of recombinant human interieukin-1 receptor antagonist in the treatment of rheumatoid arthritis. Clinical Therapeutics. 2004;26(12):1960-75.
33. Arend WP, Malyak M, Smith MF, Whisenand TD, Slack JL, Sims JE, et al. BINDING OF IL-1-ALPHA, IL-1-BETA, AND IL-1 RECEPTOR ANTAGONIST BY SOLUBLE IL-1 RECEPTORS AND LEVELS OF SOLUBLE IL-1 RECEPTORS IN SYNOVIAL-FLUIDS. Journal of Immunology. 1994;153(10):4766-74.
34. Jouvenne P, Vannier E, Dinarello CA, Miossec P. Elevated levels of soluble interleukin-1 receptor type II and interleukin-1 receptor antagonist in patients with chronic arthritis - Correlations with markers of inflammation and joint destruction. Arthritis and Rheumatism. 1998;41(6):1083-9.

35. Lin SY, Hsieh SC, Lin YC, Lee CN, Tsai MH, Lai LC, et al. A whole genome methylation analysis of systemic lupus erythematosus: hypomethylation of the IL10 and IL1R2 promoters is associated with disease activity. Genes and Immunity. 2012;13(3):214-20.
36. Asquith DL, Miller AM, McInnes IB, Liew FY. Animal models of rheumatoid arthritis. European Journal of Immunology. 2009;39(8):2040-4.
37. Iwakura Y, Tosu M, Yoshida E, Takiguchi M, Sato K, Kitajima I, et al. INDUCTION OF INFLAMMATORY ARTHROPATHY RESEMBLING RHEUMATOID-ARTHRITIS IN MICE TRANSGENIC FOR HTLV-I. Science. 1991;253(5023):1026-8.
38. Keffer J, Probert L, Cazlaris H, Georgopoulos S, Kaslaris E, Kioussis D, et al. TRANSGENIC MICE EXPRESSING HUMAN TUMOR-NECROSIS-FACTOR - A PREDICTIVE GENETIC MODEL OF ARTHRITIS. Embo Journal. 1991;10(13):4025-31.
39. Sakaguchi N, Takahashi T, Hata H, Nomura T, Tagami T, Yamazaki S, et al. Altered thymic T-cell selection due to a mutation of the ZAP-70 gene causes autoimmune arthritis in mice. Nature. 2003;426(6965):454-60.
40. Courtenay JS, Dallman MJ, Dayan AD, Martin A, Mosedale B. IMMUNIZATION AGAINST HETEROLOGOUS TYPE-II COLLAGEN INDUCES ARTHRITIS IN MICE. Nature. 1980;283(5748):666-8.
41. Holmdahl R, Rubin K, Klareskog L, Larsson E, Wigzell H. CHARACTERIZATION OF THE ANTIBODY-RESPONSE IN MICE WITH TYPE-II COLLAGEN-INDUCED ARTHRITIS, USING MONOCLONAL ANTI-TYPE II COLLAGEN ANTIBODIES. Arthritis and Rheumatism. 1986;29(3):400-10.
42. Brackertz D, Mitchell GF, Mackay IR. ANTIGEN-INDUCED ARTHRITIS IN MICE .1. INDUCTION OF ARTHRITIS IN VARIOUS STRAINS OF MICE. Arthritis and Rheumatism. 1977;20(3):841-50.
43. Brackertz D, Mitchell GF, Vadas MA, Mackay IR, Miller J. STUDIES ON ANTIGEN-INDUCED ARTHRITIS IN MICE .2. IMMUNOLOGICAL CORRELATES OF ARTHRITIS SUSCEPTIBILITY IN MICE. Journal of Immunology. 1977;118(5):1639-44.
44. Glaccum MB, Stocking KL, Charrier K, Smith JL, Willis CR, Maliszewski C, et al. Phenotypic and functional characterization of mice that lack the type I receptor for IL-1. Journal of Immunology. 1997;159(7):3364-71.
45. Asano M, Furukawa K, Kido M, Matsumoto S, Umesaki Y, Kochibe N, et al. Growth retardation and early death of beta-1,4-galactosyltransferase knockout mice

with augmented proliferation and abnormal differentiation of epithelial cells. Embo Journal. 1997;16(8):1850-7.
46. Sunaga S, Maki K, Komagata Y, Ikuta K, Miyazaki J. Efficient removal of loxP-Flanked DNA sequences in a gene-targeted locus by transient expression of Cre recombinase in fertilized eggs. Molecular Reproduction and Development. 1997;46(2):109-13.
47. Inglis JJ, Simelyte E, McCann FE, Criado G, Williams RO. Protocol for the induction of arthritis in C57BL/6 mice. Nature Protocols. 2008;3(4):612-8.
48. Zhang X, Goncalves R, Mosser DM. The isolation and characterization of murine macrophages. Curr Protoc Immunol. 2008;Chapter 14:Unit 14.1.
49. Chou RC, Kim ND, Sadik CD, Seung E, Lan YN, Byrne MH, et al. Lipid-Cytokine-Chemokine Cascade Drives Neutrophil Recruitment in a Murine Model of Inflammatory Arthritis. Immunity. 2010;33(2):266-78.
50. Seki N, Sudo Y, Yoshioka T, Sugihara S, Fujitsu T, Sakuma S, et al. TYPE-II COLLAGEN-INDUCED MURINE ARTHRITIS .1. INDUCTION AND PERPETUATION OF ARTHRITIS REQUIRE SYNERGY BETWEEN HUMORAL AND CELL-MEDIATED-IMMUNITY. Journal of Immunology. 1988;140(5):1477-84.
51. Luross JA, Williams NA. The genetic and immunopathological processes underlying collagen-induced arthritis. Immunology. 2001;103(4):407-16.
52. Chou L-W, Wang J, Chang P-L, Hsieh Y-L. Hyaluronan modulates accumulation of hypoxia-inducible factor-1 alpha, inducible nitric oxide synthase, and matrix metalloproteinase-3 in the synovium of rat adjuvant-induced arthritis model. Arthritis Research & Therapy. 2011;13(3).
53. Jhun JY, Moon S-J, Yoon BY, Byun JK, Kim EK, Yang EJ, et al. Grape Seed Proanthocyanidin Extract-Mediated Regulation of STAT3 Proteins Contributes to Treg Differentiation and Attenuates Inflammation in a Murine Model of Obesity-Associated Arthritis. Plos One. 2013;8(11).
54. Ryu J-H, Chae C-S, Kwak J-S, Oh H, Shin Y, Huh YH, et al. Hypoxia-Inducible Factor-2 alpha Is an Essential Catabolic Regulator of Inflammatory Rheumatoid Arthritis. Plos Biology. 2014;12(6).
55. Park M-J, Park H-S, Oh H-J, Lim J-Y, Yoon B-Y, Kim H-Y, et al. IL-17-deficient allogeneic bone marrow transplantation prevents the induction of collagen-induced arthritis in DBA/1J mice. Experimental and Molecular Medicine. 2012;44(11):694-705.
56. Mor A, Abramson SB, Pillinger MH. The fibroblast-like synovial cell in rheumatoid arthritis: a key player in inflammation and joint destruction. Clinical

Immunology. 2005;115(2):118-28.
57. Sasai M, Saeki Y, Ohshima S, Nishioka K, Mima T, Tanaka T, et al. Delayed onset and reduced severity of collagen-induced arthritis in interleukin-6-deficient. Arthritis and Rheumatism. 1999;42(8):1635-43.
58. Jacobs JP, Ortiz-Lopez A, Campbell JJ, Gerard CJ, Mathis D, Benoist C. Deficiency of CXCR2, but Not Other Chemokine Receptors, Attenuates Autoantibody-Mediated Arthritis in a Murine Model. Arthritis and Rheumatism. 2010;62(7):1921-32.
59. Kato H, Nishida K, Yoshida A, Takada I, McCown C, Matsuo M, et al. Effect of NOS2 gene deficiency on the development of autoantibody mediated arthritis and subsequent articular cartilage degeneration. Journal of Rheumatology. 2003;30(2):247-55.
60. Saijo S, Asano M, Horai R, Yamamoto H, Iwakura Y. Suppression of autoimmune arthritis in interleukin-1-deficient mice in which T cell activation is impaired due to low levels of CD40 ligand and OX40 expression on T cells. Arthritis and Rheumatism. 2002;46(2):533-44.
61. Li J, Hsu H-C, Yang P, Wu Q, Li H, Edgington LE, et al. Treatment of Arthritis by Macrophage Depletion and Immunomodulation Testing an Apoptosis-Mediated Therapy in a Humanized Death Receptor Mouse Model. Arthritis and Rheumatism. 2012;64(4):1098-109.
62. Martin P, Palmer G, Vigne S, Lamacchia C, Rodriguez E, Talabot-Ayer D, et al. Mouse neutrophils express the decoy type 2 interleukin-1 receptor (IL-1R2) constitutively and in acute inflammatory conditions. J Leukoc Biol. 2013;94(4):791-802.
63. Prince LR, Allen L, Jones EC, Hellewell PG, Dower SK, Whyte MKB, et al. The role of interleukin-1 beta in direct and toll-like receptor 4-mediated neutrophil activation and survival. American Journal of Pathology. 2004;165(5):1819-26.
64. Bourke E, Cassetti A, Villa A, Fadlon E, Colotta F, Mantovani A. IL-1 beta scavenging by the type IIIL-1 decoy receptor in human neutrophils. Journal of Immunology. 2003;170(12):5999-6005.
65. Colotta F, Orlando S, Fadlon EJ, Sozzani S, Matteucci C, Mantovani A. CHEMOATTRACTANTS INDUCE RAPID RELEASE OF THE INTERLEUKIN-1 TYPE-II DECOY RECEPTOR IN HUMAN POLYMORPHONUCLEAR CELLS. Journal of Experimental Medicine. 1995;181(6):2181-8.
66. Mercer F, Kozhaya L, Unutmaz D. Expression and Function of TNF and IL-1 Receptors on Human Regulatory T Cells. Plos One. 2010;5(1).
67. Townsend MJ, Fallon PG, Matthews DJ, Jolin HE, McKenzie ANJ.

T1/ST2-deficient mice demonstrate the importance of T1/ST2 in developing primary T helper cell type 2 responses. Journal of Experimental Medicine. 2000;191(6):1069-75.
68. Wald D, Qin JZ, Zhao ZD, Qian YC, Naramura M, Tian LP, et al. SIGIRR, a negative regulator of Toll-like receptor-interleukin 1 receptor signaling. Nature Immunology. 2003;4(9):920-7.
69. Nakayamada S, Takahashi H, Kanno Y, O'Shea JJ. Helper T cell diversity and plasticity. Current Opinion in Immunology. 2012;24(3):297-302.
70. Korn T, Bettelli E, Oukka M, Kuchroo VK. IL-17 and Th17 Cells. Annual Review of Immunology. 2009;27:485-517.
71. Veldhoen M, Hocking RJ, Atkins CJ, Locksley RM, Stockinger B. TGF beta in the context of an inflammatory cytokine milieu supports de novo differentiation of IL-17-producing T cells. Immunity. 2006;24(2):179-89.
72. Bettelli E, Carrier YJ, Gao WD, Korn T, Strom TB, Oukka M, et al. Reciprocal developmental pathways for the generation of pathogenic effector T(H)17 and regulatory T cells. Nature. 2006;441(7090):235-8.
73. Mangan PR, Harrington LE, O'Quinn DB, Helms WS, Bullard DC, Elson CO, et al. Transforming growth factor-beta induces development of the T(H)17 lineage. Nature. 2006;441(7090):231-4.
74. Korn T, Bettelli E, Gao W, Awasthi A, Jaeger A, Strom TB, et al. IL-21 initiates an alternative pathway to induce proinflammatory T(H)17 cells. Nature. 2007;448(7152):484-U9.
75. Nurieva R, Yang XO, Martinez G, Zhang Y, Panopoulos AD, Ma L, et al. Essential autocrine regulation by IL-21 in the generation of inflammatory T cells. Nature. 2007;448(7152):480-U8.
76. Anderson D, Yang L, Baecher-Allan C, Bettelli E, Oukka M, Kuchroo V, et al. IL-21 and TGF-beta are required for differentiation of human Th17 cells. Clinical Immunology. 2008;127:S18-S9.
77. Manel N, Unutmaz D, Littman DR. The differentiation of human T(H)-17 cells requires transforming growth factor-beta and induction of the nuclear receptor ROR gamma t. Nature Immunology. 2008;9(6):641-9.
78. Volpe E, Servant N, Zollinger R, Bogiatzi SI, Hupe P, Barillot E, et al. A critical function for transforming growth factor-beta, interleukin 23 and proinflammatory cytokines in driving and modulating human T(H)-17 responses. Nature Immunology. 2008;9(6):650-7.
79. Chung Y, Chang SH, Martinez GJ, Yang XO, Nurieva R, Kang HS, et al. Critical Regulation of Early Th17 Cell Differentiation by Interleukin-1 Signaling.

Immunity. 2009;30(4):576-87.
80. Liu X, Leung S, Wang C, Tan Z, Wang J, Guo TB, et al. Crucial role of interleukin-7 in T helper type 17 survival and expansion in autoimmune disease (Retracted article. See vol. 19, pg. 1673, 2013). Nature Medicine. 2010;16(2):191-U97.
81. Stritesky GL, Yeh N, Kaplan MH. IL-23 Promotes Maintenance but Not Commitment to the Th17 Lineage. Journal of Immunology. 2008;181(9):5948-55.
82. Li P, Spolski R, Liao W, Leonard WJ. Complex interactions of transcription factors in mediating cytokine biology in T cells. Immunological Reviews. 2014;261(1):141-56.
83. Ivanov II, McKenzie BS, Zhou L, Tadokoro CE, Lepelley A, Lafaille JJ, et al. The orphan nuclear receptor ROR gamma t directs the differentiation program of proinflammatory IL-17(+) T helper cells. Cell. 2006;126(6):1121-33.
84. Yang XO, Panopoulos AD, Nurieva R, Chang SH, Wang D, Watowich SS, et al. STAT3 regulates cytokine-mediated generation of inflammatory helper T cells. Journal of Biological Chemistry. 2007;282(13):9358-63.
85. Bruestle A, Heink S, Huber M, Rosenplaenter C, Stadelmann C, Yu P, et al. The development of inflammatory T-H-17 cells requires interferon-regulatory factor 4. Nature Immunology. 2007;8(9):958-66.
86. Yang XO, Pappu BP, Nurieva R, Akimzhanov A, Kang HS, Chung Y, et al. T helper 17 lineage differentiation is programmed by orphan nuclear receptors ROR alpha and ROR gamma. Immunity. 2008;28(1):29-39.
87. Veldhoen M, Hirota K, Westendorf AM, Buer J, Dumoutier L, Renauld J-C, et al. The aryl hydrocarbon receptor links T(H)17-cell-mediated autoimmunity to environmental toxins. Nature. 2008;453(7191):106-+.
88. Quintana FJ, Basso AS, Iglesias AH, Korn T, Farez MF, Bettelli E, et al. Control of T-reg and TH17 cell differentiation by the aryl hydrocarbon receptor. Nature. 2008;453(7191):65-+.
89. Kimura A, Naka T, Nohara K, Fujii-Kuriyama Y, Kishimoto T. Aryl hydrocarbon receptor regulates Stat1 activation and participates in the development of Th17 cells. Proceedings of the National Academy of Sciences of the United States of America. 2008;105(28):9721-6.
90. Veldhoen M, Hirota K, Christensen J, O'Garra A, Stockinger B. Natural agonists for aryl hydrocarbon receptor in culture medium are essential for optimal differentiation of Th17 T cells. Journal of Experimental Medicine. 2009;206(1):43-9.
91. Okamoto K, Iwai Y, Oh-hora M, Yamamoto M, Morio T, Aoki K, et al. I kappa B zeta regulates T(H)17 development by cooperating with ROR nuclear receptors.

Nature. 2010;464(7293):1381-U13.
92. Schraml BU, Hildner K, Ise W, Lee W-L, Smith WAE, Solomon B, et al. The AP-1 transcription factor Batf controls T(H)17 differentiation. Nature. 2009;460(7253):405-U125.
93. Ruan Q, Kameswaran V, Zhang Y, Zheng S, Sun J, Wang J, et al. The Th17 immune response is controlled by the Rel-ROR gamma-ROR gamma T transcriptional axis. Journal of Experimental Medicine. 2011;208(11):2321-33.
94. Zhang F, Meng G, Strober W. Interactions among the transcription factors Runx1, ROR gamma t and Foxp3 regulate the differentiation of interleukin 17-producing T cells. Nature Immunology. 2008;9(11):1297-306.
95. Dang EV, Barbi J, Yang H-Y, Jinasena D, Yu H, Zheng Y, et al. Control of T(H)17/T-reg Balance by Hypoxia-Inducible Factor 1. Cell. 2011;146(5):772-84.
96. Ichiyama K, Yoshida H, Wakabayashi Y, Chinen T, Saeki K, Nakaya M, et al. Foxp3 inhibits ROR gamma t-mediated IL-17A mRNA transcription through direct interaction with ROR gamma t. Journal of Biological Chemistry. 2008;283(25):17003-8.
97. Yang X-P, Ghoreschi K, Steward-Tharp SM, Rodriguez-Canales J, Zhu J, Grainger JR, et al. Opposing regulation of the locus encoding IL-17 through direct, reciprocal actions of STAT3 and STAT5. Nature Immunology. 2011;12(3):247-U84.
98. Lazarevic V, Chen X, Shim J-H, Hwang E-S, Jang E, Bolm AN, et al. T-bet represses T(H)17 differentiation by preventing Runx1-mediated activation of the gene encoding ROR gamma t. Nature Immunology. 2011;12(1):96-U124.
99. Ouyang X, Zhang R, Yang J, Li Q, Qin L, Zhu C, et al. Transcription factor IRF8 directs a silencing programme for T(H)17 cell differentiation. Nature Communications. 2011;2.
100. Yu X, Rollins D, Ruhn KA, Stubblefield JJ, Green CB, Kashiwada M, et al. T(H)17 Cell Differentiation Is Regulated by the Circadian Clock. Science. 2013;342(6159):727-30.
101. Ichiyama K, Hashimoto M, Sekiya T, Nakagawa R, Wakabayashi Y, Sugiyama Y, et al. Gfi1 negatively regulates T(h)17 differentiation by inhibiting ROR gamma t activity. International Immunology. 2009;21(7):881-9.
102. Stromnes IM, Goverman JM. Active induction of experimental allergic encephalomyelitis. Nature Protocols. 2006;1(4):1810-9.
103. Arima Y, Harada M, Kamimura D, Park J-H, Kawano F, Yull FE, et al. Regional Neural Activation Defines a Gateway for Autoreactive T Cells to Cross the Blood-Brain Barrier. Cell. 2012;148(3):447-57.
104. Luheshi NM, Rothwell NJ, Brough D. The Dynamics and Mechanisms of

Interleukin-1 alpha and beta Nuclear Import. Traffic. 2009;10(1):16-25.
105. Luheshi NM, Rothwell NJ, Brough D. Dual functionality of interleukin-1 family cytokines: implications for anti-interleukin-1 therapy. British Journal of Pharmacology. 2009;157(8):1318-29.
106. Maier JAM, Statuto M, Ragnotti G. ENDOGENOUS INTERLEUKIN-1-ALPHA MUST BE TRANSPORTED TO THE NUCLEUS TO EXERT ITS ACTIVITY IN HUMAN ENDOTHELIAL-CELLS. Molecular and Cellular Biology. 1994;14(3):1845-51.
107. Werman A, Werman-Venkert R, White R, Lee JK, Werman B, Krelin Y, et al. The precursor form of IL-1 alpha is an intracrine proinflammatory activator of transcription. Proceedings of the National Academy of Sciences of the United States of America. 2004;101(8):2434-9.
108. Buryskova M, Pospisek M, Grothey A, Simmet T, Burysek L. Intracellular interleukin-1 alpha functionally interacts with histone acetyltransferase complexes. Journal of Biological Chemistry. 2004;279(6):4017-26.
109. Kawaguchi Y, Nishimagi E, Tochimoto A, Kawamoto M, Katsumata Y, Soejima M, et al. Intracellular IL-1 alpha-binding proteins contribute to biological functions of endogenous IL-1 alpha in systemic sclerosis fibroblasts. Proceedings of the National Academy of Sciences of the United States of America. 2006;103(39):14501-6.
110. Chang S-Y, Su P-F, Lee T-C. Ectopic expression of interleukin-1 receptor type II enhances cell migration through activation of the pre-interleukin lot pathway. Cytokine. 2009;45(1):32-8.
111. Tuomela S, Salo V, Tripathi SK, Chen Z, Laurila K, Gupta B, et al. Identification of early gene expression changes during human Th17 cell differentiation. Blood. 2012;119(23):E151-E60.
112. Feng T, Wang L, Schoeb TR, Elson CO, Cong Y. Microbiota innate stimulation is a prerequisite for T cell spontaneous proliferation and induction of experimental colitis. Journal of Experimental Medicine. 2010;207(6):1321-32.
113. Bettelli E, Pagany M, Weiner HL, Linington C, Sobel RA, Kuchroo AK. Myelin oligodendrocyte glycoprotein-specific T cell receptor transgenic mice develop spontaneous autoimmune optic neuritis. Journal of Experimental Medicine. 2003;197(9):1073-81.
114. Butler JT, Ray SK, Banik NL, Beeson CC. THE INVOLVEMENT OF CALPAIN IN CD4+ T HELPER CELL BIAS. Journal of Neurochemistry. 2009;108:131-.
115. Wessendorf JHM, Garfinkel S, Zhan X, Brown S, Maciag T.

IDENTIFICATION OF A NUCLEAR-LOCALIZATION SEQUENCE WITHIN THE STRUCTURE OF THE HUMAN INTERLEUKIN-1-ALPHA PRECURSOR. Journal of Biological Chemistry. 1993;268(29):22100-4.

116. Sudo M, Kobayashi Y, Watanabe N. Presence of a cytoplasmic retention sequence within the human interleukin-1 alpha precursor. Zoological Science. 2005;22(8):891-6.

117. Baekkevold ES, Roussigne M, Yamanaka T, Johansen FE, Jahnsen FL, Amalric F, et al. Molecular characterization of NF-HEV, a nuclear factor preferentially expressed in human high endothelial venules. American Journal of Pathology. 2003;163(1):69-79.

118. Ali S, Mohs A, Thomas M, Klare J, Ross R, Schmitz ML, et al. The Dual Function Cytokine IL-33 Interacts with the Transcription Factor NF-kappa B To Dampen NF-kappa B-Stimulated Gene Transcription. Journal of Immunology. 2011;187(4):1609-16.

119. Thomas JO, Travers AA. HMG1 and 2, and related 'architectural' DNA-binding proteins. Trends in Biochemical Sciences. 2001;26(3):167-74.

120. Sims GP, Rowe DC, Rietdijk ST, Herbst R, Coyle AJ. HMGB1 and RAGE in Inflammation and Cancer. Annual Review of Immunology, Vol 28. 2010;28:367-88.

VII. Acknowledgements

I first wish to express my appreciation to Prof. Toshiki Watanabe for his supports on many points.

And also, I would like to express my deep gratitude to Prof. Yoichiro Iwakura for his guidance.

I also thank co-authors of “Interleukin-1 receptor type 2 suppresses collagen-induced arthritis by inhibiting interleukin-1 signal on macrophages”, Akiko Nakajima, Katsuko Sudo, Yang Liu, Atsuhiko Mizoroki, Tetsuro Ikarashi, Reiko Horai and Shigeru Kakuta for their help on promoting this work.

I gratefully acknowledge Prof. Jun-ichi Miyazaki for providing pCAGGS-Cre plasmid and Prof. Daisuke Kitamura for providing CD45.1 mice.

Finally, I am grateful to all colleagues in our laboratory for technical supports and helpful discussion.